Masterproef

Optimisation of the Suzuki-Miyaura-coupling and conversion from batch to continuous flow with microwaves as energy source

Promotor :
Prof. dr. ir. Leen BRAEKEN

Promotor :
Prof. dr. ir. LEEN THOMASSEN

Copromotor :
ing. LENNART CAMPS

Gezamenlijke opleiding Universiteit Hasselt en KU Leuven

Douwe Verhoeven
Scriptie ingediend tot het behalen van de graad van master in de industriële wetenschappen: chemie

KU LEUVEN | universiteit ►►hasselt

KU LEUVEN | universiteit ►►hasselt

2015•2016
Faculteit Industriële ingenieurswetenschappen
master in de industriële wetenschappen: chemie

Masterproef
Optimisation of the Suzuki-Miyaura-coupling and conversion from batch to continuous flow with microwaves as energy source

Promotor :
Prof. dr. ir. Leen BRAEKEN

Promotor :
Prof. dr. ir. LEEN THOMASSEN

Copromotor :
ing. LENNART CAMPS

Douwe Verhoeven
Scriptie ingediend tot het behalen van de graad van master in de industriële wetenschappen: chemie

universiteit
▶▶hasselt

KU LEUVEN

Preface

As a final year student of the department of Master in Chemical Engineering Technology at UHasselt and KULeuven, I had the opportunity to do research at Lab4U.

Conducting this research and writing this master's thesis was a complex task that took a lot of time and effort. Now I have managed to complete this master's thesis, I can look back on a very educational experience. Completing this master's thesis was never possible without the support and guidance of a number of people, whom I would like to thank.

In particular, I want to thank my promoter Ing. Lennart Camps for the great support, and the time and effort he has put into my research. His exquisite supervision, useful feedback on the thesis and many ideas and tips during the research were a great deal of help in carrying out this project.

Then I would like to express my gratitude towards Prof. Dr. Ir. Leen Braeken for her help in the writing of the thesis. Thanks to her ideas, thoughts, comments and critical reviews I was able to successfully write this thesis. During the research, I have learned a lot from her about structural composition and scientific writing.

Also a big thank you to my co-promoter, Prof. Dr. Ir. Leen Thomassen, who helped me very well with the experimental approach of the research. During regular meetings, her professional expertise proved to be very useful for troubleshooting. And once again, sorry for the stupid mistake I made during that meeting, I did not think that through.

I also want to thank Ing. Luc Moens for supplying the microwave reactor and his useful tips and advice for performing the experiments.

A special thank you goes to Ing. Sven Gobbert and Guy Hendriks who helped me a lot with the set-up of the continuous flow system. If there were any problems with the continuous system, I could always turn to them. Also my fellow students and roommates, Arno Corstjens and Jochim Kadivnik, thanks for your insights on my research and for helping me out if I had any questions.

My colleagues and fellow students at Lab4U, thanks for the fine collegiality. I could always go to you with all my questions and thanks to you it was a very pleasant working atmosphere.

Mom, dad, I cannot express how grateful I am to you, you always supported me and believed in me. Thank you for always being there and helping me become the person I am today.

Last, I also want to thank my friends and family for their support over the years and the good times we have together. These moments mean a lot for me, as they provide much support and affection.

Table of contents

List of tables

List of figures

Abstract

The use of microwave radiation as an energy source for chemical reactions is the last few years a popular method for fast and efficient synthesis. This master's thesis, in collaboration with Lab4U and Janssen Pharmaceuticals, has two objectives. First, the influence of microwave energy on the Suzuki-Miyaura coupling is investigated, and second, the Suzuki reaction carried out in a microwave-assisted flow process is compared with batch processing.

The Suzuki-Miyaura reaction in this study combines iodobenzene and phenylboronic acid to form biphenyl. In order to investigate the influence of microwave energy, the reaction kinetics and biphenyl yields are examined in a conventional reactor and microwave reactor. In addition, a microwave-assisted flow system and a conventional flow system are designed to compare the conversions between both flow systems and also with batch processing.

At the same temperature profile and residence time, the conversions in batch with conventional energy are 1.20 times higher than the conversions obtained in the microwave reactor. A possible explanation is a different mechanism in the transmetalation step when using microwaves. Although microwaves are less suitable for the reaction kinetics of the Suzuki-Miyaura reaction, the conversions obtained in the microwave-assisted flow are 3.15 times higher than in the conventional flow. This is due to the rapid heating effect of microwaves achieving a higher temperature within the same residence time, which is favorable for the reaction kinetics.

Abstract Nederlands

Het gebruik van microgolfstraling als energiebron voor chemische reacties is de laatste jaren een populaire methode voor snelle en efficiënte syntheses. Deze masterproef, in samenwerking met Lab4U en Janssen Pharmaceutica, heeft twee doelstellingen. Enerzijds wordt de invloed van microgolfenergie op de Suzuki-Miyaura koppeling nagegaan, anderzijds wordt de Suzuki reactie uitgevoerd in een microgolf-geassisteerd flowproces vergeleken met een batchuitvoering.

De Suzuki-Miyaura-reactie in dit onderzoek koppelt joodbenzeen en fenylboorzuur ter vorming van bifenyl. Om de invloed van microgolfenergie te onderzoeken, zijn de reactiekinetica en bifenyl-opbrengst nagegaan in een conventionele reactor en microgolfreactor. Daarnaast is een flow systeem met zowel microgolfenergie als conventionele warmte ontworpen om de conversies onderling en ten opzichte van batch te vergelijken.

Bij eenzelfde temperatuursprofiel en verblijftijd zijn de conversies in batch met conventionele energie gemiddeld 1,20 keer hoger dan die in de microgolfreactor. Een mogelijke reden hiervoor is een verschillend mechanisme in de transmetallatiestap bij gebruik van microgolven. Hoewel microgolven minder geschikt zijn voor de reactiekinetiek van de Suzuki-Miyaura-reactie, zijn de conversies in de microgolf-geassisteerde flow gemiddeld 3,15 keer hoger dan in de conventionele flow. Dit is te wijten aan het snelle opwarmingseffect van microgolven waardoor een hogere temperatuur binnen dezelfde verblijftijd gehaald wordt, wat wel gunstig is voor de reactiekinetiek.

1 Introduction

This research is performed in the context of a master's thesis to obtain the degree of Master in Chemical Engineering Technology at UHasselt and KULeuven. The research is commissioned by Lab4U, a research group of KU Leuven and UC Leuven Limburg. In this project, Lab4U cooperates intensively with Janssen Pharmaceutica, a Belgian pharmaceutical company. The mean idea of this collaboration is to gather interesting industrial problems and investigate them in more detail to get a better fundamental understanding. In industry, there is often not enough time to solve all those problems. That is where Lab4U kicks in, as it studies these problems at the request of a company in master theses or bilateral projects.

Lab4U primarily focuses on the intensification of chemical processes, purification of waste- and process water, remediation and recovery of contaminated soils and waste. This master's thesis is specifically focused on the part of process intensification [1],[2]. Janssen Pharmaceutica is a Belgian pharmaceutical company and part of the American group Johnson & Johnson, which is a multinational manufacturer of health care products [3]. Janssen Pharmaceutica supports this master's thesis by making a microwave reactor available and sharing knowledge.

The subject of this master's thesis is to investigate the influence of microwave energy on a chemical reaction. The choice to investigate the use of microwaves is because microwave radiation has become the last few years a popular energy source for chemical reactions as it is fast and efficient. In most cases, controlled microwave heating reduces reaction times and increases products yields and product quality by reducing product impurities [4].

The chemical reaction chosen to investigate is the Suzuki-Miyaura coupling reaction catalysed by palladium acetate. In this coupling reaction, iodobenzene and phenyl boronic acid react to biphenyl [5].
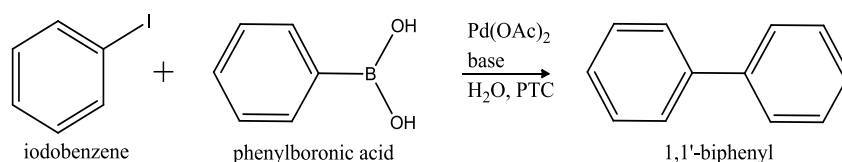
Scheme 1: Palladium acetate catalysed Suzuki reaction of iodobenzene and phenylboronic acid in water

As research topic, the first reason to choose the Suzuki-Miyaura reaction is because it is the most representative coupling reaction for the synthesis of pharmaceuticals. A second reason is that most Suzuki couplings are often inexpensive, selective and high-yielding when using catalytic levels of palladium. Finally, palladium catalysis has a high activity under mild reaction conditions. This makes the Suzuki reaction very suitable for large-scale applications in the pharmaceutical industry [6].

The use of microwave radiation on the Suzuki-Miyaura reaction is evaluated by means of two different processing methods. In the first method, the influence of microwave irradiation is evaluated by performing the Suzuki-Miyaura reaction in batch. The second method evaluates the use of microwave irradiation on continuous flow processing. Both methods are compared with conventional heating, as well in batch, as in flow. Finally, the Suzuki-Miyaura reaction performed in batch and in continuous flow are also compared.

First, the influence of microwaves on the Suzuki-Miyaura is examined in batch by carrying out the reaction in a microwave reactor and comparing it to the reaction in a conventional batch reactor. This comparison is based on the product yields and the reaction kinetics. According to Arvela et al. [7], it is possible to get high yields using the Suzuki-Miyaura coupling, both when using thermal energy as well as microwave energy. But these heating mechanisms are not exactly compared in the existing literature. Most studies on the SM-coupling are about the reaction itself and report on which components in which amounts should be added to achieve high conversions. This research is primarily interested in the use of microwaves. The quantities of components for carrying out the reaction are extracted from literature.

Second, an attempt is made to convert the reaction from batch to a microwave-assisted flow system. Therefore, a new reactor set-up has to be developed which also needs to be characterised before performing the Suzuki-Miyaura reaction on a continuous manner. Obtaining a flow reaction for the Suzuki-Miyaura reaction would have a number of advantages. According to Arvela et al. [7], the coupling reaction works very well when using microwave heating. High yields are already obtained within 7 minutes. Knowing this, performing the reaction in a batch reactor might not be the most efficient way due to the long preparation and clean-up of the reactor. Other significant benefits of a continuous process over a batch process are a more consistent product quality, improved process control, less labour intensive, increased use of capital goods and increased safety [8]. In addition, working continuously also makes it possible to work at higher pressures which ensures a higher boiling point of the solvent resulting in higher temperatures, and thus, increased reaction rates. Therefore, the continuous flow reactor is also evaluated based on the obtained product yields. This evaluation is done by comparing the microwave-assisted flow with a conventional flow and comparing flow processing with batch processing.

In order to determine the yields of the biphenyl product, a suitable analysis method must be performed. Different sources show that the analysis of the product is possible with GC/MS, GC/FID or HNMR [7],[9]. However, UV-Vis spectrophotometry is chosen as analysis method because of its ease of use and its best possibility to use it as an in-line analysis behind the continuous flow system. The UV-Vis spectrophotometrically method is then validated to verify whether it is able to determine selectively the concentration of biphenyl. In addition, a suitable sample preparation was necessary to isolate the formed biphenyl.

Finally, this research may be considered as a success when the use of microwaves on the Suzuki-Miyaura reaction performed in batch and continuous flow is successfully evaluated. This success also depends on the suitability of the analysis method, sample preparation, experimental method and set-up and characterisation of the flow system.

2 Literature

2.1 Electromagnetic radiation

Microwaves are a form of electromagnetic radiation which occur within a given frequency range. Electromagnetic radiation is a form of energy propagated through vacuum or a material medium [10].

2.1.1 Generation of electromagnetic waves

Point loads that dwell only generate a static electric field. Point loads that move at a constant speed generate an electric field and a magnetic field, but still no electromagnetic wave. Only accelerated or delayed loads (see Figure 1) can induce a changing electric field. As a result of the changing electric field, a varying magnetic field is generated. This creates, in its turn, a changing electric field and so forth. In this way, an electromagnetic wave is formed which, even in vacuum, can propagate [11]. Figure 1 represents two consecutive snapshots showing electric and magnetic fields that move outwardly departing from the vibrating loads on two conductors. The conductors are connected to an AC voltage generator [12].
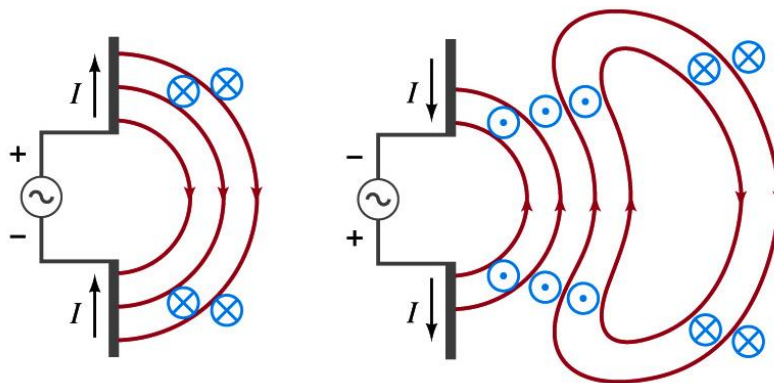
Figure 1: Principle of an antenna to excite electromagnetic waves [12]

At the left side of Figure 1, the current flows upwards, creating a magnetic field. At the right side of the figure, the current flows downwards, creating a magnetic field in the opposite direction. As a result the electric field lines align themselves and extend further to the outside as can be seen in Figure 2 [11],[12].
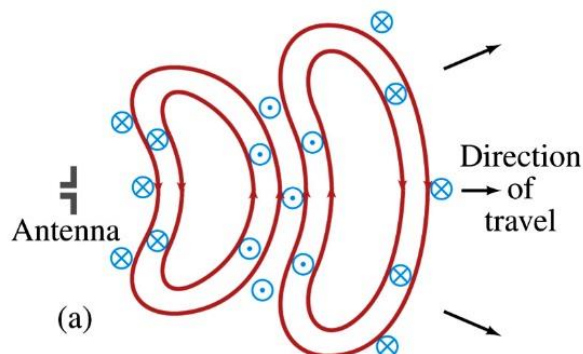
Figure 2: Radiation fields produced by a sinusoidal current in an antenna [12]

Figure 2 shows the radiation fields far away from the antenna produced by a sinusoidal current in the antenna. The closed loops represent the electric field lines and the magnetic field lines ($\otimes$ and $\odot$) form closed loops around the electric field lines [11].

The field strengths are greatest in the directions perpendicular to the vibration loads and they fall to zero along the direction of the vibration. Both fields are perpendicular to each other and to the propagation direction [11]. A schematic representation of an electromagnetic wave is shown in Figure 3 [13].

1. A sinusoidal wave with frequency f and wavelength λ travels with wave speed v_{em}.

2. $\vec{E}$ and $\vec{B}$ are perpendicular to each other and to the direction of travel. The fields have amplitudes E_0 and B_0.

3. $\vec{E}$ and $\vec{B}$ are in phase. That is, they have matching crests, troughs, and zeros.
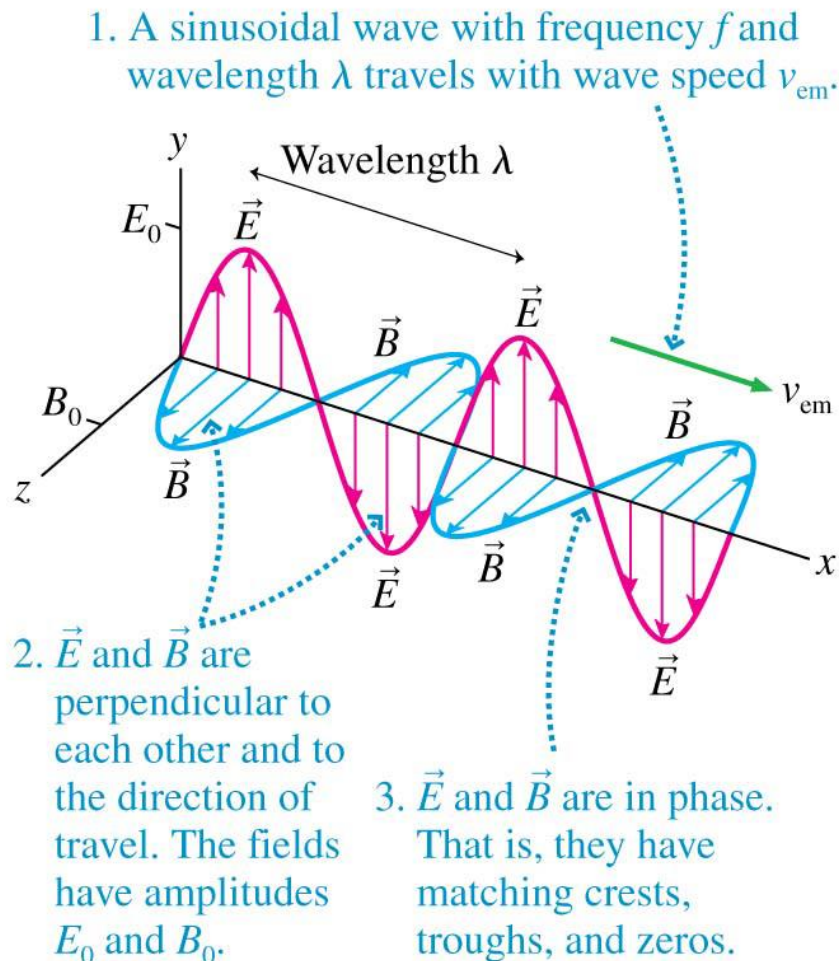
Figure 3: Schematic representation of an electromagnetic wave [13]

In the above Figure 3, the electromagnetic field is described with the electric field $\vec{E}$ (V/m) and the magnetic induction $\vec{B}$ (T). The electric- and magnetic field strengths vary at the same place at the same time from a maximum in one direction, through zero, to a maximum in the other direction. This means that both fields are in phase [11].

2.1.2 Properties of electromagnetic waves
The propagation velocity of the electromagnetic wave is shown in formula 1.

$$v = c = \sqrt{\frac{1}{\mu_0 \varepsilon_0}} \tag{1}$$

With ε_0 a constant equal to 8.85x10^{-12} F/m representing the permittivity of the vacuum. μ_0 represents the permeability of the vacuum and is equal to $4\pi 10^{-7}$ T/Am. The outcome of the above formula is most remarkable because it is exactly equal to the measured

speed of light, namely 3.00×10^8 m/s. So the propagation velocity of an electromagnetic wave in vacuum is equal to the speed of light. However, this varies when the EM wave propagates in another medium different from the vacuum [11]. In that case, the following formula 2 is valid:

$$v = \frac{1}{\mu \cdot \varepsilon} \tag{2}$$

Now, the permittivity ε and the permeability μ of the medium replace the constant quantities μ_0 and ε_0. The ratio of the velocity c in a vacuum relative to the velocity v in the medium is called the absolute refractive index n of the medium [11], this is shown in formula 3.

$$n = \frac{c}{v} = \sqrt{\frac{\varepsilon\,\mu}{\varepsilon_0\,\mu_0}} \tag{3}$$

Note that the permittivity and the permeability of the medium depend on the frequency of the electromagnetic wave. The frequencies of the electromagnetic waves are usually very high and as a result, the reorientation of the electric dipoles may not follow. This has as result that permittivity of the medium will then have a much lower value than with static fields, where the frequency is 0 Hz [11].

2.1.3 Electromagnetic spectrum

Electromagnetic radiation is described in terms of its wavelength λ, frequency f or energy E. Knowing the velocity v, it is possible to calculate the frequency from the value of the wavelength and vice versa with formula 4, because the wavelength and frequency are inversely related [10],[14].

$$\lambda = \frac{v}{f} \tag{4}$$

So when the wavelength is large, the frequency is small. The frequency and wavelength also indicate the amount of energy of the wave. This relation between the wavelength and energy is described in formula 5, where h is Planck's constant (h=6.625×10^{-34} J s) and c is the speed of light. So it is concluded that electromagnetic waves with shorter wavelengths are more energetic [15].

$$E = \frac{h\,c}{\lambda} \tag{5}$$

While there exists an inverse relationship between the wavelength and the energy, there exists a direct relationship between the energy and the frequency. Electromagnetic waves with a higher frequency are more energetic. This relationship is also shown in formula 6 [15].

$$E = h\,f \tag{6}$$

As electromagnetic waves exist over a wide range of frequencies, specific regions are classified into an electromagnetic spectrum. A schematic representation of the electromagnetic spectrum is shown in Figure 4. The electromagnetic spectrum is the distribution according to energy or, equivalently, according to the frequency or the wavelength. The range extends from zero to infinite frequencies [10],[13],[15].
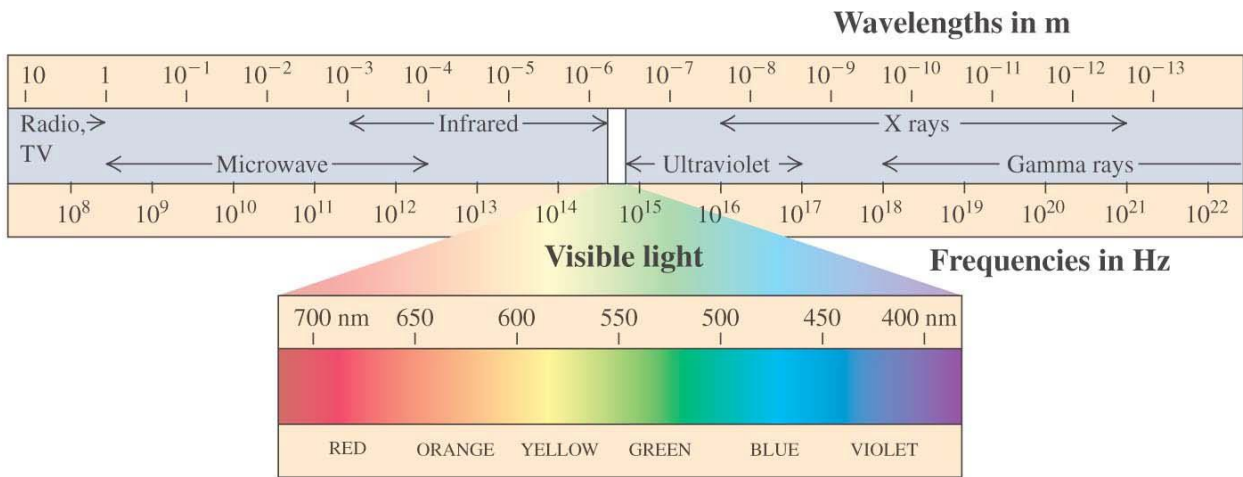
Figure 4: Electromagnetic spectrum [13]

Gamma rays and X-rays are types of EM radiation which possess the shortest wavelength, highest frequencies and in consequence the highest energy. These waves are generated by de-excitation of electrons in an atom and de-excitation of the nucleus. The low energy waves are located at the other end of the electromagnetic spectrum, these waves are generated by ac-currents. These low frequency waves include, in order of decreasing energy, radar waves, microwaves, television waves and radio waves. In the middle of the spectrum lies the energy which is known as "light". Here, infra-red light has the lowest energy, followed by visible light and ultraviolet. The human eye is capable to discriminate electromagnetic waves of different energy between 400 nm and 700 nm of wavelength. This spectrum appears as the different colours red, orange, yellow, green, blue and violet [13],[15].

However, this research focuses on the region of 30 GHz to 300 MHz of the electromagnetic spectrum. The waves that represent this region are microwaves. So this is further discussed in the next chapter [16].

2.2 Microwaves

Microwaves are a form of electromagnetic radiation located at the lower end of the electromagnetic spectrum. Frequencies of 300 to 300 000 Mhz are characteristic for microwaves, corresponding to wavelengths of 1 mm to 1 m. The microwave region of the electromagnetic spectrum is located between radio- and infrared waves, this is also shown in Figure 5 [16].
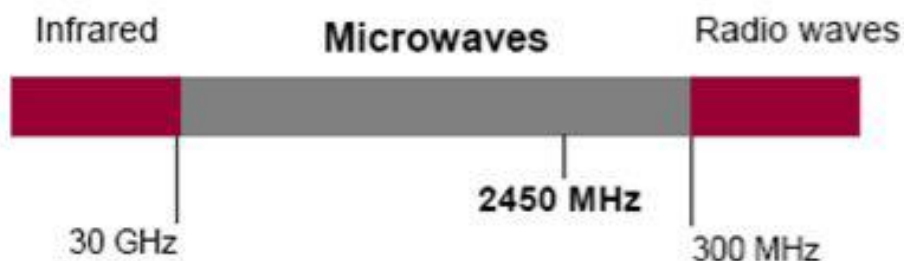
Figure 5: Situating of microwaves in the electromagnetic spectrum [16]

Industrial microwave processes generally use frequencies of 915 MHz, 2.45 GHz, 5.8 GHz and 24.124 GHz as these frequencies do not interfere with frequencies used for telecommunication and mobile phones. Especially the frequency of 2.45 GHz is applied in

microwave chemistry since this frequency is approved worldwide for commercial microwave chemistry equipment. This corresponds to a wavelength of 12.2 cm (see also formula 4). Another reason for this specific frequency is that near this frequency, the microwave energy absorption by liquid water and ice is maximal [17],[18].

2.2.1 Uses of microwaves

Microwaves have a broad field of applications. Microwave technology is extensively used for point-to-point telecommunications since microwaves are more easily focused into narrower beams than radio waves. Applications of microwaves are found in spacecraft communication, and also much of the world's data, TV and telephone communication are transmitted long distances by microwaves. Another more interesting application for this study is the heating and power ability of microwaves [18],[19].

Microwave energy is becoming an increasingly popular technique in chemistry to heat chemical reactions. This is evidenced by a large number of publications on this topic. In a lot of cases, controlled microwave heating reduces reaction times, increases product yields and product quality. A reduction of unwanted side reactions leads to lower product impurities in comparison with conventional synthetic methods. Microwaves are mainly applied in organic syntheses and in the pharmaceutical production, but there are also applications in polymer synthesis, nanotechnology and biochemical processes [4].

2.2.2 Microwave heat transfer mechanism

The energy transfer of microwaves to materials takes place by ionic conduction, dipolar polarization and interfacial polarization mechanisms. Due to the microwave radiation, the molecules move. This movement creates friction, which results in heat. Next to the heat generation, there are also local and superheated spots in the reaction solution created [17].

2.2.2.1 Dipolar polarization

When molecules are exposed to microwave radiation, the molecules that contain dipole moments will align with the applied electric field (see Figure 6). Since the electric field is an oscillation, the dipoles will constantly try to realign to follow the movement of the wave. However, at 2450 MHz the electric fields oscillate so fast that the molecules are not able to follow the oscillating field perfectly. Nevertheless, the molecules will try to align with the electric field and as a result of this continual reorientation of the molecules, friction is created, which dissipates as internal homogeneous heating [17].
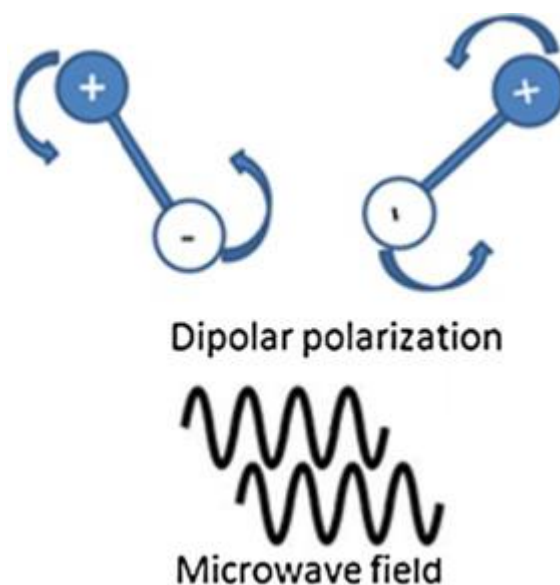
Figure 6: Dipolar polarisation under microwave conditions [17]

Commonly used microwaves possess an irradiation frequency of 2450 MHz, which means that the electric field of the wave oscillates $4,9 \cdot 10^9$ times per second. Consequently, the heating of the solution with microwaves is directly dependent on the dielectric properties of that solution, which are the dielectric constant ε', also known as permittivity, and dielectric loss ε''. These dielectric properties are of greatest importance in microwave processing. The dielectric constant ε' determines how much energy is reflected and how much energy is absorbed by the molecule. So it is a value for the ability of a molecule to be polarized by an electric field. The dielectric loss factor ε'' is a measure of the efficiency of the conversion of the absorbed microwave energy to heat. The dielectric properties are also used to calculate the ability of a substance to convert electromagnetic energy to heat energy at a given temperature and frequency, which can be seen in formula 7 [18],[20].

$$\frac{\varepsilon''}{\varepsilon'} = \tan \delta \tag{7}$$

Tan(δ) is the dissipation factor of the sample and it is in fact the most important property in microwave processing. It indicates the ability of the material to convert absorbed energy into heat. High values of the dissipation factor δ indicates large susceptibility to microwave energy. Polarized molecules have a higher dielectric loss factor, which means that higher conversions from microwave energy to heat are achieved [20].

Since the ability of a molecule to absorb microwave radiation is a function of its polarizability (e.g. a function of its dipole moment), only polar molecules are able to interact with microwave radiation. Compounds such as water, ethanol, which possess high dielectric constant will tend to heat rapidly using microwave irradiation. Less polar molecules such as aliphatic and aromatic hydrocarbons or molecules who possess no net dipole moment poorly absorb microwave irradiation. This has the result that mixtures with microwave active components and microwave inactive components are often used. When the solvent absorbs the microwave energy and the reagents are non-absorbing, there is no significant difference between the microwave energy and conventional heating. But then again, a mixture with reagents that selectively absorb microwave energy in a non-absorbing solvent will lead to larger product rates [20]. The system used in this study is similar to the first system as water is used as solvent which possesses a high dielectric constant, so selective heating does not occur.

20

2.2.2.2 Ionic conduction

Ionic conduction is when charged molecules are moved forth and back through the sample by the electric field of the microwave irradiation (see Figure 7).
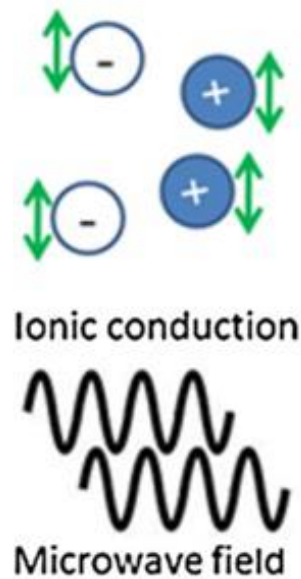
Figure 7: Ionic conducting under microwave conditions [17]

By this movement, the molecules collide into each other, which converts kinetic energy into heat. In addition, the energy interacts very rapidly with the molecules so that the molecules get no time to relax. This has the consequence that the generated heat, in short times, can be much greater than the overall temperature resulting in localized superheating [17],[20].

2.2.2.3 Interfacial polarisation

The interfacial polarisation method is considered as a combination of dipolar polarisation and ionic conduction. This occurs mainly in heating systems containing a conducting material dispersed in a non-conducting material. For example, a metal oxide in a polar solvent [17]. In these systems, accumulation of charges occurs at the interface because of an external field. Figure 8 shows an example of how free charges accumulate in an electric field causing interfacial polarisation.
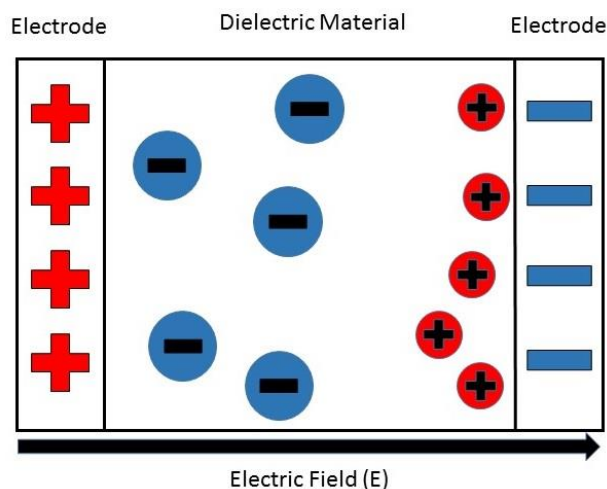
Figure 8: Free positive charges in a dielectric material migrating towards the negative charged electrode [21]

As shown in Figure 8, free charges can accumulate in an electric field. The electric field will cause an imbalance of the charges because of the insulating properties of the dielectric material. In order to maintain charge neutrality, the mobile charges will migrate in the dielectric material causing interfacial polarisation [21].

2.2.3 Microwave effects

Microwave heating uses the ability to convert electromagnetic radiation into heat. This energy is then used for the reaction to take place. This technique offers new possibilities in synthetic chemistry, especially in reactions that require heating. It was noticed that the application of microwaves in chemistry provides a significant reduction in reaction time in comparison to conventional heating. Reactions which take more than hours or days, can be run in considerably shorter time of several minutes to even seconds. There are two groups of theories that explain the reduction of reaction time when microwave heating is used instead of conventional conditions [16],[20].

The first group of theories says that microwaves provide a sudden, sometimes uncontrollable temperature growth of the reaction mixture. This leads to an increase of the reaction rates according to the common kinetic laws, which in its turn leads to a reduction of the reaction time. However, the kinetics and mechanism of the reactions still stay the same [20].

According to the second group of theories, there is a specific effect of microwave activation during microwave irradiation of the reaction mixture. This effect is called a non-thermal effect or the specific microwave effect and is a result from the interaction of the electric field with the molecules in the reaction medium. The specific microwave effect is capable of accelerating the reaction kinetics in a way that cannot be done with conventional heating. This is explained based on the Arrhenius kinetic law shown in Formula 8 [20],[22].

$$k = k_0 \, e^{\frac{-E_a}{R\,T}} \tag{8}$$

In formula 8, k is the reaction rate coefficient, k_0 is the Arrhenius pre-exponential factor, E_a is the activation energy, R is the gas constant and T is the temperature. The non-thermal effects have an influence on the orientation of polar molecules, which affects either the pre-exponential factor k_0 or the activation energy E_a in formula 8. The pre-exponential factor k_0 represents the probability of efficient molecular collision. When a microwave field is applied on a dielectric material, it induces rapid rotation of the molecular dipoles. This rapid rotation provides an increase of the probability of contact between molecules resulting in a higher collision efficiency k_0 and thus, an increase of the reaction rate [22].

The other non-thermal effect is to lower the activation energy E_a which can also be represented as ΔG. This effect is explained with reference to formula 9 where ΔG consists of an enthalpy term (ΔH) and an entropy term (ΔS) [22].

$$\Delta G = \Delta H - T\Delta S \tag{9}$$

Due to the microwave irradiation, a more ordered environment is created as consequence of dipolar polarisation. However, this ordered environment is constantly being reversed by the changing electromagnetic field. As the molecules are not capable of aligning with the applied field, more chaos is created which increases the entropy term which at its turn decreases ΔG. So referring to formula 8, it is considered that this causes

an increase of the reaction rate, which is definitely not caused by the bulk temperature of the reaction mixture [17],[20],[22].

2.2.4 Comparison of microwave heating with conventional heating

In contrast to conventional heating, microwaves cause more volumetric heating of the sample (see Figure 9). This means that more extensive heating inside the sample is conducted in comparison with outer layers of the material, while conventional heating first transfers heat to the surface of the material then followed by the inner part, which is called wall heating [17],[20].
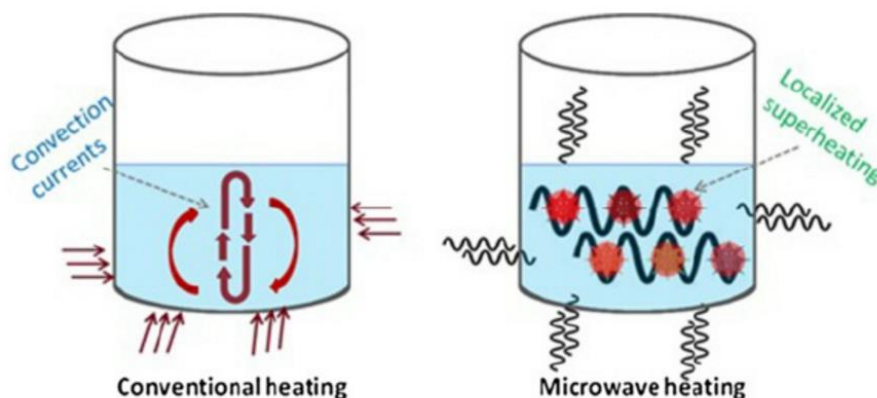
Figure 9: Conventional and microwave heating mechanisms [17]

Because of this wall heating effect, a lot of energy is lost to the environment through convection and conduction of materials. This results in higher surface temperatures that cause heat transfer from the outer surface to the inner part of the sample solution. Figure 10b shows the temperature gradient as an effect of both heating methods. The temperature gradient of the sample where microwaves are used shows clearly that the temperature of the whole volume is evenly and simultaneously in contrast to the conventional heating method [17].
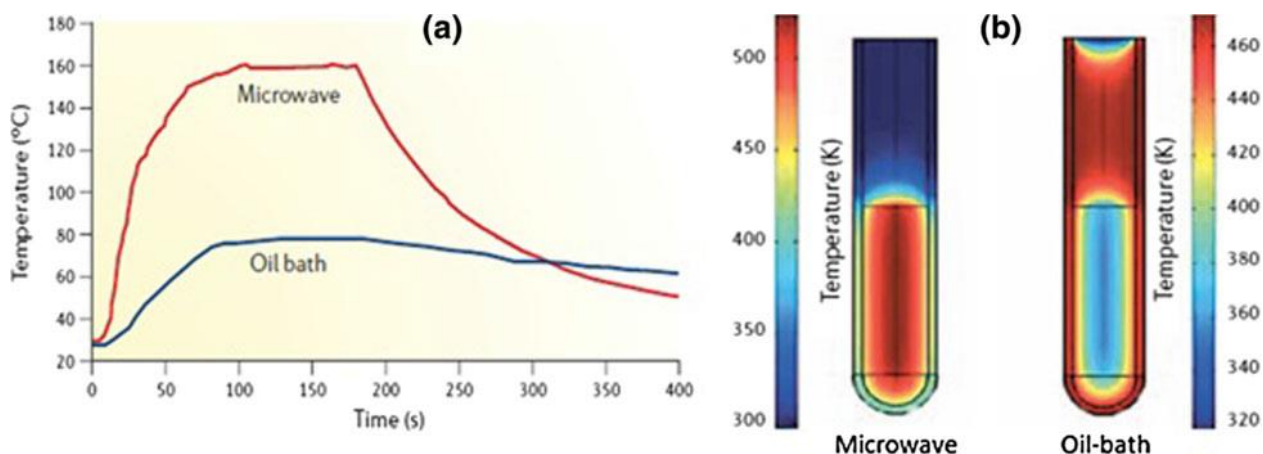
Figure 10: a) Comparison of temperature profiles b) Thermal behaviour in microwave and conventional heating methods [17]

In Figure 10a, a temperature profile for both heating methods is shown. It is clear that the temperature of solvents increases fast and cools down quickly when microwave irradiation is used. This is in contrast to conventional heating where the heating and cooling rates are low [17].

Other important differences between the mechanism of microwave heating and conventional heating are given in Table 1 [23].

Table 1: Comparison of microwave heating and conventional heating [23]

Conventional heating	Microwave heating
The vessel is in physical contact with the heating source which is at a higher temperature (for example, oil bath, steam bath etc.)	There is no need for physical contact of the vessel with the temperature source. The vessel is held in microwave cavities.
The highest achievable temperature (for an open vessel) is limited by the boiling point of the solution or the maximum temperature of the jacket.	The temperature of the mixture can be higher than the boiling point because of the effect of superheating.
All the compounds in the mixture are heated equally with a slight temperature difference from the jacket to the middle of the reactor	Specific components in the mixture can be heated selectively.

The characteristics of microwaves, either singly or in combination, show benefits that are not available with conventional heating or processing methods. This provides alternative possibilities for processing a wide variety of materials but gives also new problems by making some materials very difficult to process. For example, there are materials that possess ionic or metallic conductivity. When the bulk of a material consists out of these materials, it cannot be effectively processed due to the poor penetration of the microwaves. Also, materials containing insulators with low dielectric loss factors are difficult to heat because of their minimal absorption of the microwave energy. Because of these facts, microwave heating of these types of materials is problematic so it is not always possible to apply microwave energy [18].

2.2.5 Microwave system

Over many years, a large investment has been made in the development of microwave processing systems for a wide range of applications. In general, a microwave processing system consists of a microwave source, an applicator to deliver the power to the sample, and a system to control the heating. There are different types of microwave sources such as vacuums tubes and solid state devices, but the magnetron is the most common microwave source in material processing applications. The magnetron will be further discussed in the next chapter. As an applicator, multi-mode (e.g., home ovens) and single-mode are mostly applied. In multi-mode, numerous modes are excited simultaneously, while one resonant mode is excited in single-mode. To control the temperature in microwave heating processes, variation of input power or pulsed sources are generally used [18].

2.2.5.1 Generation of microwaves

There is a great diversity of microwave generators. Currently available microwave generators include klystrons, klystrodes, power grid tubes, magnetrons, traveling wave tubes, crossed-field amplifiers and gyrotrons. The choice of a suitable generator mainly depends on the performance of power and frequency, but also other performance factors like gain, noise, linearity, stability etc. must be considered. Within those choices, the magnetron is one of the most common microwave generators in microwave ovens and in

industrial ovens. This is because the magnetron produces the usual microwave frequencies and it is also preferred economically. Therefore, there is a further focus on the principle of the magnetron [18].

Magnetron

A magnetron is a high power microwave oscillator which converts the potential energy of electrons near the cathode to radio frequent energy. Figure 11 shows a schematic representation of a magnetron [24].
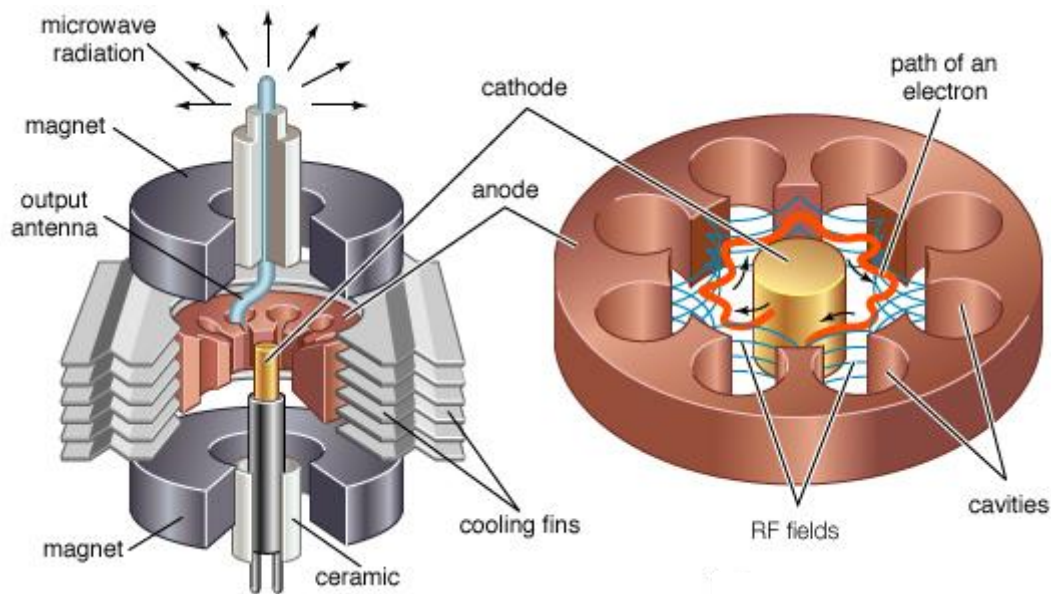
Figure 11: Typical elements of a magnetron [25]

A magnetron is a thermo-ionic diode which exists of an anode and a directly heated oxide-coated cathode. Electrons are emitted by the heated oxide-coated cathode. These emitted electrons are attracted to the anode which consists of narrow cavities, who ensure that the anode oscillates with a specific frequency. Mostly, these cavities possess a 180° phase difference with respect to the adjacent resonant cavity (see also + and – in Figure 12) so the correct frequency is obtained. This 180° phase difference is maintained by connecting the alternate cavities with two thin wire straps, which ensure the correct phase relationship. Then, a strong axial magnetic field induced by the anode deflects the electrons as shown in Figure 12, where the blue lines represent a stable magnetic field and the red lines represent the electrons emitted by the hot cathode [20],[26].
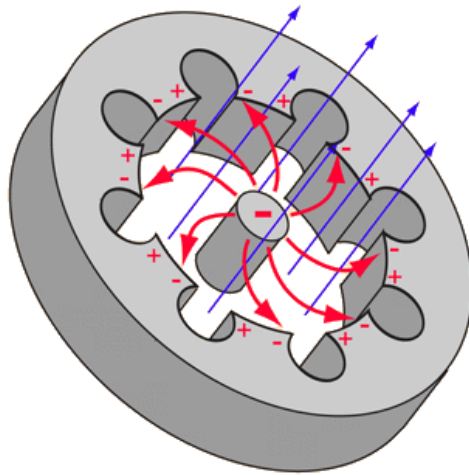
Figure 12: Electrons emitted in a magnetron and deflected by the magnetic field [26]

The electrons are forced into groups by the electromagnetic resonances from the cavity. These groups spin around in the magnetron as can be seen as the red line in figure. During the time that the electrons travel from the cathode to the anode, a large part of their energy is given to the electromagnetic field of the cavities. The path of the electrons is different from the spiral shape because of the interaction with magnetic field of the cavities. In fact, the electrons follow a complex path, in which their speed constantly changes and their movement periodically comes closer and further from the anode. Eventually, the electrons end up with a relatively low speed at the anode and the oscillation is removed from the anode via an antenna to emit the microwave [20],[22],[24],[26].

Solid state generator

The microwave reactor used in this study generates microwaves with a solid state generator. Therefore, the solid state generator is further explained. In contrast to a magnetron generator, a solid state generator creates power in stage using solid-state devices. Herein, each stage consists of a transistor-based amplifier to increase the power of the previous stage [27].
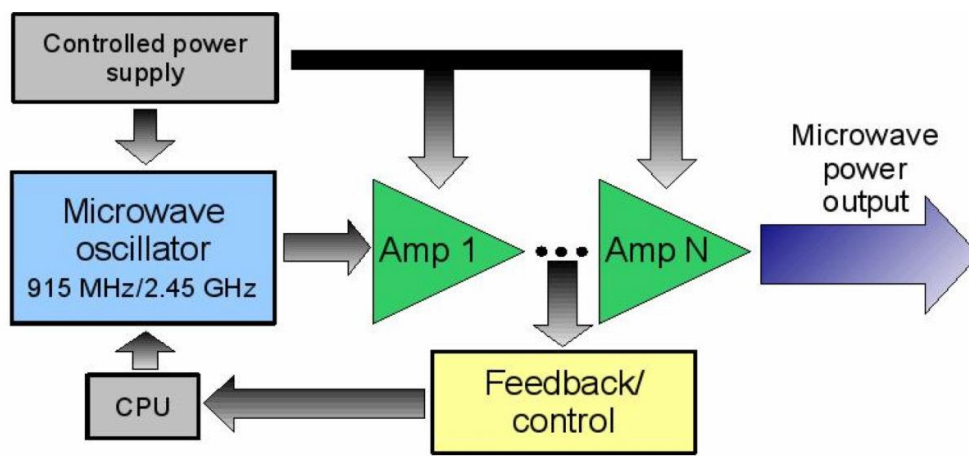
Figure 13: Scheme of a solid-state generator [27]

Some advantages of the solid-state generator are low-power control, more stable output, good robustness and mostly a smaller, lighter unit. Also, when using a solid state generator, the pre-amplified signal can be monitored and controlled much easier than in

magnetron generators. Disadvantages of the solid stage generator include lower output power (< 150 W) and lower efficiency (< 30 %). This lower efficiency causes a lot of heat production, which needs to be dissipated [27].

2.2.5.2 Microwave applicators
There are two types of microwave applicators that can be used in laboratory. A distinction is made between multi-mode microwave reactors and single mode microwave reactor [18],[20].

Multi-mode applicators

Figure 14 shows a diagram of the microwave field distribution in a common multi-mode parallel synthesis reactor. Multimode reactors have larger holes which ensure that the microwaves are more chaotic and arrive at several places in the reactor vessel.
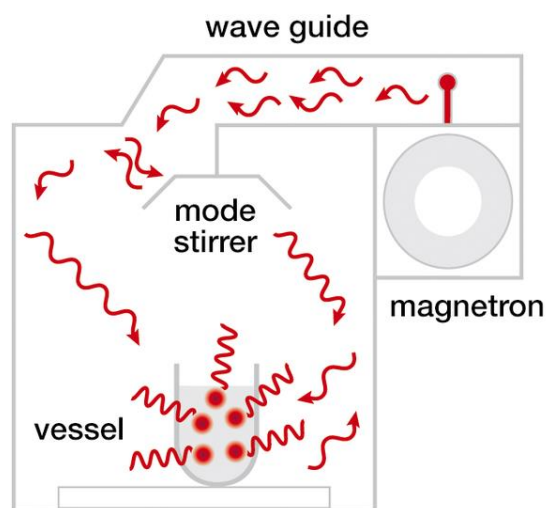
Figure 14: Microwave field distribution in a multi-mode applicator [28]

A multi-mode applicator is comparable with domestic microwave ovens. The main features of such a multi-mode applicator are [18]:

- A good method for bulk processing applications;
- A low sensitivity for product geometry or positioning;
- A moderate to high efficiency;
- An easy adaptability to batch or continuous flow;
- A size which is dependent on the dimensions of the product;
- A good uniformity of the microwaves.

Within a multi-mode applicator, the microwaves are reflected by the walls over a large cavity, so multiple modes of the microwaves interact with the sample. Although the sample is rotated in the cavity and high microwave power is used, the density of the field around the sample is low. This results in poor performance for small-scale reactions [22],[28]. In addition to this disadvantage, the use of multi-mode applicators still have some other limitations [20]:

- The temperature is difficult to measure accurately;
- The power that arrives at the sample is not accurately tuneable;
- As the distribution of the electric field in the cavity results from multiple reflection off the walls, the electric field is heterogeneous.

Mono-mode applicators

The cavities of mono-mode applicators are much smaller and the microwave irradiation is directly focused on the sample as represented in Figure 15 [28].
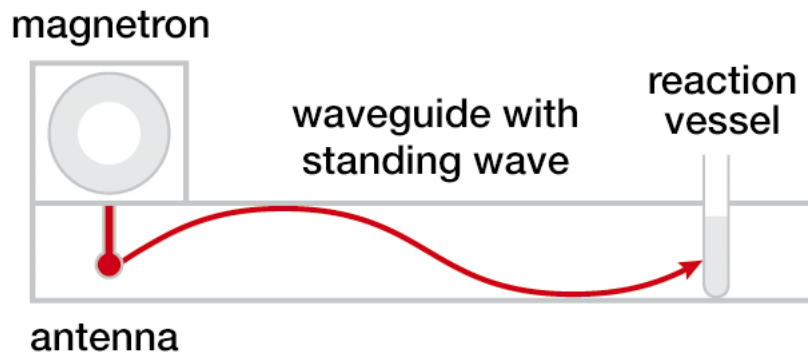
Figure 15: Microwave distribution in a mono-mode applicator [28]

A high microwave field density is obtained due to the focussing of the microwaves. This results in very fast heating rates. Additionally, the mono-mode applicator also has other advantages such as [18],[28]:

- Possibility of high fields;
- Possibility of high efficiency;
- Able to operate in standing or traveling wave configuration so local or uniform heating is possible;
- Able to heat both low-loss and high-loss materials;
- Matching the fields to product geometry;
- Compatibility with continuous flow.

However, the use of single-mode applicators also involves some limitations that must be considered. Single-mode applicators are more product specific and can be very sensitive to changes in products characteristic, geometry and positioning. Therefore, to use a single-mode applicator, it may require automatic controls and feedback to ensure a good performance. So the design of a single-mode applicator can become more expensive [18].

2.3 The Suzuki-Miyaura coupling

2.3.1 Cross coupling reactions

The use of cross-coupling reactions has grown into a very important strategy for forming carbon-carbon bonds. This importance has grown because it provides key steps in the building of a complex molecule from a simple precursor. Cross coupling reactions combine two molecular components with the formation of a new bond. This formation is often catalysed by a transition metal such as Pd and Ni. Many studies have been performed on the improvement of the reaction conditions for cross-coupling, including tests on a wide variety of substrates, functional groups and amounts of catalyst [29],[30],[31].

But this study focusses on the influence of microwave irradiation on a particular cross-coupling reaction. More specific, the most widely exploited cross-coupling reaction protocol developed by Suzuki and Miyaura in 1979. Therefore, the Suzuki-Miyaura coupling is discussed more specifically in the next section [6],[32].

2.3.2 Principle

The Suzuki-Miyaura coupling performed in this study uses a $Pd(OAc)_2$ catalyst and Na_2CO_3 as a base. The overall equation for this reaction is shown in Scheme 2
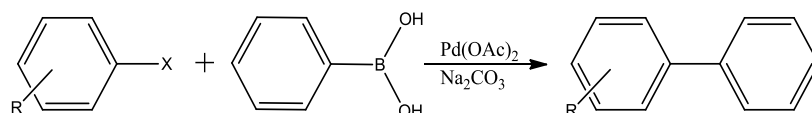
Scheme 2: Suzuki-Miyaura coupling of arylhalides and phenylboronic acid

The Suzuki-Miyaura coupling of organoboron compounds with arylhalides catalysed by palladium is versatile and a widely used reaction, especially for the forming of biaryls. The structure of a biaryl is shown in Figure 16, where R and R' can represent all types of organic groups [6],[7].
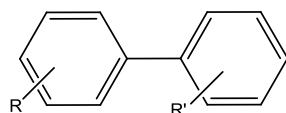
Figure 16: Structure of biaryl

The biaryl structure which is formed in this study possesses no functional groups on the biaryl structure. R and R' represent both a hydrogen-atom in this case, so the formed biaryl structure in this study is called biphenyl (see Figure 17).
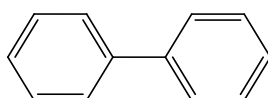
Figure 17: Structure of biphenyl

2.3.3 Reaction Mechanism

The traditional Suzuki-Miyaura coupling of aromatic boron compounds with aromatic halides was first observed in 1981. This reaction uses a phosphine-based palladium catalyst under heterogeneous conditions providing selectively the coupled product. Based on the presence of a Pd catalyst and NaOH as the base, the reaction mechanism of the Suzuki Miyaura coupling is explained [29].

The catalytic cycle is divided in 3 main steps, namely the oxidative addition, the transmetalation and the reductive elimination. Scheme 3 shows an overview of the SM coupling mechanism in perspective of the Pd catalyst [6],[29],[33]. In Scheme 3, following abbreviations suggest a couple of possible structures:

- R = alkyl or H;
- R^1 = aryl, alkenyl or alkyl;
- R^2 = aryl, alkenyl, alkyl or allyl;
- X = Cl, Br, I.
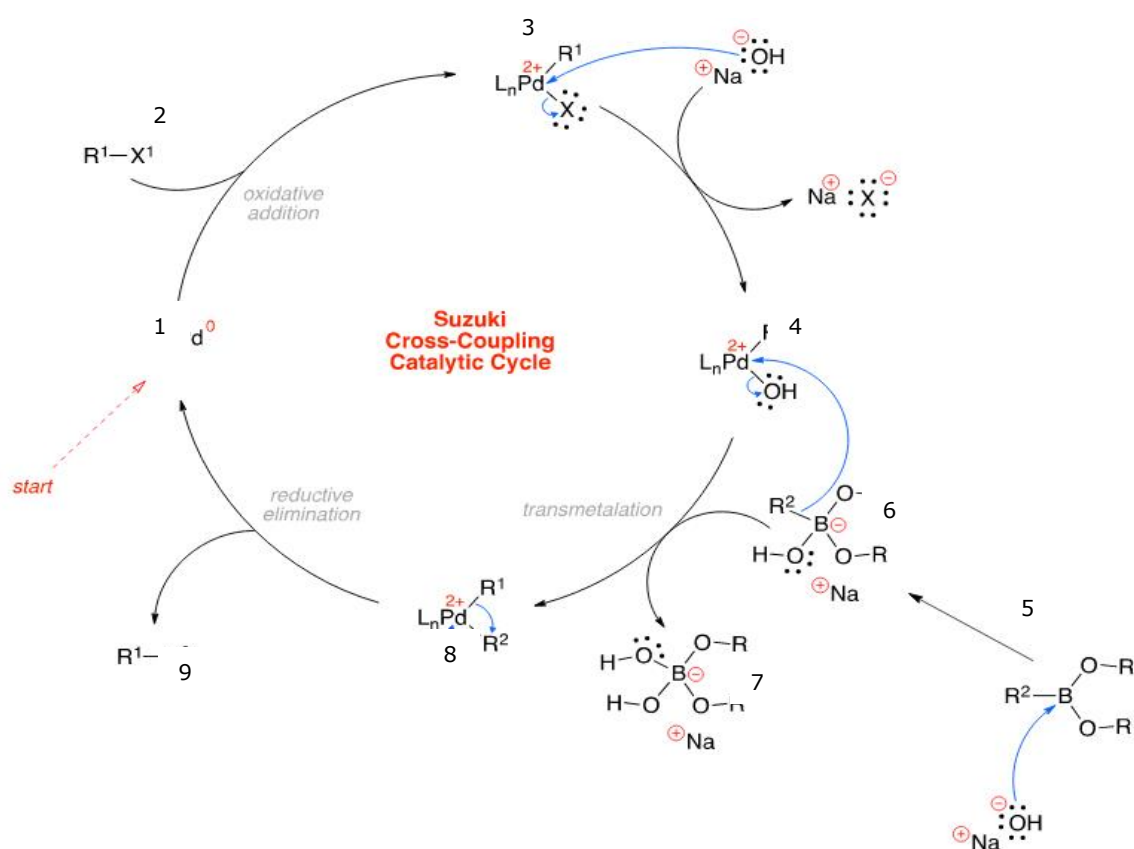
Scheme 3: Suzuki-Miyaura reaction catalytic cycle [34]

The mechanism starts with the oxidative addition of the organohalide (2) to the Pd-catalyst (1). By this oxidative addition a organopalladium(II) complex (3) has formed wherein the oxidation stage of Pd is increased from zero to two and the organohalide is reduced. Thereafter the organopalladium(II) complex (3) reacts with NaOH exchanging its halogen for a hydroxyl group and so creating an intermediate form (4). NaOH also forms a borate (6) from reaction with the organoborane (5) making the R^2-group of the organoborane more nucleophile. This is necessary for the transmetalation step where the R^2-group replaces the hydroxyl group of the intermediate (4). As a result of the transmetalation step, the organopalladium complex (8) is formed. Finally, the reductive elimination of the organopalladium complex forms the biaryl product (9) and restores the original palladium catalyst. So the catalytic cycle is completed and can start over again [34],[35],[36].

30

2.3.3.1 Oxidative addition

The first step of the catalytic cycle is the oxidative addition. The requirements for an oxidative addition is a metal complex with empty coordinated sites and a substrate. In this case the metal complex is the palladium and the substrate is the organohalide. The oxidative addition can proceed via different pathways such as a concerted pathway, a SN_2-type pathway, an ionic pathway or a radical pathway [37],[38].

In order to know which pathway is followed, a closer look at the organohalide is necessary. In this study, iodobenzene is used as the organohalide. The carbon atom in the C-X bond of iodobenzene is sp^2-hybridized. Oxidative additions of sp^2-hybridized C-X bonds prefer the concerted mechanism which occurs in one step. Two open coordination sites of Pd interact with the organohalide to form an intermediate. Due to the interaction, the palladium oxidises by two electrons. This is also shown in Scheme 4 [38],[39],[40].
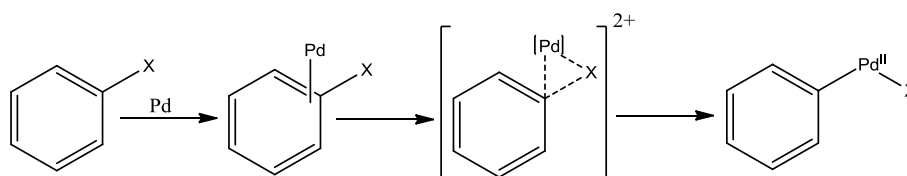
Scheme 4: Concerted oxidative oxidation of arylhalide with palladium

From the point of view of the palladium catalyst, the oxidation is associated with the generation of two ligands. In this case, the two ligands are the aryl compound and the halogen group. On this way, the organopalladium(II) complex is formed. However, the resulting ligands in an oxidative addition are standing in the cis-formation (see Scheme 5). Subsequently, the organopalladium(II) complex isomerizes to the trans-formation because this is a more stable formation [36],[37].
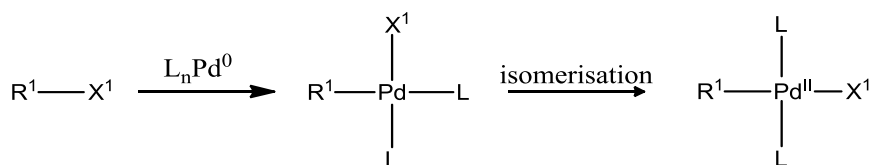
Scheme 5: Oxidative addition of the organohalide to the Pd-catalyst

The reactivity of this step depends on the leaving group of the organohalide. The tendency of a group to act as a leaving group is called nucleofugacity. In case of organohalides, the iodide ion possesses the largest nucleofugacity, followed by Br^- >> Cl^- > F^-. As iodobenzene is used in this study, the halide group I^- is easily split off, which is favorable for the reaction rate, knowing that the oxidative addition is often the rate-determining step. This also induces that the oxidative addition in this study probably is not the rate-determining step because of the iodo-group [36],[41],[42].

2.3.3.2 Transmetalation

As the oxidative addition and the reductive elimination are well understood, less is known about the transmetalation step. According to Lenox and Lloyd-Jones [43], the transmetalation can proceed via two different pathways. By these two different pathways the role of the base is crucial for the distinction between the different mechanisms [33].

In the first pathway, the base reacts with the boronic acid to form a four-coordinated borate. This tetrahedral borate is more nucleophilic making it able to associate with the organopalladium(II) complex formed in the oxidative addition. This first pathway is called the boronate pathway and is shown as pathway A in Scheme 6. In the second pathway, the base reacts via a nucleophilic attack with the organopalladium(II) complex to a more

reactive alkoxo-palladium complex. This pathway is called the oxo-palladium pathway and is shown as pathway B in Scheme 6 [6],[33],[36],[43].
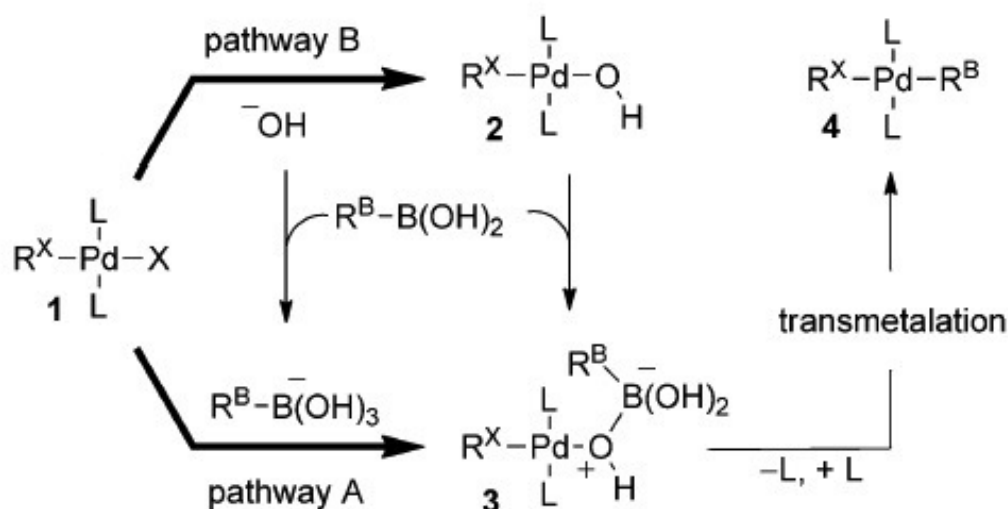
Scheme 6: Two possible pathways of transmetalation in Suzuki-Miyaura coupling [33]

To the present day, there is still no definitive evidence of the correct pathway in the transmetalation. Several studies of Amatore and Jutand, Hartwig, and Schmidt led to the conclusion that the transmetalation occurs between the boronic acid and hydroxo-palladium(II) complex (pathway B). However, this only applies with some certainty to the Suzuki-Miyaura reaction of aryl boronic acids. There are also data reported indicating that transmetalation could occur between the palladiumhalide and the boronate (pathway A). So pathway A should not be ruled out [6],[33],[44].

After the pathways, in both cases a common key intermediate (see **3** in Scheme 6) is formed, which unfortunately remains elusive to this date. This intermediate undergoes a transmetalation where the ligands switch places with each other to give the new palladium(II)complex (see **4** in Scheme 6). This mechanism is also shown in Scheme 7 [33],[45].
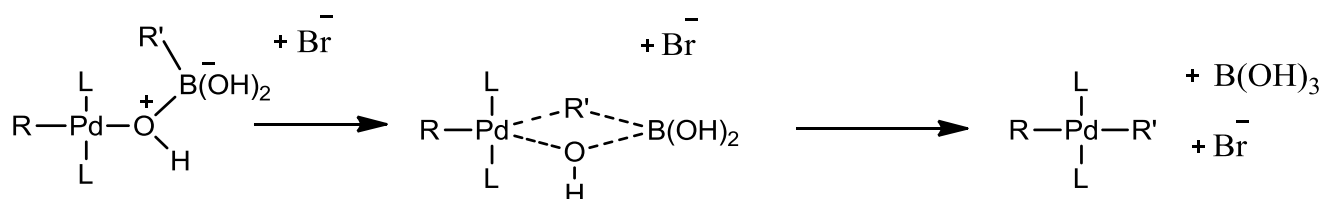
Scheme 7: Intermediate form transmetalates to the organo palladium(II)complex [33]

2.3.3.3 Reductive elimination

The reductive elimination mechanism is in fact the opposite of the oxidative addition mechanism [38]. The palladium(II) complex eliminates the biaryl product and regenerates the palladium(0) catalyst.
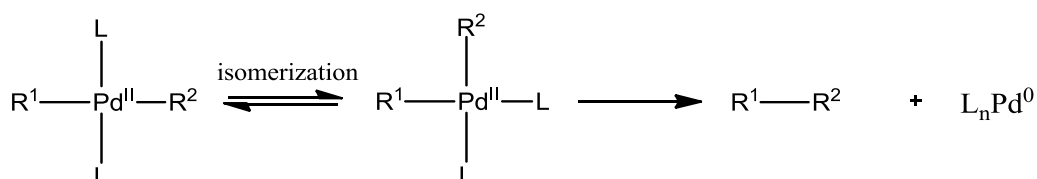
Scheme 8: Reductive elimination

32

Before the reductive elimination can occur, the palladium(II) complex needs to isomerate from trans to the cis complex. Once the cis formation is achieved, palladium(II) is reduced by two electrons. This is accompanied by the loss of the two ligands, which in this case are the benzene rings. On this manner the biphenyl product is formed and the palladium catalyst is regenerated [45],[46].

2.3.4 Variations on the Suzuki-Miyaura coupling

To focus on the use of microwave irradiation on the SM coupling, a model reaction has to be chosen. So the optimization of the reaction circumstances and reagents is done based on literature study. In this chapter, different possibilities of reagents, solvents, bases etc. are explained. Also the amounts of reagents, catalyst loads, amounts of base and reaction circumstances are examined based on the research studies of Liu et al. [9] and Arvela et al. [7].
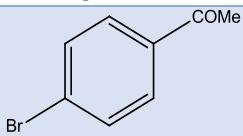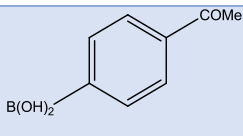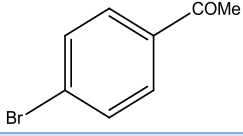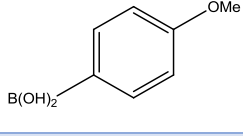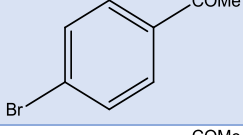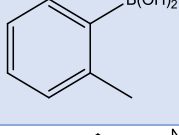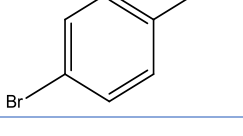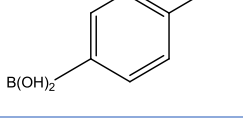
2.3.4.1 Boron reagents

The Suzuki-Miyaura coupling uses organoboron compounds under palladium catalysis. This organoboron is a non-metallic molecule so the bond between carbon and boron is almost a completely covalent bond. This covalent carbon-boron bond ensures that it is too inert to protonate in the presence of water and acids. But in the presence of bases, the reactivity of the organo-boron compound can be greatly improved. Other facts for the use of organo-boron compounds include [6],[32]:

- A good stability of organoboronic acids to water, air and heat;
- A wide variety of functional groups are possible on organoboron compounds;
- A low toxicity.

The boron reagent is the nucleophilic component in the SM-coupling. Influences on the nucleophilicity of the boron compound have, therefore, an influence on the reactivity. The more nucleophilic boron reagents will thus result in higher yields. Factors such as the positive inductive effect and positive mesomeric effect ensure that the electron pair element (Boron) becomes more negative and so more nucleophilic [41],[43]. Different kinds of boron reagents have been tested in several studies. Here, the resulting yields with these boron reagents are shown in table 2 [7].

Table 2: Suzuki-type coupling of 4-bromoacetophenone with different kinds of boronic acids

entry	arylhalide	Boronic acid	Yield (%)
1			94
2			91
3			99
4			63

The reactions in Table 2 are carried out on 1 mmole scale in water using sodium carbonate as a base and TBAB as an additive. Microwave irradiation of 150 W is used, where the temperature ramped from room temperature to 150°C and held for 5 min [7].

The results shown in Table 2 show that the reaction proceeds better when the functional group is small and performs an electron withdrawing effect. This can be concluded from the product yield obtained with (4-acetamidophenyl) boronic acid as this functional group performs a strong electron-donating effect on the benzene ring. Here, the reactivity of the boronic acid depends on the electron density of the benzene ring. When the benzene ring is electron-poor, it benefits the carbon-boron bond as this bond will be more polarised resulting in a better reactivity for the transmetalation.

However, since phenylboronic acid is used as the boron component in the most relevant studies for this research, the Suzuki-Miyaura coupling in this study is performed with phenylboronic acid.

2.3.4.2 Aryl halides

In chapter 2.3.3.1 it is explained that among other things, the reactivity of the reaction depends on the leaving group of the organohalide. Bromides or iodides are the most suitable substrates for the SM-coupling, since the nucleofugacity of chlorides is lower and thus, chlorides are a worse leaving group resulting in a significant slower reaction rate. Functional groups with an electron-withdrawing effect also have a positive effect on the reactivity of the aryl halide compound. By these aryl halide compounds, a wide range of functional groups are possible and a number of these have been tested in the study of Liu et al. [9],[35]. Table 3 shows some of these arylhalides in the Suzuki-Miyaura reaction with phenylboronic acid. The reaction which is carried out is shown in Scheme 9 [9].
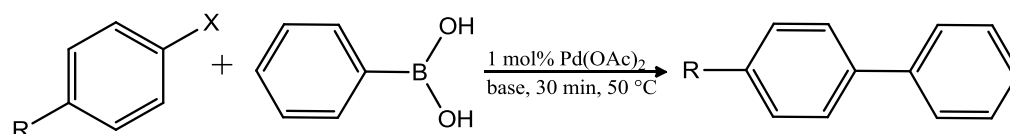
Scheme 9: SM-reaction of various arylhalides with phenylboronic acid

Table 3: SM-reaction of various aryl halides [9]

entry	X	R	Time (h)	Yield (%)	Entry	X	R	Time (h)	Yield (%)
1	Br	4-OMe	0.5	95	10	Br	4-NO$_2$	0.25	96
2	Br	3-OH	0.5	98	11	I	4-OMe	0.5	97
3	Br	2-NH$_2$	0.5	94	12	I	H	0.4	99
4	Br	4-NH$_2$	0.5	98	13	I	4-NO$_2$	0.25	99
5	Br	2-Me	0.5	95	14	Cl	4-NO$_2$	3	98[a]
6	Br	4-Me	0.5	97	15	Cl	4-COCH$_3$	28	52[a]
7	Br	H	0.3	97	16	Cl	4-Me	28	22[a]
8	Br	4-COCH$_3$	0.3	98	17	Cl	4-Me	0.5	4[a]
9	Br	4-CN	0.3	98					

[a]The reaction temperature was 120 °C.

It is clear that the SM coupling is tolerant to a wide range of functional groups. Even with electron-deficient aryl bromides, good yields are obtained. Entry 14 even gives good product yields with chloride as the leaving group. This is because of the presence of the

nitro-group which is an electron-withdrawing group. By this electron-withdrawing effect, the benzene ring becomes more positive because the electrons are extracted from the ring. This electron-poor benzene ring is more advantageous for the oxidative addition with the palladium catalyst resulting in a better reaction and thus, a better product yield.

2.3.4.3 Phase-transfer catalyst
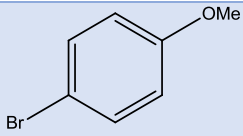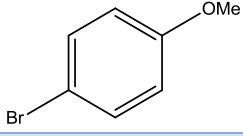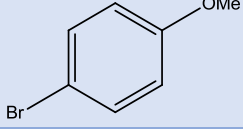
In case of heterogeneous systems, two or more insolvable phases are created, with no contact and thus no reaction between both reactants. To overcome this barrier, a phase transfer catalyst (PTC) is added to the system. The PTC facilitates the migration of a reagent from one phase to another where the reaction occurs. For example, ionic reactants are soluble in a polar or aqueous phase but insoluble in an organic phase unless a PTC is added [41],[47].

Mostly quaternary ammonium salts are used for anions and crown ethers for cations. In this study tetrabutylammoniumbromide or TBAB is used as the quaternary ammonium salt [7],[47].

Arvela et al. report that when the reaction mixture is not stirred, two phases are distinguished. The lower phase is the aqueous layer containing the base and the upper organic layer contains the organic substrates. According to Arvela et al. it is believed that the TBAB occurs in both phases and that the reaction takes place at the interface between the aqueous and organic phase. Here, it is thought that the phase-transfer catalyst has two roles. The first role is to facilitate the solvation of the organic substrates in the solvent. The second role is to form a boronate complex with the boronic acid. On this manner, the boronic acid gets activated and enhances the rate of the coupling reaction [7].

Alternative phase-transfer agents are also possible. For example, mixtures of water and ethanol give comparable yields to a water-TBAB mixture. Arvela et al examined some different types of water-PTC systems. The obtained yields with these systems are shown in Table 4 [7].

Table 4: Suzuki coupling reaction of 1-bromo-4-methoxybenzene with trans-2-phenylvinylboronic acid in various reaction mixtures [7]

entry	arylhalide	Reaction medium	Yield (%)
1	OMe — Br	H_2O/TBAB	81
2	OMe — Br	H_2O/EtOH	26
3	OMe — Br	H_2O/EtOH/TBAB	82

The reactions shown in Table 4 are performed on 1 mmole scale with a $Pd(OAc)_2$-catalyst. Microwave irradiation of 150W was used with a temperature ramping from room temperature to 150°C and held for 5 min [7]. From the results shown in Table 4, it is concluded that in the presence of TBAB as the phase-transfer catalyst significant higher yields are obtained. Therefore, the reaction in this study is performed in water as the solvent and with the presence of a phase transfer catalyst such as TBAB.

Also, Liu et al investigated the use of PEGs[1] as PTC in water to perform the Suzuki-Miyaura reaction. They report that the application of a $Pd(OAc)_2$-H_2O-PEG system is an efficient catalytic medium for the SM-reaction of aryl iodides and bromides. This system for the coupling of aryliodides is even more efficient than the $Pd(OAc)_2$-H_2O-TBAB system. This higher efficiency would be due to the properties of PEG as co-solvent and PTC [9].

Since the $Pd(OAc)_2$-H_2O-PEG system is an effective medium for the SM reaction, PEG is also used as PTC in this study. The amount and the choice of PEG is based on the study of Liu et al. They investigated the effect of the chain length of PEG and the amount on the SM-reaction. Within PEG with a molecular weight between 600, 1000, 2000, 4000 and 6000, the best results were obtained by PEG having a large chain length. Here, PEG 2000, PEG 4000 and PEG 6000 showed the best results [9].

The effect of the amount of PEG 2000 was also investigated. These tests were executed with 4-bromotoluene and phenylboronic acid on millimolar scale. Figure 18 shows the results of the amount of PEG 2000 for the SM-reaction at 50°C for 30 minutes [9].
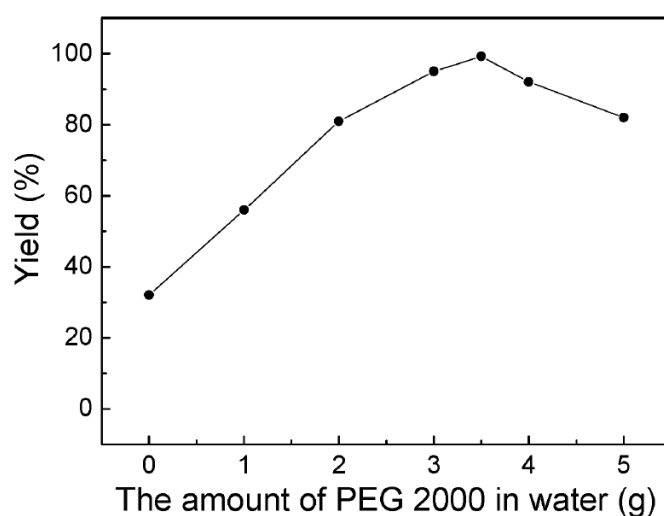
Figure 18: Effect of PEG 2000 on the SM reaction in water [9]

Beside the fact that PEG 2000 functions as a phase-transfer catalyst, PEG 2000 also serves as a co-solvent. So when adding bigger amounts of PEG 2000, the whole reaction system is more diluted and better dissolved which leads to a better contact of the reagents, catalyst and base. However, at 3.5 g of PEG 2000, all the components are already dissolved completely, so adding more PEG 2000 only leads to more dilution of the reactor system.

2.3.4.4 Catalyst
There are a lot of catalytic systems for the Suzuki-Miyaura reaction. Mainly, the SM-reaction is carried out in the presence of a Pd-type catalyst, but also other catalysts like nickel and even iron catalysts are possible. Since the Pd-type catalysts are the most common catalysts for the SM-reaction, these will be further discussed [48],[49].

There are two ways to use palladium-type catalysts for the reaction. The first one is where a preformed catalyst such as $Pd(PPh_3)_4$ or $Pd(PBu_3)_2$ is added to the system. The second is where the catalyst can be formed in situ by using a palladium source such as $Pd_2(dba)_3$ or $Pd(OAc)_2$ with the necessary ligand. The choice of the ligand also has an influence on the reaction. When the ligand has a strong σ-effect (for example

---

[1] Polyethylene glycol

trialkylphosphines), the electron density around the metal increases which accelerates the oxidative addition [49].

In order to know the amount of the catalyst, the effect of the palladium concentration was investigated in the study of Arvela et al. The reactions were run on 1 mmole scale and were heated with microwaves of 150 W. The temperature raised from room temperature to 150 °C and was held for 5 min. The results are shown in Table 5 [7].

Table 5: Effect of Palladium concentration on the coupling of 4-bromoacetophenone and phenylboronic acid [7]

entry	Pd concentration	Yield (%)
1	50 ppb	18
2	100 ppb	48
3	1 ppm	93
4	2.5 ppm	94

Table 5 shows that good yields are obtained from a palladium concentration of 1 ppm and higher. At lower catalyst concentrations, the product yield significantly lowers which means that the palladium catalyst is crucial in the Suzuki-Miyaura reaction. At higher catalyst concentration, no additional benefits are detected so in this study, the concentration of the $Pd(OAc)_2$ catalyst is kept at 1 mole%.

2.3.4.5 Base

The Suzuki-Miyaura coupling takes place in the presence of a base. For the explanation of the role of the base, a reference is made to chapter 2.3.3.2. The choice of the base is very important for the SM reaction. Stronger bases such as NaOH, NaOMe and TlOH perform well in THF/H_2O systems, while weak bases such as K_2CO_3 and K_3PO_4 perform better in DMF solvents [50].

Liu et al. investigated different kinds of bases for the $Pd(OAc)_2-H_2O-PEG$ system. The performed Suzuki-Miyaura reaction is shown in Scheme 10 and the results are shown in Table 6 [9].
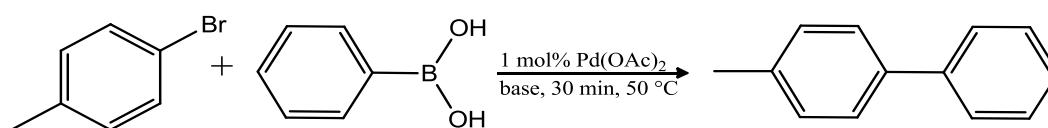
Scheme 10: SM-coupling of bromotoluene with phenylboronic acid with various bases

Table 6: Comparison of different kinds of bases on the SM-coupling in $Pd(OAc)_2-H_2O-PEG$ [9]

entry	base	Reaction medium	Yield (%)
1	Na_2CO_3	H_2O/PEG	97
2	K_2CO_3	H_2O/PEG	95
3	K_3PO_4	H_2O/PEG	96
4	KOH	H_2O/PEG	70
5	KF	H_2O/PEG	86
6	NaOAc	H_2O/PEG	47
7	Et_3N	H_2O/PEG	76

Na_2CO_3, K_2CO_3 and K_3PO_4 are demonstrated as suitable bases for the coupling because the highest yields are delivered with these bases. Therefore, Na_2CO_3 is chosen as the suitable base in this research.

2.3.4.6 Solvent

The key role of the solvent is to dissolve the base which is necessary for the activation of the boron component. Different solvents were tested in the study of Liu et al. The combination of PEG with a nonpolar solvent resulted in low yields. Also with an aprotic polar solvents, low yields were obtained, but mixtures of PEG 2000 and polar protic solvents give better yields (see Table 7). Therefore, the combination of PEG and H_2O is chosen as the solvent for this study [9].
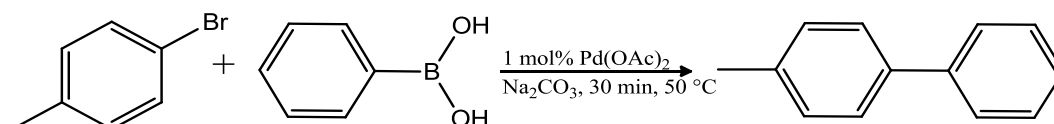
Scheme 11: Reaction conditions of the SM reaction with various media

Table 7: Effects of the reaction medium on the SM-coupling of bromotoluene with phenylboronic acid [9].

entry	Reaction medium	Yield (%)
1	PEG	11
2	PEG/toluene	32
3	PEG/DMF	24
4	PEG/CH_3CN	32
5	PEG/dioxane	15
6	PEG/acetone	21
7	PEG/H_2O	97
8	PEG/methanol	97
9	PEG/ethanol	72
10	PEG/propanol	40
11	PEG/2-propanol	41

3 Methods and materials

3.1 Suzuki-Miyaura reaction

The Suzuki-Miyaura coupling of iodobenzene and phenylboronic acid is carried out nearly the same as described in literature. Two reaction ways will be examined, which differ in the applied phase transfer catalyst as Arvela et al. [9] used TBAB[2] as a phase transfer catalyst while Liu et al [12] used PEG 2000[3]. Both yields are determined and compared to each other.

The products used in this study for carrying out the Suzuki-Miyaura reaction are shown in Table 8, which also shows the product specifications- and information.

Table 8: Product specifications

Substance	Purity (%)	Supplier	CAS number
Phenylboronic acid	95	Sigma Aldrich	98-80-6
Iodobenzene	98	Sigma Aldrich	591-50-4
Pd(OAc)$_2$	98	Sigma Aldrich	3375-31-3
H$_2$O (milli Q)	1	/	/
TBAB	> 98	Sigma Aldrich	1643-19-2
PEG 2000	99	Sigma Aldrich	25322-68-3
Na$_2$CO$_3$	100	VWR	497-19-8

3.1.1 TBAB system

The Suzuki-Miyaura reaction performed in the study of Arvela et al. is carried out using water as a solvent with the addition of TBAB as the phase-transfer catalyst. In their study, the reaction is performed in a glass vessel with a capacity of 10 ml with a sealed septum [7]. The reaction vessel of the batch reactors in this study have a maximum capacity of 100 ml for the EasyMax® 102 and 80 ml for the Miniflow® 200SS. Since the volume level in the reactor needs to be big enough to be stirred, a minimum volume of 40 ml is a requirement. Therefore, the amounts of the components in the study of Arvela et al. have to be scaled-up to a minimum volume of 40 ml. The upscaling is based on the molar quantities.

According to the study of Arvela et al. [7] 1.0 mmole arylhalide, 1.3 mmole arylboronic acid, 3.7 mmole Na$_2$CO$_3$, 1.0 mmole TBAB and 2 ml of water are placed in a 10 ml glass tube. These amounts result in an overall volume of 2.688 ml. To obtain a volume of 40 ml, an upscale of 14.88 is necessary. This upscaling gives following amounts shown in Table 9.

---

[2] Tetra-n-butylammonium bromide
[3] Polyethylene glycol

Table 9: Up-scaled amounts of reagents for the SM reaction with TBAB as PTC

	iodobenzene	phenylboronic acid	water	Pd(Oac)2	Na2CO3	TBAB	total
density (g/ml)	1.823	1.13	1	2.19	2.532	1.148	
MM (g/mole)	204.01	121.93	18.02	224.5	105.99	322.38	
m%	0.98	0.95	1	0.98	0.99	1	
n (mole)	0.015	0.019	1.652	0.000002	0.055	0.015	
m_{pure} (g)	3.036	2.359	29.763	0.0004	5.836	4.798	45.792
m_{total} (g)	3.098	2.483	29.763	0.0005	5.895	4.798	
V (ml)	1.699	2.197	29.763	0,0002	2,328	4,179	40.167
conc (M)	0.370	0.482			1.371	0.370	

The results in Table 9 are used to prepare the reactor solution. The mass quantities are kept the same for each experiment. This applies to both the experiments with the microwave reactor as with the conventional reactor.

3.1.2 PEG system

The amounts for carrying out the reaction with PEG 2000 as the phase-transfer agent are based on the study of Liu et al [9]. In their study, a mixture of 1.0 mmole bromobenzene, 1.5 mmole phenylboronic acid, 2 mmole Na_2CO_3, 1 mole % $Pd(OAc)_2$, 3.5 g PEG and 3.0 g water is prepared. This results in an overall volume of 6.261 ml.

Likewise for the PEG-system, the values of the reagents also need to be up-scaled in order to obtain a total volume of 40 ml. However, the amounts for the PEG 2000 system are not kept the same as the study of Liu et al. In order to compare the PEG 2000 system with the TBAB system, the same amounts as the TBAB system are held. This results in following amounts of the reagents and solvents (see Table 10).

Table 10: Up-scaled amounts of reagents for the SM reaction with PEG 2000 as PTC

	iodobenzene	phenylboronic acid	water	Pd(OAc)2	Na_2CO_3	PEG 2000	total
density (g/ml)	1.823	1.13	1	2.19	2.532	1.21	
MM (g/mole)	204.01	121.93	18.02	224.51	105.99	2000	
m%	0.98	0.95	1	0.98	1	1	
n (mole)	0.015	0.019	1.652	1.99E-06	0.055	0.015	
m_{pure} (g)	3.036	2.359	29.763	0.0004	5.836	29.763	
m_{total} (g)	3.098	2.483	29.763	0.0005	5.895	29.763	
V (ml)	1.699	2.197	29.763	0.0002	2.328	24.598	60.586
conc (M)	0.246	0.319			0.909	0.246	

Also, literature indicates for the PEG method a bigger amount of PEG 2000 compared to TBAB used in the TBAB method. However, this induces one difference. Since PEG 2000 is a much bigger molecule than TBAB, the molecular mass of PEG 2000 is 6.20 times bigger than the molecular mass of TBAB. This means that the required mass of PEG 2000 is 6.20 times more than the required mass of TBAB. The consequence of this is that the volume of the phase transfer catalyst is 24.598 ml for PEG 2000 instead of 4.179 ml for TBAB. So the total volume of the PEG 2000 system is 60.586 ml, while the volume of the TBAB system is 40.167 ml. This results in different concentrations since the volume of the PTC has an influence on the concentration of the reagents.

3.2 Experiments in the batch reactor

3.2.1 Conventional batch reactor

The conventional reactor used in this study is the EasyMax® 102 from Mettler Toledo. This reactor is shown in Figure 19.

Overhead stirrer

Temperature sensor

Reactor vessel

Display
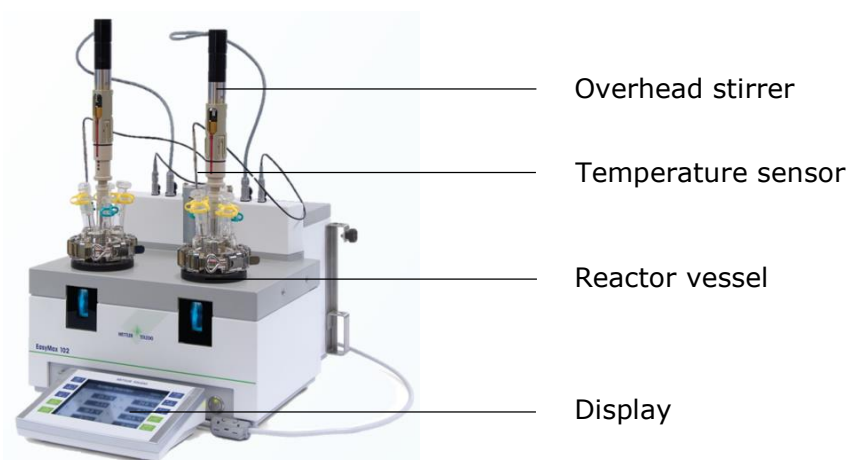
Figure 19: EasyMax® 102 batch reactor from Mettler Toledo [51]

The EasyMax® 102 consists of a reactor vessel with a maximum volume of 100 ml. The reactor can be cooled and heated within a temperature range of -40°C to 180 °C. The temperature is solid state controlled: heating is performed electrically while a Peltier element provides the cooling. The reactor temperature is measured with a Pt100 sensor. In addition, the reactor is equipped with an overhead stirrer which reaches stirring rates between 50 rpm and 1000 rpm. The EasyMax® 102 allows precise control of reaction parameters such as temperature and stirrer rpm. All these measurements and setting are recorded and shown on the display [52].

3.2.1.1 Settings of the conventional batch reactor

The reaction kinetics are investigated in the EasyMax® 102. For comparison with the microwave reactor, all the reaction parameters are held the same. Once the reactor vessel is filled with all the reaction substances, the temperature starts to ramp from room temperature to the desired temperature in 30 minutes. This temperature program is shown in Figure 20 and the EasyMax® controls the temperature to keep it at the desired temperature.
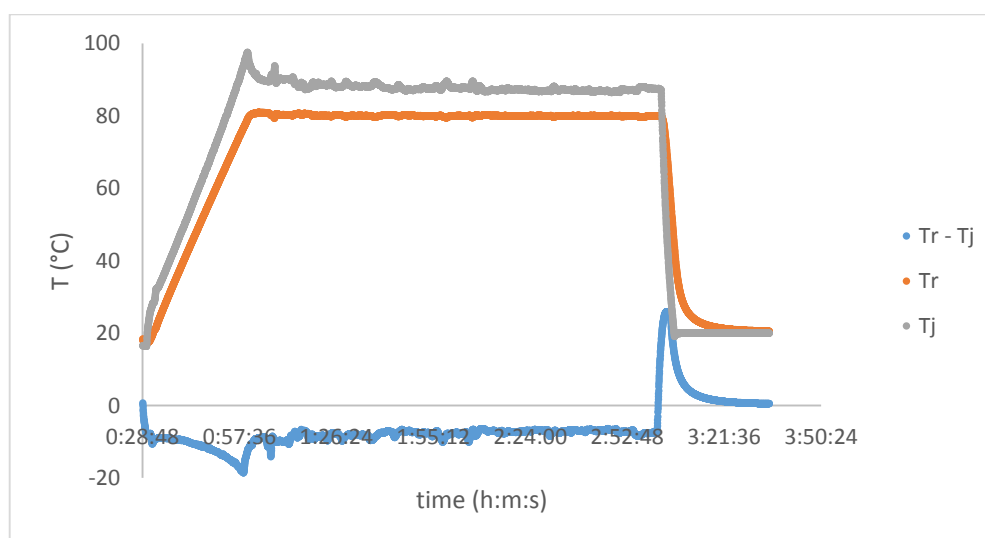
Figure 20: Temperature profile in the EasyMax®

The stirring bar is set to 515 rpm to make sure that a homogeneous solution is obtained. This value is chosen in the beginning of this study and kept the same for each experiment.

3.2.2 Microwave batch reactor

The microwave reactor used in this study, is the Miniflow® 200SS from Sairem. The Miniflow® 200 SS is shown in Figure 21.
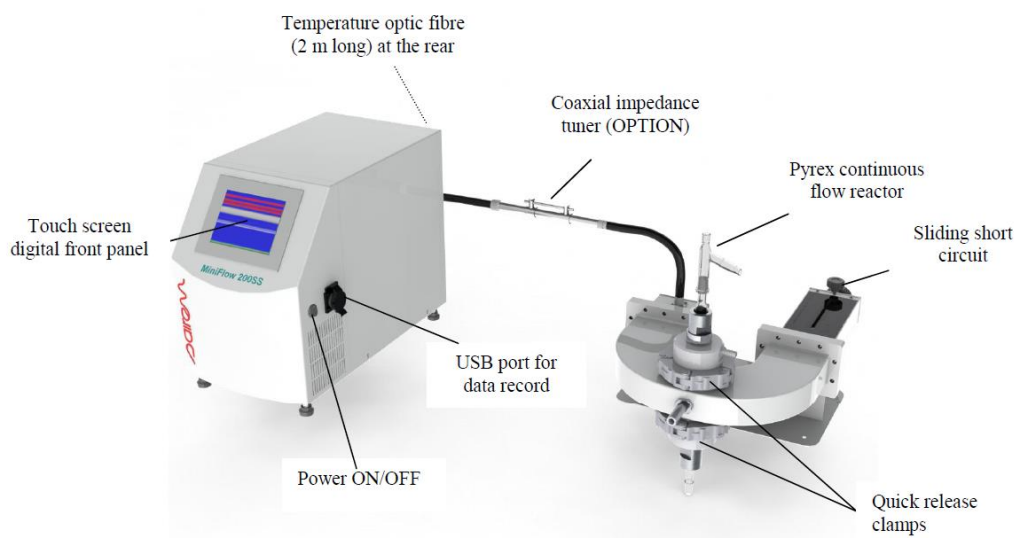
Figure 21: Miniflow® 200SS with continuous flow reactor in TE cavity [53]

As shown in Figure 21, it is possible to perform reactions in continuous flow. This set-up will be further discussed in chapter 3.3. In addition, there are also accessories to make the batch set-up. This set-up is shown in Figure 22.
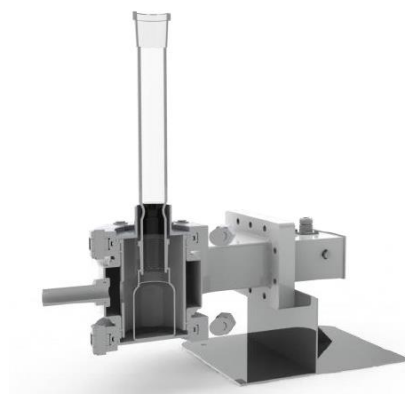
Figure 22: Batch reactor in the Miniflow® 200SS [53]

The frequency of the Miniflow® 200SS is 2450 MHz but can vary between 2430 and 2470 MHz in steps of 0.1 MHz. The power of the reactor can be adjusted from 0 to 200 W with 1 W increment. To create the microwaves, a solid state generator is used (see also 2.2.5.1).

With the software of the Miniflow® 200SS, parameters such as the reaction time, maximum temperature and maximum power are pre-set. The Miniflow® 200SS measures and records automatically the temperature, the transmitted power and the reflected power. The temperature of the reactor solution is measured with a thermometer made out of optical fibers. This is necessary because the thermometer may not absorb any

microwaves as this could increase the temperature resulting in false temperature measurements. The generated microwaves are transported via a coaxial cable to the reactor vessel. This reactor vessel can be equipped with a magnetic stirrer or an overhead mechanical stirrer [53].

The amount of reflected power can be minimalized by a sliding bar. This bar shifts a mirror to set the path length of the microwaves. By doing this, the incoming wave and reflected wave can be put in phase, so the maximum amplitude of the waves arrives at the reactor vessel. Consequently, maximum absorption of the microwave will occur. Note that the mirror is made out of metal since metal reflects microwaves without any absorption [53].

3.2.2.1 Settings of the microwave-assisted batch reactor
Since all the reaction conditions have to be held the same as in the conventional reactor, the same temperature profile is set. The Miniflow® 200SS has two options to control the temperature. The first type is normal or thermal mode and the second type is microwave power:

- MW power: this type sets the reaction time and the power of the Miniflow®. The power of the microwave reactor is kept constant when using this type;
- Normal mode: this type sets the reaction time and the temperature. Now the Miniflow® changes the microwave power to reach the set temperature.

In order to obtain a similar temperature profile as the EasyMax® 102, the temperature needs to be controlled manually. The power is set manually with the MW-power option and controlled by checking the temperature as a function of the time. Once the temperature reaches the desired value, the mode is switched to normal so the temperature is held at the desired value. The temperature profile and the required power of the Miniflow® 200SS is shown in Figure 23.
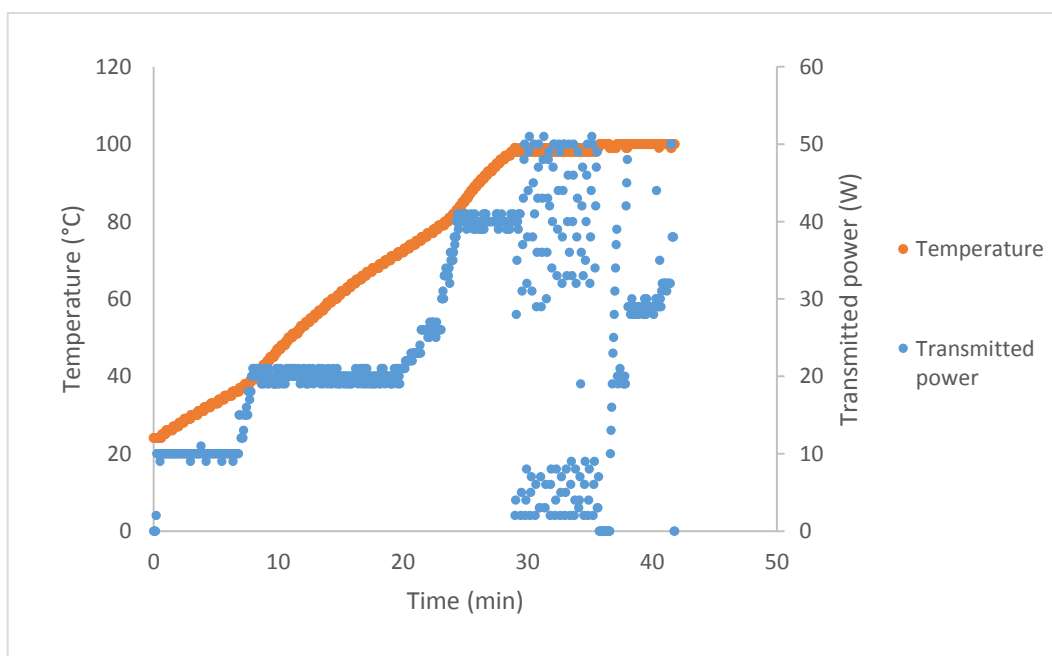
Figure 23: Temperature profile and set power of the Miniflow® 200SS

In Figure 23, the measured temperature forms a linear increasing profile within the first 30 minutes. After 30 minutes, the temperature remains constant at 100 °C. Due to the bigger heat losses at higher temperatures, the set power needs to be higher at higher temperature. From the moment the temperature reaches the desired temperature, which

in this case is equal to 100°C, the mode is switched to normal. In this mode, the Miniflow® 200SS maintains the temperature by switching on and off. This is also reflected in the large variation of the transmitted power.

The Miniflow® 200SS uses a magnetic stirring bar, so the mixing is not identically the same as in the EasyMax® 102. The stirring is one of the few possible variables which needs to be investigated as discussed further in chapter 4.1.7.

3.2.3 Performing the SM-reaction in batch

In order to examine the influence of microwaves on the SM-reaction of iodobenzene and phenylboronic acid, the reaction is performed in the presence of microwaves or conventional heating as energy source. The yields of the product biphenyl are investigated as a function of the time and the reaction kinetics are determined. Based on these data, the influence of microwave irradiation is demonstrated.

To compare the data of the conventional method with the microwave method, it is important that all the reaction conditions are held the same. In that case, all other effects than the microwave heating effect are ruled out. This is done by maintaining the following procedure when performing the reaction.

The amounts of phenylboronic acid, PTC, base, catalyst and solvent are weighed precisely as described in Table 9 and Table 10 (see chapter 3.1.1 and 3.1.2). Note that in the beginning, no iodobenzene is added. Otherwise the reaction already starts from the moment the iodobenzene is added, which results in incorrect values for the conversion to biphenyl. Once all the components with the exception of iodobenzene are added in the reactor vessel, the reaction conditions are applied. So the reactor is stirred and heated to the desired temperature.

When the desired temperature is reached, the iodobenzene is added. Instead of weighing the necessary amount of iodobenzene, a volume of 1.7 ml is added using a graduated pipette. The volume of 1.7 ml corresponds to the needed amount of 3.098 g or 0.015 mole. From the moment iodobenzene is added to the reactor, the reaction starts and the time is recorded. Subsequently, several samples are taken after different reaction times to create a view of biphenyl yields as a function of the time.

3.2.3.1 Sampling

In order to display the reaction kinetics and the biphenyl yields, multiple samples are taken periodically. Since the samples are analysed with UV-Vis spectrometry, it is important that the background of the sample does not interfere with the measurement of biphenyl. That is why an attempt is made to isolate the biphenyl from the reactor solution. Biphenyl is a nonpolar organic substance. This is confirmed by the solubility of biphenyl in water which is only 4.45 mg/l [54]. Biphenyl is isolated using hexane since hexance extracts all the biphenyl and it does not interfere with the spectrum of biphenyl in the UV-Vis spectrometer. Hexane is also used to make further dilutions of the biphenyl samples.

While recording the reaction time, samples of 1 ml are taken from the resulting suspension in the reactor. These sample are added to a prepared volume of 15 ml hexane. By adding the samples to the 15 ml hexane, the sample cools down immediately to room temperature so the reaction of iodobenzene and phenylboronic acid stops directly. Two phases are formed in the solution, where the lower aqueous phase is the reactor solution and the upper phase consists of hexane. Herein, the non-polar substances of the reactor solution are extracted and transferred to the organic hexane phase. These non-polar substances include mainly biphenyl and iodobenzene. Since the

organic phase also contains iodobenzene, a possible interference will need to be considered in the analysis.

For a good preservation of the samples, the organic phase needs to be separated from the aqueous phase because even at room temperature the reaction continues at a very low reaction rate. So as long the organic phase is not separated from the aqueous phase, further reaction could still occur. Therefore, the samples are examined whether further reaction occurs. The results for the stability of the samples is shown in Figure 24.
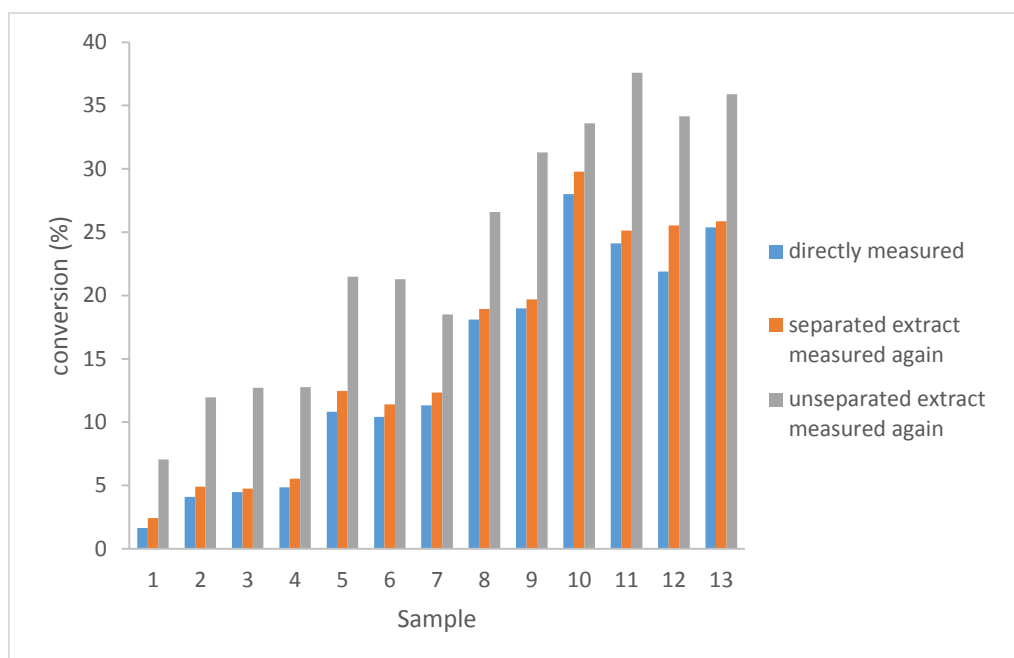
Figure 24: Stability and preservation of the samples

In Figure 24, the "separated extract measured again" represents the samples which are extracted and separated from the aqueous phase. Thereafter, these samples are measured directly (see "directly measured") and measured after five days of storing at room temperature. "Unseparated extract measured again" represents the samples which are not separated from the aqueous phase and also measured after five days of storage.

The samples that are separated and measured after five days, show a conversion that is relative 9.23 % higher than the samples which are measured directly. However, as this deviation is so small, it could be due to the measurement against the blanc. Since a different blanc is used, it affects all the measurements similarly resulting in an overall trend such as observed. So it may be concluded that the samples can be stored for minimal five days after separating the organic phase from the aqueous phase. However, in this study, most samples are measured directly after obtaining them.

The samples that are not separated and stored for five days, show a conversion that is relative 90.76 % higher than the samples which are measured directly. This corresponds to a significant increase of the conversion so it is concluded that further reaction occurs when the aqueous phase and organic phase are not separated. Therefore, it is necessary that the organic phase needs to be separated from the aqueous phase. When this is done, the samples are longer tenable.

3.2.4 Comparison of microwaves to conventional heating on the SM-coupling

To successfully compare microwave heating to conventional heating, all reaction conditions have to be kept the same to ensure that the results only depend on the heating source. Therefore, the stability of the catalyst and the influence of stirring were investigated for both heating systems to exclude possible interferences. The repeatability of the experimental method is also studied.

3.2.4.1 Repeatability of an experiment

To verify whether the results are representative, the repeatability of the experimental method is examined. The reaction performed in the TBAB-water medium at 80 °C in the conventional reactor is repeated and the concentration gradient of biphenyl is followed relative to the reaction time. These concentrations of biphenyl are plotted against the reaction time for both experiments. The concentration gradients of both experiments as a function of the reaction time are shown in Figure 25. Based on these concentration gradients, it is possible to check if the experimental method is robust.
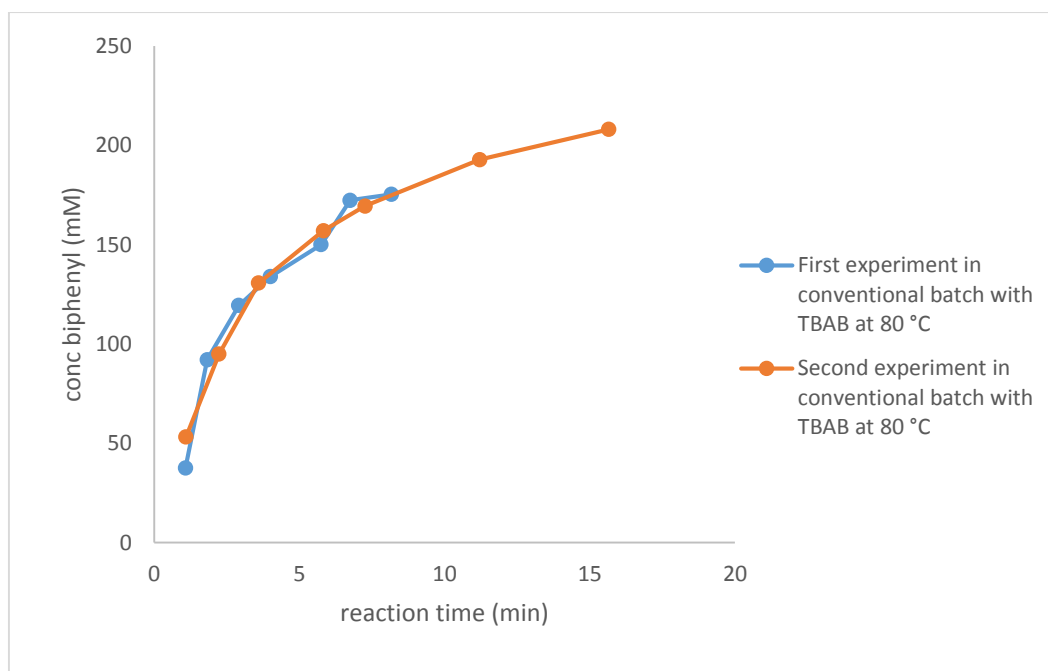
Figure 25: Repeatability of the method of experiment

From the results shown visually in Figure 25, it is clear that the concentration gradients of biphenyl obtained during the reaction look very similar and therefore shows a good repeatability. As a result, it is concluded that the experimental method is correct to obtain representative results.

3.2.4.2 Deactivation of the Pd-catalyst

Catalyst deactivation is a possible phenomenon in which the catalyst loses its activity or its selectivity over the time. This deactivation could lower the reaction rates. The catalyst can be deactivated by chemical, mechanical or thermal manners. These manners include poisoning, fouling, thermal degradation, vapor formation, vapor–solid and/or solid–solid reactions, and attrition/crushing [55].

This part investigates the thermal degradation and attrition of the catalyst since the other ways of catalyst deactivation a more unlikely. Thermal degradation induces the loss

46

of the catalytic surface area, support area and active phase-support reaction due to thermal effects. This could be possible since the reactor solution is heated to elevated temperatures of at least 80 °C. Attrition is the loss of catalytic material due to abrasion, which could occur due to continuously stirring of the solution at 515 rpm. The other types of catalyst deactivation are rather chemical and mechanical (fouling) types which are due to impurities of the catalytic system. These impurities are more unlikely as the reactor solution consists of pure reagents and other pure components [55].

Thermal degradation and attrition of the catalyst are investigated for the reaction conditions that are usually maintained, but with the difference that these conditions are maintained during extreme times. The reason why these longer times are held is to investigate if the reaction still proceeds identically to the reaction performed with the normal conditions. If both reactions still proceed the same, it can be concluded that no catalyst deactivation occurs at the maintained reaction conditions. Also, because of the fact that the reaction parameters are tested in extreme conditions, it is then made sure the parameters will not interfere at normal conditions.

Following steps are performed to test the catalysis deactivation experimentally. The reactor solution (TBAB-H_2O medium) is prepared as normal with the addition of the Pd(OAc)$_2$ catalyst and without iodobezene. Subsequently, the reactor solution is heated to 80 °C in the conventional reactor and stirred at 515 rpm similar to the normal execution of the reaction. After the three hours, iodobenzene is added to the reactor solution to initiate the reaction. From this point on, the concentration gradient of formed biphenyl is followed as a function of the reaction time. The results of the test after three hours of preheating are shown in Figure 26 and compared with the results obtained by normal conditions.
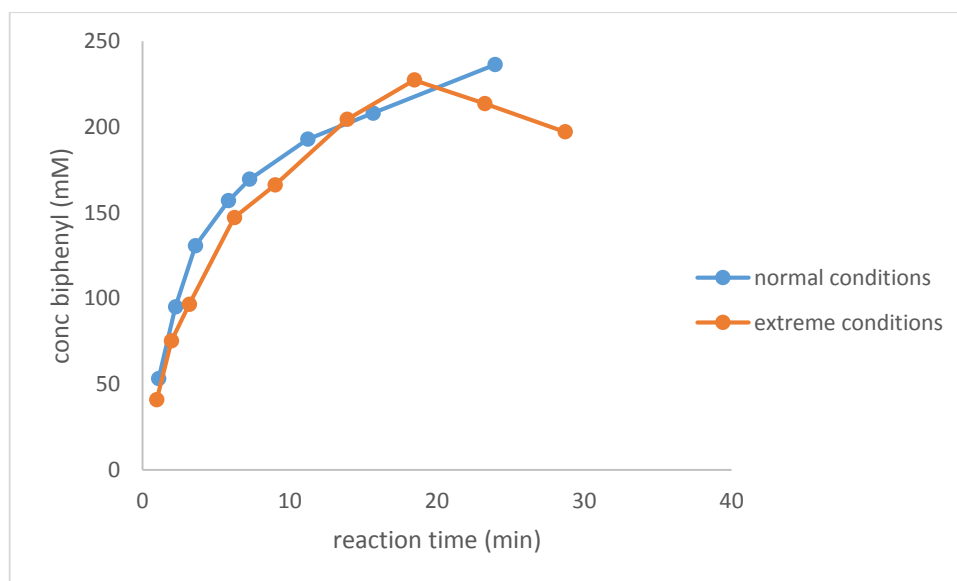
Figure 26: Test on catalyst deactivation in a conventional heating system

No significant differences between the concentration gradients of biphenyl are detected. Therefore, it is concluded that no catalyst deactivation occurs within 3 hours at the maintained reaction conditions of 515 rpm stirring speed and a temperature of 80 °C. The small deviations are due to standard errors made in the experimental and analytic method.

In addition, also a sample is taken after the three hours of stirring and heating. This is still without the addition of iodobenzene so no reaction is possible. As a result, it is expected that no absorption will be detected. The measurement of the sample showed an absorbance of 0.071 which corresponds to a biphenyl concentration -7.43 mM. This value

is unreal given that the concentration cannot be less than zero. However, the value does not differ much from zero mM, so it may be stated that no biphenyl has formed yet.

3.2.4.3 Influence of stirring

One of the main differences between the experiments performed in the conventional reactor and the microwave reactor is the stirring unit. As discussed in chapter 3.2.1 and 3.2.2, the stirring in the EasyMax® happens with an overhead stirrer controlled by the EasyMax®, while the stirring in the Miniflow® happens with a magnetic stirrer. To know whether the stirring unit has an influence on the reaction rate, an overhead stirring unit is placed inside the microwave batch reactor as shown in Figure 27. Then, the product yields obtained with the overhead stirring unit are compared to the yields obtained with the magnetic stirring unit. In order to obtain the yields, the SM-reaction with the TBAB-water medium is performed at 60 °C in the microwave reactor. The results for the different stirring set-ups are shown in Figure 28.

Figure 27: Overhead stirring set-up in the microwave reactor
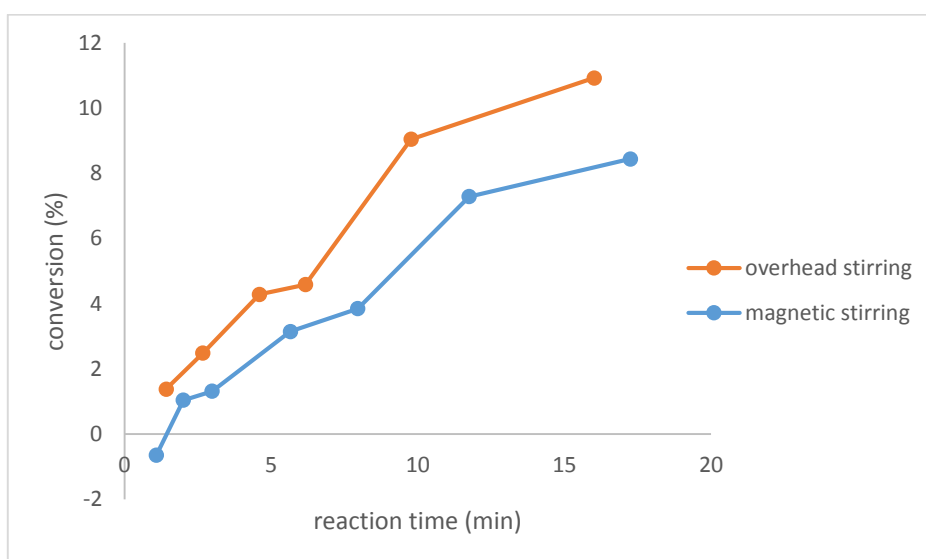
Figure 28: Influence of the stirring set-up in the microwave batch reactor

The stirring speed of the overhead stirrer is 810 rpm. The exact stirring speed of the magnetic stirrer is not known, but it is always made sure that the stirring of the solution was visually detected. In Figure 28, it is graphically shown that the yields obtained with the overhead stirrer are in general a bit higher than the yields obtained with the magnetic stirrer. Namely, the conversions obtained with overhead stirring are relative 42.86 % higher than the conversions obtained with magnetic stirring. This is a big deviation, although, this deviation is mainly due to the low product yields so that a deviation of only 1 % already can provide a relative deviation of 40 %. However, as the average deviation is only 1.4 %, it is decided that the stirring method has no significant influence on the product yield. As a result, the magnetic stirrer is further used by the experiments performed in the microwave reactor because the magnetic stirrer is more practically.

3.3 Continuous flow reactor

In order to test the influence of a continuous system with microwaves as energy source, a microwave-assisted flow set-up is built as represented in Figure 29.
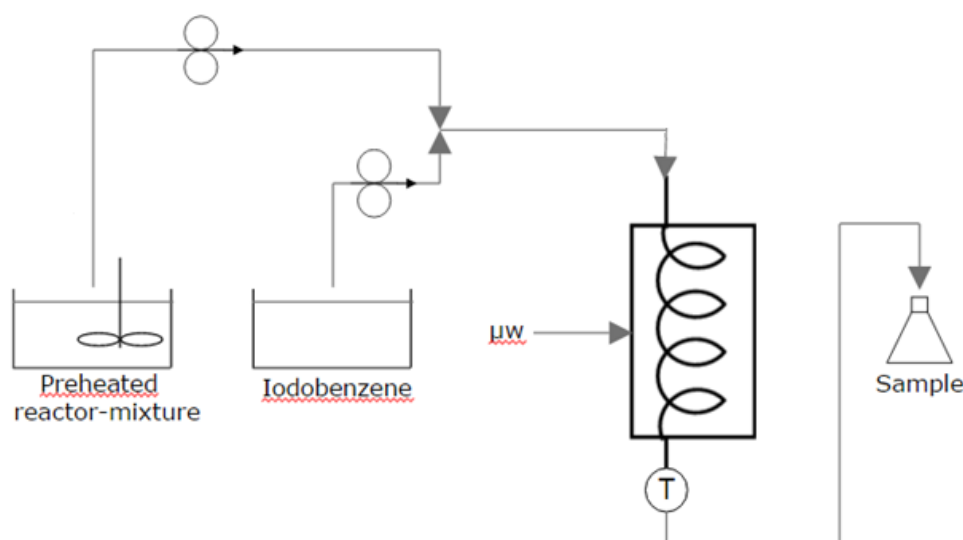
Figure 29: Schematic representation of the continuous flow set-up

In order to investigate the influence of microwaves on the continuous system, the reagents can only be mixed just before the reactor. Otherwise, the reagents could already react before the reactor, which would give incorrect results. Therefore, the reagents are kept in different beakers and pumped separately. Just before the reactor inlet, a T-piece is set as shown in following Figure 30 to mix the reagents.
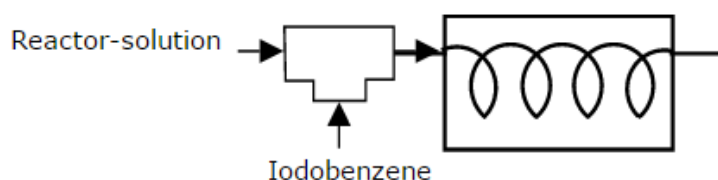
Figure 30: Positioning of the T-piece before the reactor inlet

Based on the schematic representations shown in Figure 29 and Figure 30, the microwave-assisted flow set-up is built. This set-up is shown in Figure 31.

Figure 31: Microwave-assisted flow set-up

The reactor solution (1) contains all the reagents, catalysts and solvents except iodobenzene, with the exact amounts and composition given in chapter 3.1. The other flow contains pure iodobenzene (2), which is a fluid at room temperature. Since phenylboronic acid is more diluted than iodobenzene, a much bigger flowrate of the reactor solution is necessary to keep the molar ratio the same as in the batch experiments. That is why the positioning of the T-piece (3) is executed as shown above in Figure 30. The larger flow of the reactor-solution goes straight in to the reactor inlet. Perpendicular on this flow, the much lower flowrate of iodobenzene is added and is dragged by the reactor-solution. When the flows are positioned differently, the larger flow of the reactor-solution pushes back the iodobenzene flow, so that no iodobenzene is added to the reactor inlet.

To pump the reactor-solution in the correct concentration, it has to be completely dissolved. Phenylboronic acid is soluble in most polar organic solvents and is poorly soluble in hexanes and carbon tetrachloride, and the solubility in water is only 25 g/l. Therefore, the reactor-solution needs to be heated to at least 52 °C. At this temperature all the components are dissolved. In order to compensate heat losses in the tubing, the reactor-solution is heated to 80 °C with the hot plate (4) to make sure all the components stay dissolved before reaching the reactor inlet. After the reactor inlet the microwaves transmitted to the reactor vessel (5) keep the solution at sufficient temperature. The calculations for the heat losses in the tubing will be further explained in chapter 3.3.1.3.

The tubing used for the continuous flow system exists of Polytetrafluoroethylene (PTFE), also known as Teflon. It is very non-reactive, because of the strength of carbon–fluorine bonds, and therefore suitable as tubing for reactive and corrosive chemicals. The main reason for using Teflon tubing, is its low dielectric constant ($\varepsilon = 2.1$). The fact that PTFE has excellent dielectric properties makes it very suitable to use it in the presence of microwave irradiation. The low dielectric constant also ensures that this type of tubing does not absorb any microwave energy so that no energy losses will occur due to the tubing.

After the reactor outlet, a thermocouple (6) is placed to record the temperature. Again with the calculations of the heat losses in chapter 3.3.1.3, it is possible to calculate the temperature of the solution in the reactor when the flow and length of the tubing is known.

As shown in Figure 31, peristaltic pumps (7), (8) are used to regulate the flowrates. Peristaltic pumps are very simple as they do not need any valves, seals or glands. It only needs a compressible tube which is squeezed between a roller and a track on an arc of a circle. By squeezing the compressible tube, a seal at the point of contact is created. As the roller keeps rotating, the seal moves forwards. When the roller has passed the tube, the tube returns to its original state creating a vacuum which pulls the fluid in the inlet. When the first roller just passes the compressible tube, the next roller compresses the tube at the beginning. On this manner, the fluid is isolated between the seals and gets pushed forward by the rollers [56].

Peristaltic pumps have the advantages that no backflow and siphoning occur. Also the pump effectively seals the tube when it is inactive. These pumps are suitable for a lot of fluids, including viscous, shear-sensitive and fluids containing suspended solids. In addition, they are also suitable for metering, dosing and dispensing [56]. In fact, the dosing is better with peristaltic pumps than with syringe pumps. Syringe pumps were also tested to pump the reagents, but failed to realize a precise dosage.

3.3.1 Characterisation of the continuous flow
Before carrying out the reaction in continuous flow, the flow set-up has to be characterised. This includes calibration of the pumps, calibration of the flow set up, characterisation of the heat losses, solubility of the reactor solution and the settings of the reactors.

3.3.1.1 Calibration of the pumps
In the flow set-up, two pumps are used. The first pump is the Watson Marlow 120U, shown in Figure 32. This pump is used to set the flow of the reactor solution. As the reactor-solution occupies the greatest volume, this pump sets the highest flow.

The flexible tubing used for the compression in the pump has an internal diameter of 2.4 mm. Originally, a flexible tubing of 0.8 mm internal diameter is used, but too much clogging occurs due to the suspended Pd particles. By replacing the new flexible tubing, the problem of clogging was solved.

Figure 32: Watson Marlow 120U peristaltic pump

In order to obtain accurate flows, a calibration of the Watson Marlow 120U pump is executed. The calibration is conducted with water by using the flexible tubing of 2.4 mm internal diameter. The resulting flow is tested as a function of the set rpm by weighing

the amount of water over a given time interval. The results for the calibration are shown in Table 11 and plotted graphically in Figure 33.

Table 11: Calibration of the Watson Marlow 120U pump

set rpm	V (ml)	time (min)	flow (ml/min)	regression
7	3.453	1	3.453	3.425
4.6	2.151	1	2.151	2.330
9.14	4.373	1	4.373	4.402
2	1.067	1	1.067	1.144
18	8.804	1	8.804	8.444
23	11.005	1	11.005	10.725
46	21.313	1	21.313	21.219
34	15.267	1	15.267	15.744
R²	0.998634			
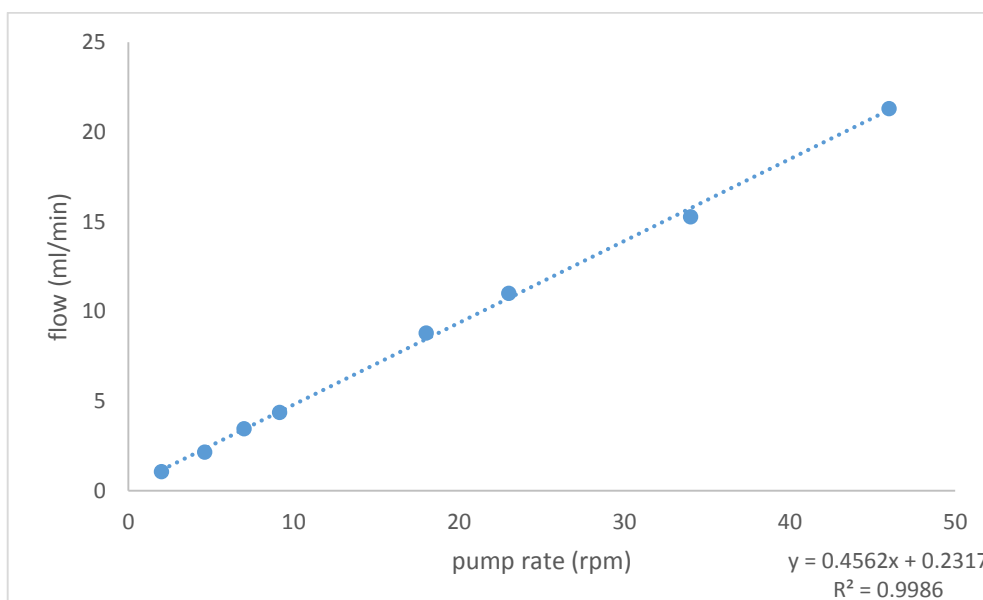
Figure 33: Calibration curve of the Watson Marlow 120U pump

The correlation between the results is 0.998634. This indicates that the obtained flows are a good representation of the set rpm despite the standard deviation of 0.284 obtained with the regression analysis. This is due to the wide range of flows that are tested, but this is necessary because a wide variety of flows are tested in the continuous flow system. The equation of the calibration is shown in formula 10.

$$Flow = 0.4562 \times set\ rpm + 0.2317 \qquad (10)$$

The second pump used in the flow set-up is the Watson Marlow 520S peristaltic pump (see also Figure 34). This pump sets the flow of iodobenzene.

Figure 34: Watson Marlow 520S peristaltic pump

Since the volume of iodobenzene is much less than the volume of the reactor-solution, the set flow of this pump is much lower than the set flow of the reactor-solution. A flexible tubing of 0.8 mm internal diameter is used. The smaller diameter allows lower flows, which is ideal for the iodobenzene flow. As the iodobenzene is a pure liquid with a relative low viscosity (1.74 mPa.s at 15 °C), no problems due to clogging are expected. The calibration of the Watson Marlow 520S is performed similar to the calibration of the Watson Marlow 120U pump. The results are shown in Table 12 and plotted graphically in Figure 35.

Table 12: Calibration of the Watson Marlow 520S pump

set rpm	V (ml)	time (min)	flow (ml/min)	regression
41.2	2.752	1	2.752	2.744
44.9	2.997	1	2.997	2.996
30	1.969	1	1.969	1.982
15	0.959	1	0.959	0.960
7.5	0.455	1	0.455	0.450
R^2	0.999949			
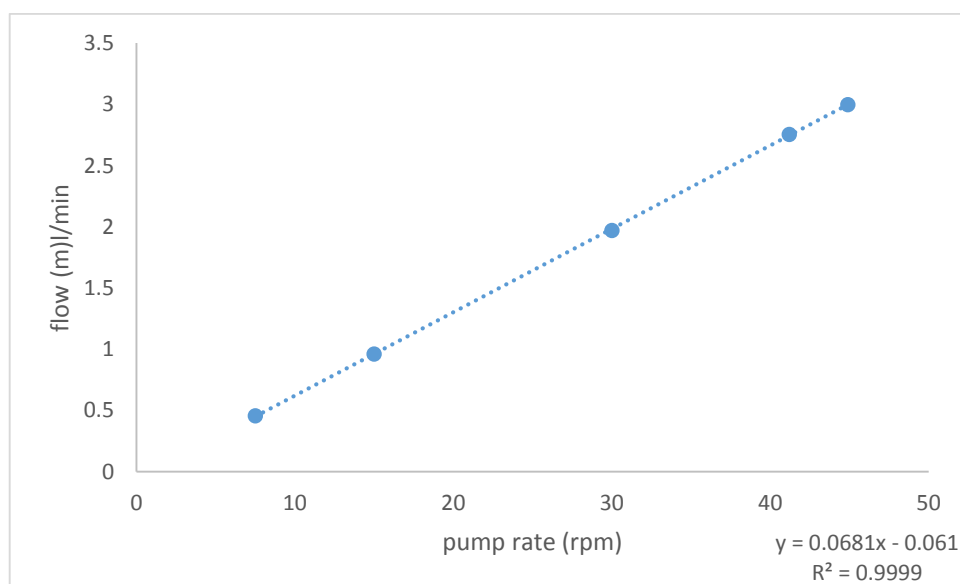
Figure 35: Calibration curve of the Watson Marlow 520S pump

The high correlation value and the relatively low standard deviation of 0.00915 proves that the calibration of the Watson Marlow 520S is very precisely. Equation 11 shows the relation between the set rpm and the resulting flow.

$$\text{Flow} = 0.0681 \times \text{set rpm} - 0.061 \qquad (11)$$

In comparison with the equation of the Watson Marlow 120U, the scope of equation 11 is 6.70 times lower. This is due to the internal diameter of the flexible tubing used by the different pumps. The internal diameter of the tubing used by the Watson Marlow 520S pump is 0.8 mm and the internal diameter of the tubing used in the other pump is 2.4 mm. This means that the surface area of the cross-section of the tubing used by the Watson Marlow 520S pump is 9 times smaller than the tubing used by the Watson Marlow 120U pump. This ratio is approximately equivalent to the ratio of the slopes, so the values of the slopes are a normal representation.

3.3.1.2 Calibration of the flows in the continuous system

The flows of both reagents must be aligned with each other so that the same molar ratio as in the batch reactor is obtained. Otherwise, the results would not be representative to compare them with the results obtained in the batch systems. Therefore, the flow of the reactor solution is used to calculate the flow of iodobenzene. However, the viscosity of the reactor solution and the length of tubing provide a pressure drop over the reactor. This pressure drop induces lower overall flows than expected which results in longer residence times. The longer residence times would result in higher conversions for a specific flow. In order to correct this incident, the flow of the reactor-solution is calibrated over the whole reactor. By doing this, the influence of the pressure drop over the reactor is compensated.

The calibration is performed by holding all the reaction conditions the same as when the reaction is performed. These reaction conditions include the power of the reactor, and using the reactor solution during calibration. In this way the viscosity of the reactor blend is also taken into account. To calibrate the flow in the reactor set-up, different pump rates are set. Then, the resulting flow is measured at the end of the tubing after the reactor. The volume is measured by weighing the amount of reactor solution before and after a time interval. Then with the density of the reactor solution, it is possible to calculate the volume over the time interval. This results in following flows as a function of the pump rates (see Figure 36 and Table 13). Here, the experiments are carried out in duplicate and these are the results which are obtained after a test on outliers is executed.
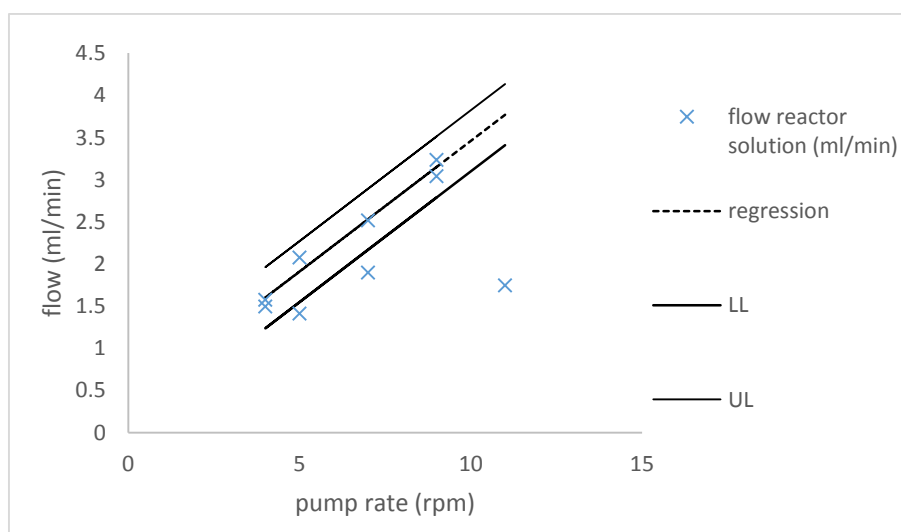
Figure 36: Calibration of the flow in the continuous reactor set-up

The outliers can be explained by the fluctuations in the flow. Fluctuations are due to the viscosity of the reactor solution and the pressure drop in the flow reactor. Also, all the measurements follow each other quickly. Therefore, it is possible that the flow at the end of the reactor has not got time enough to adapt to the set pump rate. However, without the outliers, the correlation is 0.978 which means that the flow at the end of the reactor is a good indication for the pump rate. So the pump rate can be used to set a specific flow through the reactor without much fluctuations.

The flow of the iodobenzene solution is based on the flow of the reactor solution to achieve identical molar ratios as in the batch experiments. Table 13 shows the corresponding iodobenzene pump rate, based on the pump rate of the reactor solution pump. Note that the outliers of 5, 7 and 11 rpm in Figure 36 are not used to calculate the corresponding flow of iodobenzene.

Table 13: Characterisation of the flows in the continuous reactor set-up

pump rate (rpm)	m (g)	V (ml)	time (min)	flow reactorsolution (ml/min)	flow PBA (mole/min)	Mole-ratio	flow IB (mole/min)	flow IB (ml/min)	pump rate IB (rpm)
9	0.545	0.473	0.169	2.805	0.000924	1.3	0.000711	0.081	2.1
9	1.182	1.025	0.389	2.638	0.000868	1.3	0.000668	0.076	2.0
7	1.61	1.396	0.640	2.183	0.000719	1.3	0.000553	0.063	1.8
5	1.907	1.654	0.919	1.800	0.000593	1.3	0.000456	0.052	1.7
4	1.263	1.095	0.844	1.298	0.000427	1.3	0.000329	0.038	1.4
4	1.435	1.245	0.911	1.366	0.00045	1.3	0.000346	0.040	1.5

Since the reactor solution consists of multiple substances, an average density is calculated based on the weighed amounts. The reactor solution for this experiment consists of 2.495 phenylboronic acid, 29.862 g water, 0.001 g $Pd(OAc)_2$, 5.892 g Na_2CO_3 and 29.821 g PEG 2000. This solution corresponds to an overall mass of 68.071 g and an overall volume of 59.043 ml, resulting in a density of 1.153 g/ml. All further density-calculations of the reactor-solution are performed the same as the calculation in this example.

With the concentration of phenylboronic acid in mole/ml, the flow of phenylboronic acid in moles/min is calculated. From the experiments in batch, it is known that the mole-ratio of phenylboronic acid to iodobenzene is equal to 1.3. With this value, the required flow of iodobenzene is determined. Note that this flow is displayed in mole iodobenzene/min and is converted to ml/min by multiplying the flow in mole/min with $\frac{MM}{m\% . \rho}$. Finally, with the calibration of the Watson Marlow 520S pump, the necessary pump rate is calculated.

3.3.1.3 Heat losses
By characterizing the heat losses, it is possible to determine the temperature just before the reactor and just after the reactor. These temperatures are determined by measuring the temperature at the beginning and at the end of the tubing.

In order to characterise the heat losses, a Wilson plot has been prepared. This plot is prepared by putting the PTFE-tubing of 7 m in a hot water bath. In this way, the solution at the end of the tubing has the same temperature as the hot water bath. After the hot water bath, a part of the tubing (e.g. 1 m) is placed outside the hot water bath, so it can cool down due to the lower temperature of the room. By measuring the decreased temperature at the end of this tubing as a function of the set flow, it is possible to determine the overall heat-transfer coefficient U.

By plotting the inverse of the overall heat-transfer coefficient as a function of the inverse of the flow, a linear relationship can be obtained. With this relationship, the temperature drop caused by the environment is characterised and used to determine the temperature at the beginning and at the end of the continuous reactor. The set-up of the experiment is shown in Figure 37 and Figure 38.
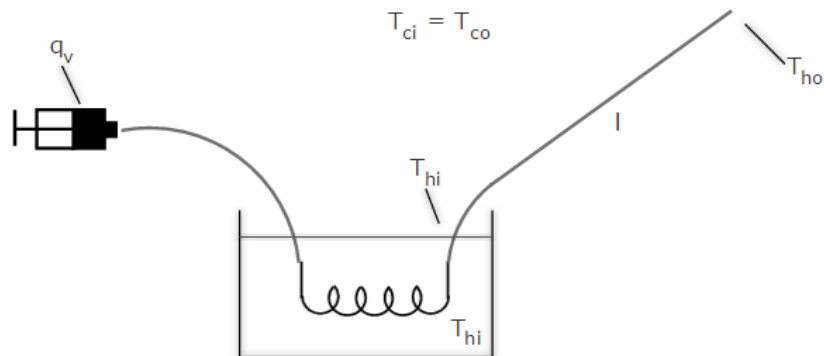
Figure 37: Schematic set-up for the determination of the overall heat-transfer coefficient

Figure 38: Experimental set-up for the determination of the overall heat-transfer coefficient

In the experiment, water is used since this corresponds well to the reaction solution, which also mainly consists of water. The flow q_v is set with a syringe pump. T_{hi} is the temperature of the hot water bath, and is also equal to the temperature at the beginning part of the tubing placed out the hot water bath. T_{ho} is the measured temperature at the end of the tubing and l is the length of the tubing placed outside the hot water bath. This is also the length where the temperature decreases due to the environment temperature. Different flows q_v, temperature T_{hi} and lengths l are examined during this experiment. Here, the parameters and results are shown in Table 14.

flow (ml/min)	l (m)	T_{hi} (°C)	T_{ho} (°C)	T_{room} (°C)	1/flow (min/ml)	1/U (m².K/W)
1	0.885	81.9	39.1	24.5	1	0.029
3	0.885	81.9	60.7	24.5	0.33	0.029
0.3	0.885	81.9	25	24.5	3.33	0.028
0.6	0.885	81.9	30.8	24.5	1.67	0.030
1.5	0.885	81.9	47.7	24.5	0.67	0.029
3	0.885	90.7	65.4	24.5	0.33	0.028
1	0.885	90.7	40.8	24.5	1	0.028
0.3	0.885	90.7	25.4	24.5	3.33	0.031
0.3	0.45	90.7	30	24.5	3.33	0.027
0.45	0.45	90.7	37.1	24.5	2.22	0.027
1	0.45	90.7	55.8	24.5	1	0.027
3	0.45	90.7	75.7	24.5	0.33	0.026

In order to calculate the overall heat-transfer coefficient, the exchanged heat flow $\dot{Q}$ over the tubing outside the hot water bath needs to be calculated. Formula 12 shows the calculation for the exchanged heat.

$$\dot{Q} = \dot{m} \, . \, c_p \, . \, \Delta T \qquad (12)$$

In this formula, ΔT is the difference between the temperature T_{ho} measured at the end of the tubing and the temperature T_{hi} of the hot water bath. Since water is used as the medium for testing the heat losses, the heat capacity c_p is 4.1818 J/g.K. The value of the mass flow $\dot{m}$ represents the quantity of water per time which is cooled down in the tubing placed outside the hot water bath. This value is calculated with the flow q_v and the density of water ρ. The calculation is shown in formula 13.

$$\dot{m} = \rho \, . \, q_v \qquad (13)$$

Finally, when the exchanged heat flow is known, the overall heat-transfer coefficient is calculated with formula 14. Here, the exchanged heat flow is expressed in J/s or W, the heat exchange surface A is expressed in m² and the logarithmic temperature difference is expressed in K. This induces that the overall heat-transfer coefficient U is expressed in J/s.m².K or W/m².K.

$$U = \frac{\dot{Q}}{A \, . \, \Delta T_{lm}} \qquad (14)$$

In formula 14, A is the surface where heat transfer is possible, so this is the same as the mantle of the tubing outside the hot water bath, which is equal to formula 15.

$$A = d \, . \, \pi \, . \, l \qquad (15)$$

ΔT_m is the logarithmic temperature difference, this is calculated with following formula 16.

$$\Delta T_{lm} = \frac{[(T_{hi} - T_{co}) - (T_{ho} - T_{ci})]}{ln\left[\frac{T_{hi} - T_{co}}{T_{ho} - T_{ci}}\right]} \qquad (16)$$

In this formula 16, T_{ci} and T_{co} are equal to the environment temperature.

The results for the inverse of the overall heat-transfer coefficient are plotted relative to the inverse of the flow. This Wilson plot is shown in Figure 39.
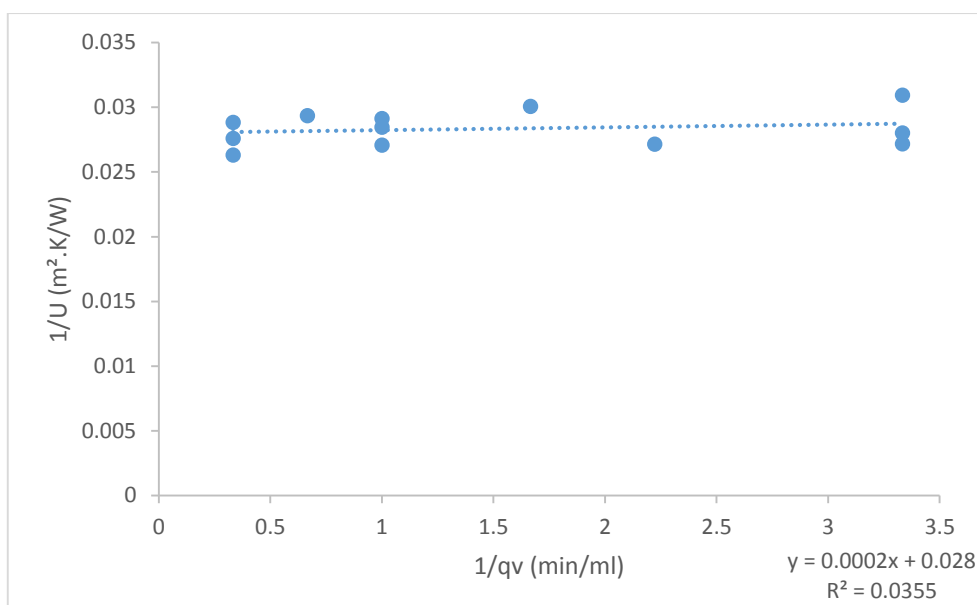
Figure 39: Wilson plot

The equation of the Wilson plot is shown in formula 17.

$$\frac{1}{U} = 0.0002 * \frac{1}{q_v} + 0.028 \qquad (17)$$

The slope of the Wilson plot is 0.0002. This is a really low value which approaches zero. This means that the flow has almost no influence on the overall heat-transfer coefficient. This is also clear in Figure 39 where the relation between $1/U$ and $1/q_v$ is represented by a nearly planar straight line. This also explains why a low correlation factor is obtained. It is a fact that correlations obtained by flat, horizontal lines are always low because in these cases, the values differ immediately more fiercely.

However, this is no problem for the calculation of the temperature drop in the reactor system, because the overall heat-transfer coefficient does not deviate fiercely in contrast to the flow. So when the flow in the reactor is known, the corresponding heat-transfer coefficient is calculated based on the relation between the $1/q_v$ and $1/U$. In this way, the heat losses due to the environment temperature are characterised.

3.3.1.4 Settings in the microwave-assisted and conventional-assisted flow

In order to examine the influence of microwaves on the continuous flow system, the maximum power of the microwave reactor is selected. The maximum power of the reactor is maintained during the whole reaction and is equal to 200 W. Since the reactor solution is not a clear liquid, the reflected power is a lot higher in comparison with the use of pure water. In addition, in comparison with pure water, the reactor solution consists of more substance with a lower dielectric constant. So less power of the microwaves is absorbed. This results in an average reflected power of 87 W resulting in an average absorbed power of 113 W (see also Figure 40).
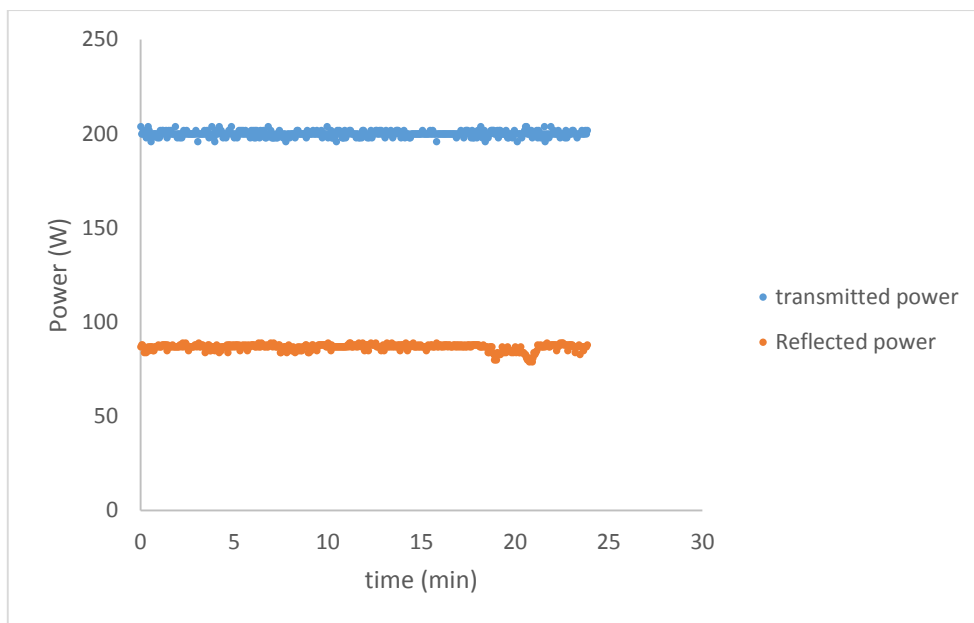
Figure 40: Transmitted- and reflected microwave power in the continuous system

As shown in Figure 40, the transmitted power is 200 W, this is much higher than in the batch reactor where the transmitted power reaches maximum 50 W (see Figure 23). This is due to the fact that in a batch reactor only a maximum temperature of 100 °C can be achieved. Higher temperatures are not possible in the batch reactor because of the pressure limit. This is not the case by a continuous flow system, here, the tubing can resist higher pressures which induces that higher temperatures than 100 °C are possible. That is also why a higher power can be transmitted to the flow set-up.

Both in the microwave-assisted flow experiments and the conventional flow experiments, the reactor solutions are preheated to 80 °C to dissolve all the components. The other variables such as flowrate and reactor length are all kept the same in the conventional flow. The only difference is the heating source, which is a hot water bath heated to 90 °C in the case of the conventional flow system.

3.4 Analytical method

To determine the yield and the concentration of the formed biphenyl product of the reaction, a suitable analysis of the samples is required. UV-Vis spectrophotometry is found as a suitable analysis method. Here, the GENESYS™ 10S Vis Spectrophotometer of Thermo fisher Scientific (see Figure 41) is used to measure the samples.

Figure 41: GENESYS™ 10S Vis Spectrophotometer of Thermo fisher Scientific

The UV-VIS absorption spectrum (Figure 42) shows that biphenyl exhibits a maximum absorption at a wavelength of 247.5 nm with a molar extinction coefficient of 16000 cm^{-1}/M.
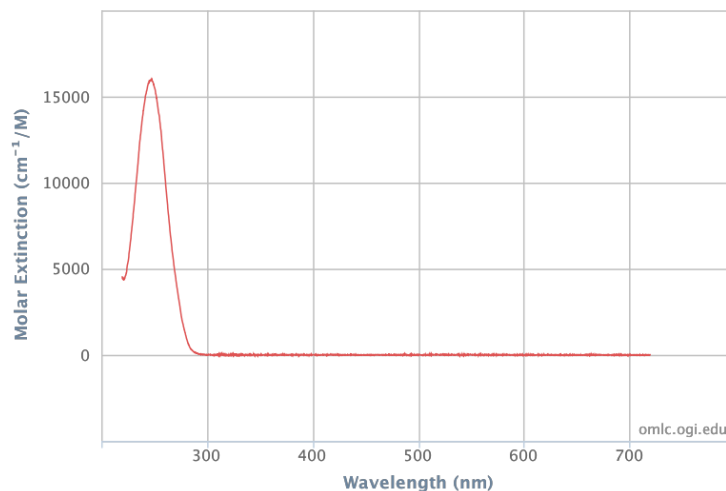
Figure 42: Optical absorption measurement of Biphenyl in cyclohexane made by R.-C. A [57]

Subsequently, all the samples in this study are measured with UV-Vis spectrometry at the wavelength of 247.5 nm. The sample preparation, validation of the analysis etc. is further explained in chapter 3.4.1 to 3.4.8.

The reason of this choice of analysis method is its ease of use. Originally, it was considered to implement an in-line analysis method after the continuous system, so that is why UV-Vis spectroscopy is selected as the analysis method. However, UV-Vis spectroscopy has a disadvantage, namely, the UV-vis spectrophotometer cannot distinguish between biphenyl and the reagents or other by-products. Therefore, it has to be made sure that the analysis is capable of measuring biphenyl selectively and accurately. This is done by the validation of the method, which includes linearity, repeatability, reproducibility, detection limit and selectivity.

3.4.1 Measurement of biphenyl

The literature study showed that biphenyl exhibits a maximum absorption at a wavelength of 247.5 nm. 247.5 nm lies in the ultraviolet part of the spectrum and therefore, special cuvettes to measure in the UV region are used. More specific, quartz cuvettes are used for the measurement because the organic solvent solves plastic disposable cuvettes. Thereafter, different dilutions of a biphenyl standard solution are made to verify the spectrum of biphenyl. Since biphenyl is a non-polar molecule, a non-polar solvent needs to be used. Therefore, hexane is used as solvent to make the dilutions and as the blanc in all the measurements. The spectrum of biphenyl is recorded by means of the VISIONlite™ 5 Software and this spectrum is shown in Figure 43.
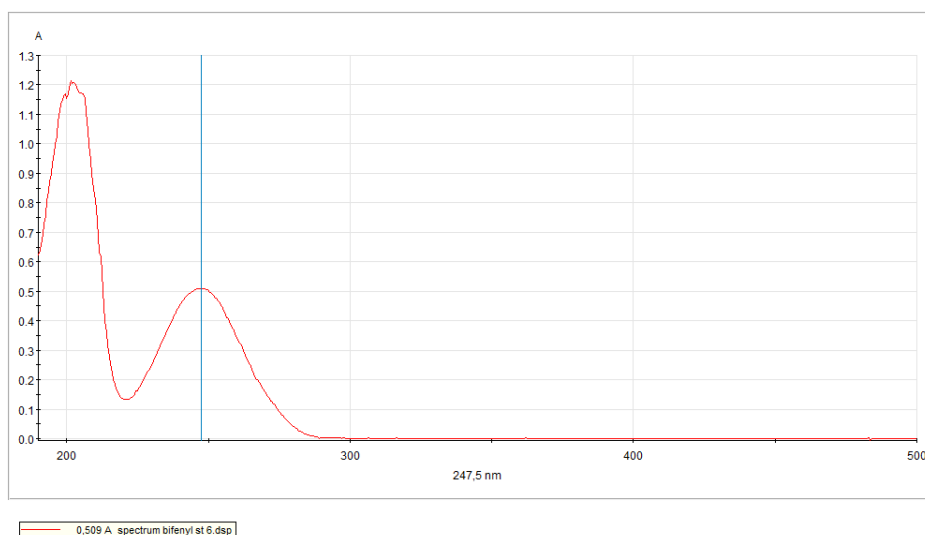
Figure 43: Scan of the biphenyl-spectrum

This spectrum corresponds well to the data from the literature. Here, it is clear biphenyl shows a maximum absorption at 247.5 nm.

3.4.2 Linearity of biphenyl

Since UV-Vis spectroscopy is not an absolute method, a calibration curve is necessary to measure the concentration of biphenyl. Therefore, a big dilution serie is prepared to test the range and linearity of the analysis method. The dilutions made for testing the linearity are shown in Figure 44.
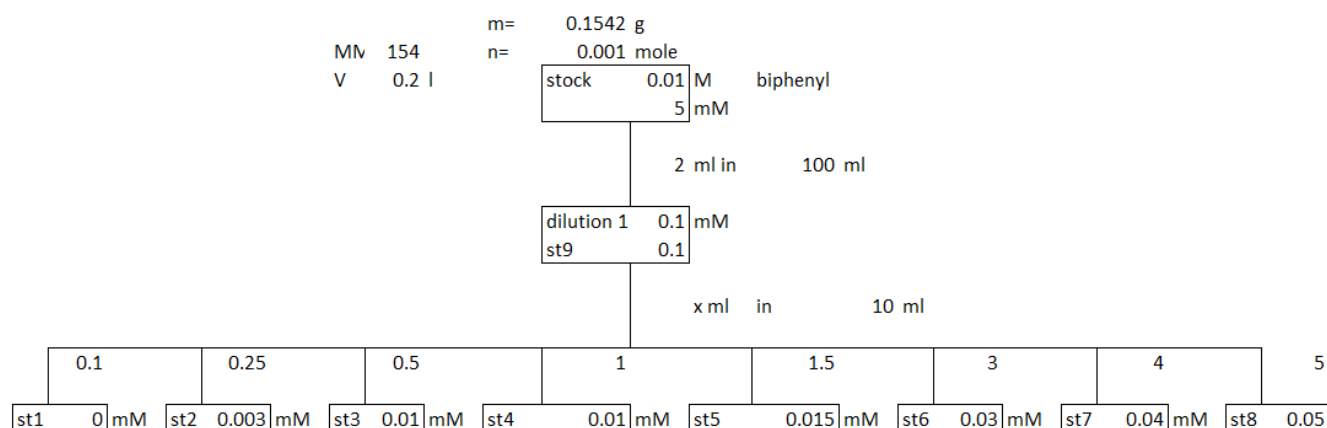
Figure 44: Dilution scheme of biphenyl in hexane

These dilutions are measured relative to a hexane blanc. The measured absorptions are plotted as a function of the concentration in order to obtain a calibration curve. The calibration curve is shown in Figure 45. Here, outliers are not included in the calibration curve.
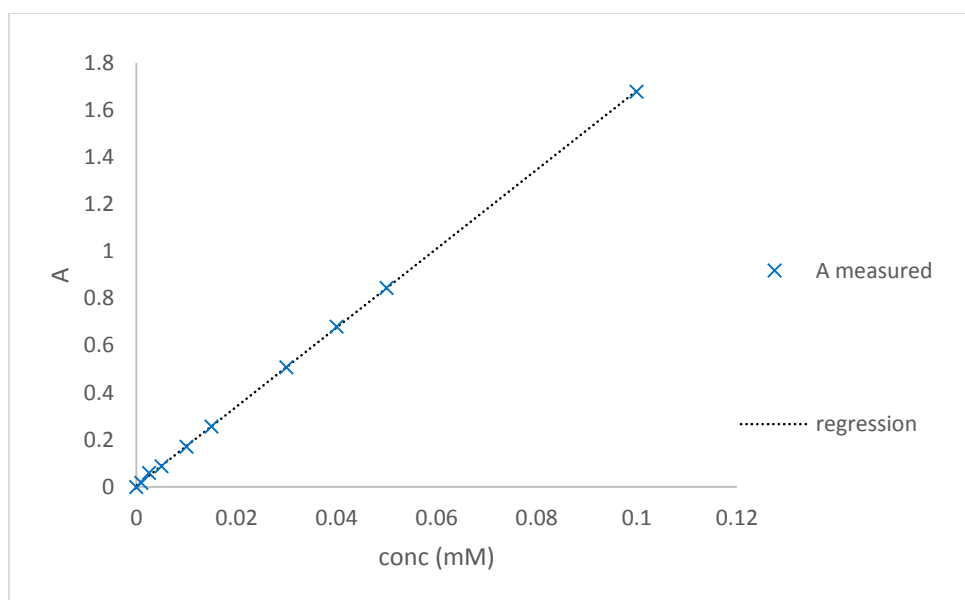
Figure 45: Calibration curve of biphenyl in hexane

A regression analysis is performed, the results of the calibration curve provide a correlation factor R² of 0.9999, so it is concluded that a linear relation exists between the concentration of biphenyl and the measured absorbance. This relation is represented by the equation shown in Formula 18.

$$A = 16.761 * concBF + 0.0063 \tag{18}$$

The calibration curve is tested on outliers outside the 95 % confidence interval. The lower limit and upper limit are calculated with a t-value and the standard deviation. The t-value is 1.895, the standard deviation is 0.005437 and the results are shown in Table 15.

Table 15: Test of outliers in the 95 % confidence interval

concBF (mM)	A measured	regression	LL	UL
0	0	0.006	-0.004	0.017
0.001	0.018	0.023	0.013	0.033
0.0025	0.059	0.048	0.038	0.059
0.005	0.089	0.090	0.080	0.100
0.01	0.172	0.174	0.164	0.184
0.015	0.257	0.258	0.247	0.268
0.03	0.509	0.509	0.499	0.519
0.04	0.681	0.677	0.666	0.687
0.05	0.846	0.844	0.834	0.855
0.1	1.68	1.682	1.672	1.693
5	3.419	83.809	83.799	83.819

The standard solution of 5 mM lies outside the 95 % confidence interval, and can thus be regarded as an outlier. This also means that the analysis method is only linear within a range from 0.001 mM to 0.1 mM.

3.4.3 Stability of the calibration curve

The stability of this calibration curve is also tested whether it is possible to use the same calibration curve during multiple experiments. The biphenyl standard solutions are stored in a naturally lit room at room temperature for six days. Thereafter, the samples are again measured with the UV-Vis photometer. The results are plotted in the same graph (Figure 46) as the original calibration curve to compare them.
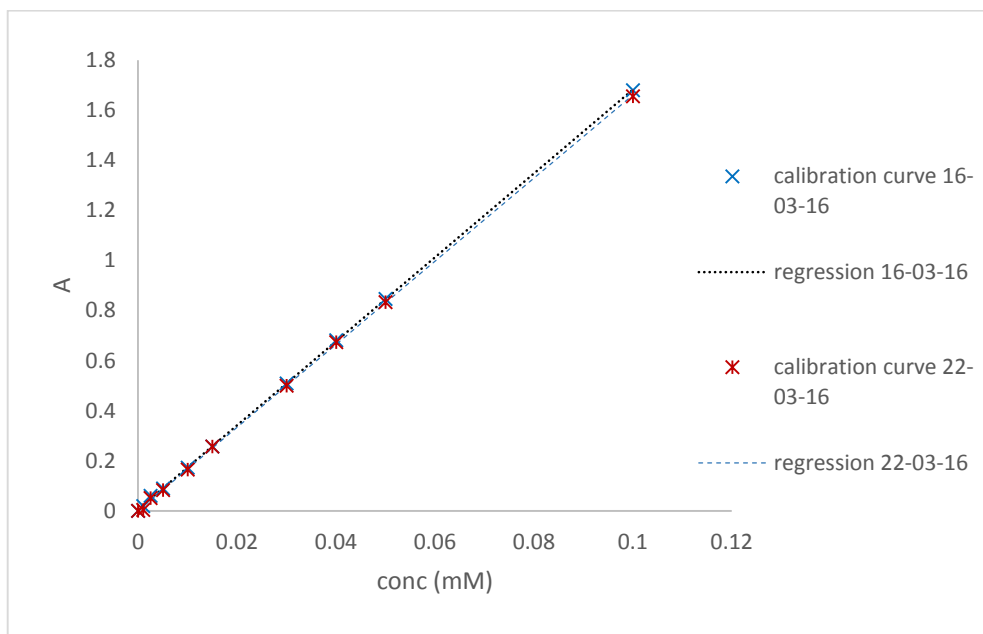
Figure 46: Stability of the calibration curve

At first sight of Figure 46, the results are very similar to each other. In addition, the correlation and equation are also very likewise. The correlation R^2 of the calibration curve measured after one week is 0.9998 and the equation is shown in formula 19.

$$A = 16.601 * concBF + 0.0011 \qquad (19)$$

The slope, the intercept and the correlation are similar to the original calibration curve, so it is concluded that the calibration curve is stable. Therefore, the calibration curve can be used for determining the concentration in multiple experiments. So the calibration curve is used for all the measurements in this study.

3.4.4 Detection limit

The detection limit is the lowest quantity of biphenyl that can be distinguished from the absence of biphenyl, so in other words a blanc. The detection limit is determined by measuring a sample with a concentration close to the blanc value. Therefore, the same sample needs to be measured multiple times (e.g. 8 times) to determine the standard deviation. Afterwards the detection is calculated based on three times the standard deviation (see formula 20).

$$DL = 3 . s \qquad (20)$$

A sample obtained after reaction in the EasyMax® is diluted to a concentration which gives an absorbance near the blanc value. This dilution is repeated 8 times and the results are shown in Table 16.

Table 16: Determination of the detection limit

sample	A	conc (mM)
bl	0.016	0.00058
1	0.191	0.01102
2	0.187	0.01078
3	0.176	0.01012
4	0.181	0.01042
5	0.196	0.01132
6	0.177	0.01018
7	0.185	0.01066
8	0.18	0.01036
	t	1.94318
	average	0.01061
	stdev	0.00039
	LL	0.00985
	UL	0.01137
	DL	0.00117

The results are tested within the 95 % confidence interval, but no outliers have been detected. From the results, a detection limit of 0.00117 mM is found. This is the lowest concentration that can be detected representatively.

3.4.5 Repeatability

The repeatability is one of the ways to express the precision of a serie of measurements. It is the variation of the values obtained by measuring the same sample multiple times. This measurement needs to be carried out under the same conditions. The same conditions can be understood by the same person, with the same method, using the same measurement equipment and consumables, and within a short period of time.

One sample after reaction in the EasyMax® is taken and extracted with hexane. The reason for taking a sample out of the EasyMax® is to take the background matrix of the sample into account. The sample is diluted to obtain a concentration within the linear range of the analysis method. This same sample is diluted multiple times on the same way and measured against the same blanc. The results are shown in Table 17.

Table 17: Repeatability of the analysis method

sample	A	conc (mM)
1	0.672	0.03972
2	0.681	0.04025
3	0.66	0.03900
4	0.672	0.03972
5	0.662	0.03912
6	0.67	0.03960
7	0.674	0.03984
8	0.666	0.03936
	stdev	0.00038
	average	0.03958
	percentage stdev	0.959 %

The percentage standard deviation is even less than 1 %, so it can be concluded that the repeatability of is the method is good. This means that the analysis method is suitable for precise and accurate measurements.

3.4.6 Reproducibility

The reproducibility is a representation of the degree of similarity between the measurements of the same analysis method, obtained under different measurement conditions. Following conditions are maintained to test the reproducibility:

- The same measuring principle;
- The same measurement method;
- The same reference standard;
- The same instrument;
- The same place;
- Different conditions;
- Different time span;
- Several observers.

One sample is taken after reaction in the EasyMax® and again extracted with hexane and diluted within the linear range of the analysis method. This same sample is diluted multiple times on the same way and measured against the same blanc. However, in contrast to the repeatability, the samples are diluted on different days and by different persons. The results are shown in Table 18.

Table 18: Reproducibility of the analysis method

sample	time measured	A	conc (mM)
1	day 1	0.671	0.03966
2	day 2	0.688	0.04067
3	day 3	0.7	0.04139
4	day 4	0.664	0.03924
5	day 5	0.713	0.04216
6	day 6	0.678	0.04008
7	day 7	0.679	0.04013
8	day 8	0.656	0.03876
		stdev	0.00105
		average	0.04026
		percentage stdev	2.599

The percentage standard deviation is 2.599 %. This is still a low value, so it can be concluded that the reproducibility of is the method is good. This means that the analysis method is suitable for precise and accurate measurements.

3.4.7 Selectivity

In order to test whether the analysis method measures the biphenyl concentration selectively, all the components used in the SM-reaction were examined to detect possible interferential with the spectrum of biphenyl. Since all the components except iodobenzene are bad solvable in a non-polar organic solvent such as hexane, it is possible that these components are not transferred to the hexane phase. This has as

result that the components probably will not interfere because of their insolubility in hexane.

Sodiumcarbonate, TBAB and $Pd(OAc)_2$ do not possess a big conjugated system, so these components do not show an absorption in the UV-Vis region. This is verified by investigating their spectra and it is concluded that these components do not interfere at a wavelength of 247.5 nm. However, it could be possible that the substances PEG 2000, phenylboronic acid and iodobenzene interfere with the measurement at 247.5 nm as these substances possess a conjugated system. Therefore, their spectra are investigated.

The spectra of PEG 2000, iodobenzene and phenylboronic acid are examined by dissolving them in hexane and afterwards a scan is made with the UV-Vis spectrophotometer. The concentrations are based on their concentrations in the reactor-solution. So these concentrations are an extreme case for the selectivity, as the samples are normally diluted at least 1500 times. The results of these components are shown in Table 19 and their spectra is shown in Figure 47.

Table 19: Interference of phenylboronic acid, PEG 2000 and iodobenzene in hexane

	phenylboronic acid	PEG 2000	iodobenzene
m (g)	0.0217	0.3894	0.686
V (ml)	50	50	10
conc (mM)	3.38[1]	3.89[1]	336.3
dilution	10	10	/
conc (mM)	0.34	0.39	336.3
A measured	0.026	0.003	4.349
Interference	no	no	yes

[1]Does not dissolve completely

PEG 2000   Phenylboronic acid   Iodobenzene
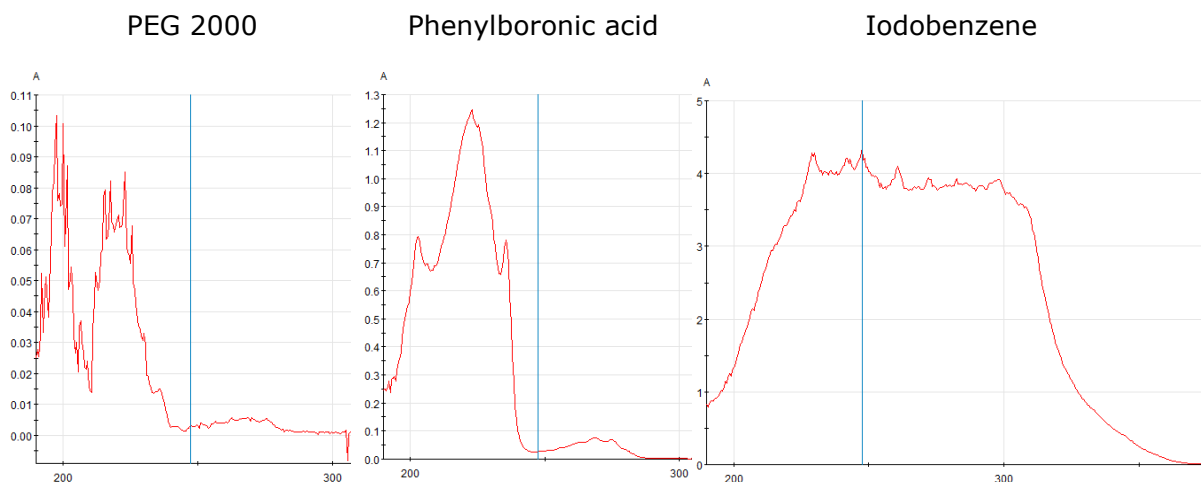
Figure 47: Spectra of PEG 2000, phenylboronic acid and iodobenzene in hexane

It is concluded that phenylboronic acid and PEG 2000 do not interfere with the measurement of biphenyl as shown by their spectra in Figure 47. This conclusion is based on that fact that PEG 2000 and phenylboronic acid do not show an absorption at 247.5 nm.

However, the results in Table 19 and the spectrum in Figure 47 show that iodobenzene has an interference at the wavelength of 247.5 nm. This interference is further investigated in the next chapter 3.4.8.

3.4.8 Interference of iodobenzene

As iodobenzene interferes with the measurement of biphenyl, a solution has to be found. This solution is based on the fact that the SM-reaction uses iodobenzene and converts it to biphenyl. Also iodobenzene is always added in the lowest amount in contrast to phenylboronic acid. So it is concluded that every mole of the formed biphenyl is a product of the same amount of moles of iodobenzene. Knowing that this is a relation between iodobenzene and biphenyl, it is possible to distinguish the concentration of iodobenzene and biphenyl. To distinguish the concentration of biphenyl and iodobenzene, two aspects are necessary. The first one is to know the amount of iodobenzene that is added at the beginning of the reaction. The second one is to find also a linear relation between the measured absorbance and the concentration of iodobenzene. Therefore, a calibration curve of iodobenzene is drafted based on the dilutions shown in Figure 48.
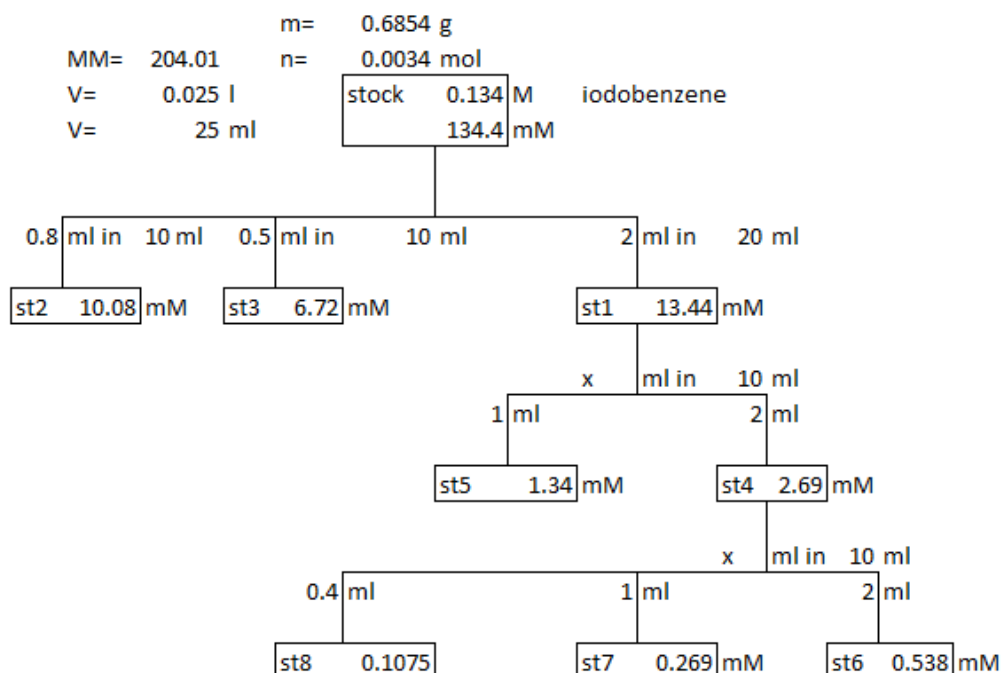
Figure 48: Dilution scheme of iodobenzene in hexane

The dilutions are measured at the same wavelength of 247.5 nm and in contrast to a hexane blanc solution. The results are shown in Table 20.

Table 20: Results for the calibration curve and test on outliers

sample	conc (mM)	A	regression	LL	UL
st1 (outlier)	13.439	3.986	7.996	7.994	7.999
st2 (outlier)	10.079	3.938	5.997	5.994	5.999
st3 (outlier)	6.719	3.62	3.997	3.995	4.000
st4	2.688	1.598	1.598	1.596	1.600
st5	1.344	0.799	0.798	0.796	0.801
st6	0.538	0.317	0.318	0.316	0.321
st7	0.269	0.159	0.159	0.156	0.161
st8	0.108	0.063	0.063	0.060	0.065
t-value	2.353				
stdev	0.00101				

The test on outliers outside the 95 % confidence interval proves that the samples 1, 2 and 3 are outliers. So the linear range for the determination of iodobenzene goes from 0.108 mM to 2.688 mM. With these values, the calibration curve is drawn (see Figure 49) and the equation is drafted (see formula 21). The correlation R² amounts 0.999998 which indicates a good linear relation.

$$A = 0.5951 * concIB - 0.00143 \tag{21}$$
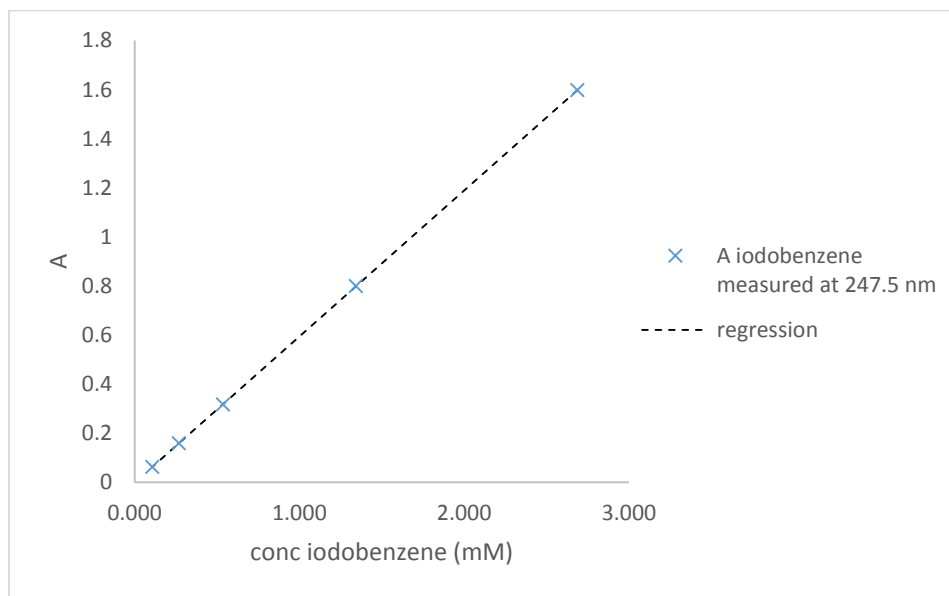
Figure 49: Calibration curve of iodobenzene measured at 247.5 nm

The slope of the equation of biphenyl amounts 16.761, while the slope of the equation of iodobenzene only amounts 0.5951. So the slope of biphenyl is 28.16 times bigger than the slope of iodobenzene, this means that the concentration of biphenyl has a much higher influence than iodobenzene on the measured absorbance. However, even as the interference of iodobenzene is small (1-28.16), a formula is designed to take this small interference into account. The reasoning and arrangement of this formula are described below.

The measured absorption can be divided in two values. The first absorption is the contribution by biphenyl and the second absorption is the small contribution by iodobenzene. This is represented by formula 22.

$$A_{measured} = A_{biphenyl} + A_{iodobenzene} \tag{22}$$

The absorptions of biphenyl and iodobenzene are obtained by measuring the concentration of iodobenzene and biphenyl in the sample. That is why the calibration curve of biphenyl and the calibration curve of iodobenzene were prepared. The equations are shown in formula 18 and 21. By putting formula 18 and 21 in formula 22, an overall formula (23) with both components is created.

$$A_{measured} = 16.761 * c_{BP} + 0.00632 + 0.5951 * c_{IB} - 0.00143 \tag{23}$$

Now, a relation between the concentration of biphenyl and the concentration of iodobenzene has to be found. Since iodobenzene is converted to biphenyl, it is known that the concentration of biphenyl in the reactor is equal to the concentration of iodobenzene which has reacted (formula 24). The concentration of iodobenzene at a certain time in the reactor is similar to the concentration of iodobenzene in the beginning of the reaction subtracted by the concentration of iodobenzene that is reacted (formula 25).

$$c_{BP} = c_{IB\ reacted} \tag{24}$$

$$c_{IB} = c_{IB,0} - c_{IB\ reacted} \tag{25}$$

Formula 24 and 25 are filled in formula 23 and is further elaborated and converted to the concentration of biphenyl. The dilution of the sample needs also to be taken into account. This dilution factor is multiplied by the beginning concentration of iodobenzene. Finally, the resulting equation is shown in formula 26.

$$c_{BP} = \frac{A - 0.5951 * c_{IB,0} * dilution factor - 0.004894}{16.166} \tag{26}$$

On this way, the representative concentration of biphenyl is calculated. This concentration allows to calculate the original concentration of biphenyl in the reactor when the dilution factor is taken into account. The concentrations of biphenyl are used to determine the reaction kinetics and the biphenyl yields.

When the concentration of biphenyl that has formed during the reaction is known, it is possible to calculate the yields. The yields are determined by looking at the amount of iodobenzene that is still left in the reactor. The concentration of iodobenzene in the reactor can be determine with formula 25. With the concentration of iodobenzene in the beginning of the reaction and the concentration of iodobenzene after a specific reaction time, it is possible to calculate the yield when using formula 27.

$$Xa = \frac{c_{IB,0} - c_{IB}}{c_{IB,0}} \tag{27}$$

4 Results and discussion

The results of this study are divided in 4 main parts. First, the reaction kinetics are determined by approaching the reaction by an order system. These reaction kinetics are important in the following parts to compare the different methods.

The second part investigates and discusses the use of microwaves as energy source for the Suzuki-Miyaura reaction and compares them to the conversion of the biphenyl product and the reaction kinetics obtained in a conventional system. In this part, the influence of several variations between the two methods are also investigated. These variations include hydrolysis of the catalyst, the effect of stirring and the use of a different phase transfer agent.

In the third part, the results of the use of microwaves in a continuous system are shown and discussed. These results include product yields and are discussed based on the comparison with a conventional flow system.

At least, performing the reaction in flow is compared with the reaction carried out in batch. This comparison is based on the product yields obtained after comparable reaction times.

4.1 Suzuki-Miyaura reaction in batch

4.1.1 Determination of the reaction order
The Suzuki-Miyaura reaction consists of a three step reaction mechanism as explained in chapter 2.3.3 and Scheme 12.
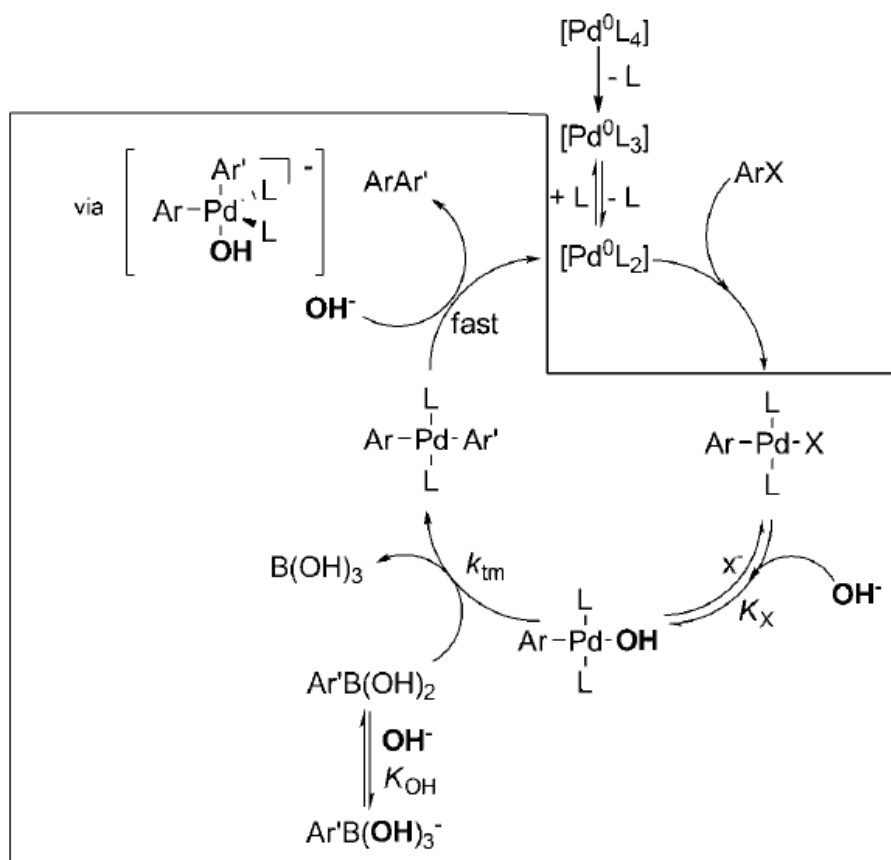
Scheme 12: Different steps of the catalytic cycle of the SM-coupling [42]

Mostly, the oxidative addition is considered the rate-determining step of the catalytic cycle. However, according to Amatore et al., the Suzuki-Miyaura reaction performed in this study is considered fast as an aryliodide e.g., iodobenzene is used. Amore et al. considered the transmetalation (rate constant k_{tm}) as the rate-determining step, assuming that the reductive elimination is fast enough. Then, the overall rate could be formulated as shown in formula 28, with the apparent rate constant k_{obs} given in formula 29 [42].

$$rate = k_{obs} \cdot [Pd^{II}]_{total} \tag{28}$$

$$k_{obs} = k_{tm} \cdot [ArB(OH)_2] \cdot C_0 \cdot \frac{1}{1+K_{OH}[OH^-]} \frac{K_x[OH^-]}{[X^-]+K_x[OH^-]} \tag{29}$$

Formula 28 shows that the rate depends on the concentration of the Pd^{II} complex, which is formed in the transmetalation step. Since k_{obs} depends on the concentration of X^- and OH^-, it is difficult to make a pseudo-first order approximation because $[X^-]$ and $[OH^-]$ are susceptible to variations during the reaction. However, the reaction performed in this study uses an excess of base so the term $[OH^-]$ can be considered as a constant during the reaction. $[X^-]$ on the other hand, is not in excess, so this term varies from the initial concentration which is near zero to C_0 at the end of the reaction.

The determination of the reaction kinetics in this study is based on the research of Amatore et al. In their study, the reaction kinetics were followed by monitoring the formation of the two products during the transmetalation/reductive elimination steps. These two products are Pd^0L_3 and ArAr' (see also Scheme 12), which are formed in stoichiometric amounts at the same reaction rate in the reductive elimination step. As these products are formed in stoichiometric amounts, it is possible to just monitor the amount of ArAr' (or biphenyl in this study). However, in this study, the reaction kinetics are determined by following the concentration of iodobenzene. This is possible because amount of reacted iodobenzene is equal to the amount of formed biphenyl.

The concentration gradient of iodobenzene is determined by taking several samples out of the reactor while the reaction still proceeds. Here, the reaction solution is stirred to obtain a homogeneous sample. Thereafter, the concentration of unreacted iodobenzene is determined after analysing the concentration of biphenyl. The concentration of iodobenzene can be calculated from the initial concentration of iodobenzene and the concentration of the formed biphenyl as shown in formula 30. In addition, the concentration of biphenyl is calculated as earlier explained in chapter 3.4.8.

$$C_{IB} = C_{IB,0} - C_{BP} \tag{30}$$

To determine the reaction rate equation, three different approaches have been investigated. The first approach is in accordance with a pseudo first order. This reaction rate equation is shown in formula 31 (for the calculation, reference is made to the appendix 6.1.1). The second approach is a standard second order of the first type, the disadvantage of this second order is that an assumption is made in which the concentrations of both reagents are held the same. This results in the reaction rate equation shown in formula 32 [58] (for calculation see appendix 6.1.2).

1st type of second order: $2A \rightarrow P$

2nd type of second order: $aA + bB \rightarrow pP$

However, in the Suzuki-Miyaura reaction performed in this study, the initial mole-ratio of phenylboronic acid to iodobenzene is 1.3. So the concentrations are not practically the same. That is why a third approach is made, this approach is the second type of the second order. In this approach, the different concentrations of phenylboronic acid and iodobenzene during the reaction are taken into account. This approach for the reaction rate equation is shown in formula 33 [58] (calculation see appendix 6.1.3).

Pseudo first order

$$\ln|c_{IB}| = c_{PBA,0}.k.t + \ln|c_{IB,0}| \tag{31}$$

First type of the second order

$$\frac{1}{c_{IB}} = k.t + \frac{1}{c_{IB,0}} \tag{32}$$

Second type of the second order

$$\ln|c_{IB}| - \ln|c_{IB} + c_{PBA,0} - c_{IB,0}| = (c_{PBA,0} - c_{IB,0}).k.t + \ln|c_{IB,0}| - \ln|c_{PBA,0}| \tag{33}$$

All these equations are linear relationships. So, by plotting the obtained concentration of iodobenzene as function of the reaction time, a linear relation should be obtained. These linear relations are examined and compared by looking at the correlation coefficients. Therefore, multiple experiments at different temperatures and different reaction circumstances are performed to determine which reaction rate equation gives the best approximation.

Figure 50 shows the concentration gradient of iodobenzene as function of the reaction time. This experiment is performed with TBAB as transfer agent on a temperature of 80 °C obtained in the EasyMax®. The reaction solution is preheated to 80 °C and thereafter, iodobenzene is added to start the reaction. This iodobenzene is not preheated, but this has no influence on the reactor temperature since the volume of iodobenzene is very small in comparison with the volume of the reactor solution. The moment of iodobenzene addition is equal to a reaction time of 0 minutes.
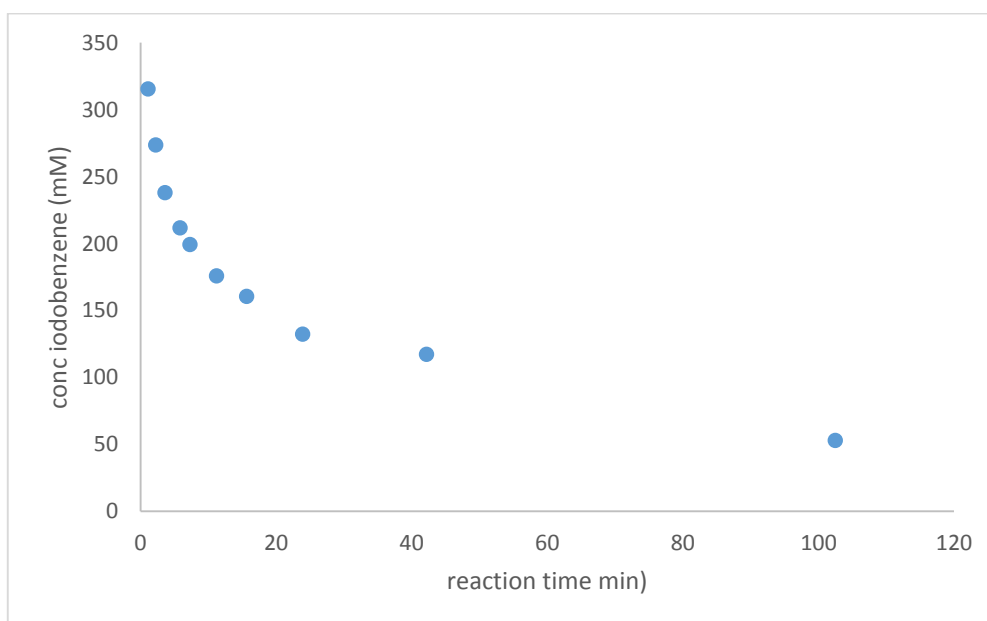
Figure 50: Concentration gradient of iodobenzene at 80 °C

The curve of the concentration gradient looks visually good. However, at first sight it is not possible to determine which approach is preferable. Therefore, the concentrations are edited as indicated in formulas 31, 32 and 33 and plotted as a function of the reaction time to obtain a linear curve. The curves for each approximation are shown in Figure 51, Figure 52 and Figure 53.
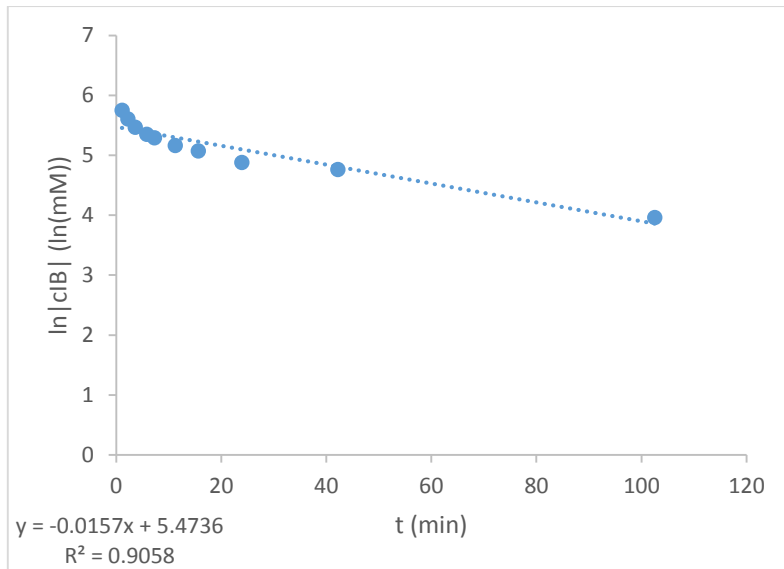
Figure 51: Pseudo first order approximation
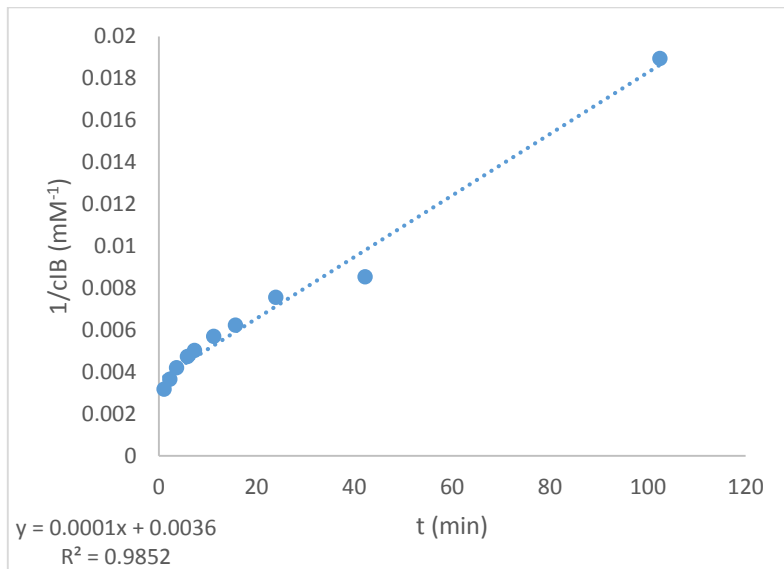
Figure 52: First type of the second order approximation
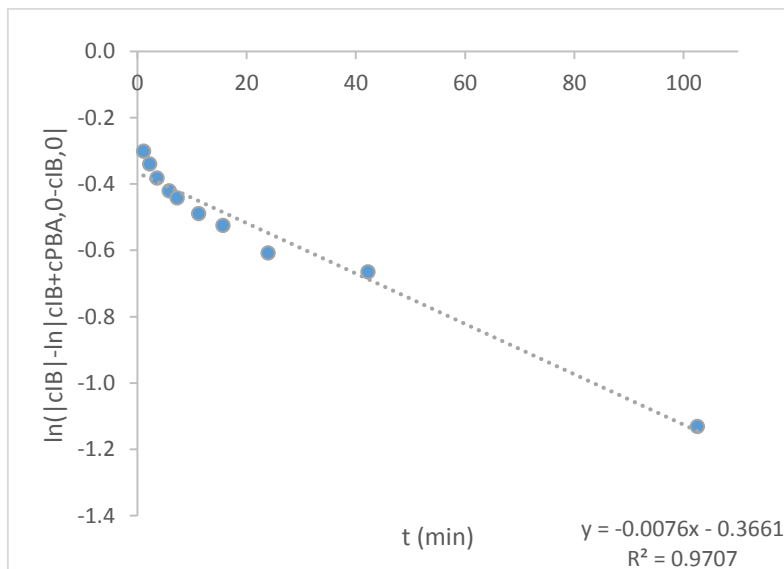
Figure 53: Second type of the second order approximation

73

The second order reaction rate equations seem to be the best approximation of the SM-reaction investigated in this study. In order to obtain more certainty about the order system of the reaction, more experiments are carried out. Here, the experiments are carried out similar to the experiment in the EasyMax® at 80 °C with TBAB as the transfer agent. The correlation factors are examined for each reaction rate equation and are summarised in Table 21.

Table 21: Approximation of the Suzuki-Miyaura reaction

Experiment	correlation-factor		
	pseudo first order approach	1st type 2nd order approach	2nd type 2nd order approach
1	0.9631	0.9806	0.9764
2	0.9058	0.9852	0.9707
3	0.9719	0.9975	0.9903
4	0.9595	0.962	0.9614
5	0.9733	0.9769	0.9761
6	0.9175	0.9489	0.9408
7	0.916	0.947	0.9376
8	0.9195	0.9739	0.9578
9	0.9485	0.9946	0.9829
10	0.9751	0.9776	0.9804
11	0.9443	0.979	0.9708
12	0.9847	0.9928	0.9998
13	0.9672	0.9825	0.9858

It can be concluded from the values of the correlation that the second order equations are a better approach than the pseudo first order equation. The first type and second type of the second order are both comparable to each other. Globally, the correlations obtained with the 1st type of the second order equations are a bit better than these obtained with the 2nd type. In addition, the 1st type of the second order is an easier method for the approximation of the Suzuki-Miyaura reaction, so in the investigated SM-coupling is approached by the 1st type of a second order reaction. This approach will also be used as the base to determine the reaction kinetics in order to examine the use of microwaves as energy source.

Despite that the correlation factors obtained with the first type of the second order approximation are the best, these correlation factors are still not that high. This is, among other things, due to spread of the experimental- and analysis method. Also, at the beginning of the reaction, the concentration gradient does not look like it can be linearly approximated (see Figure 52). This is also verified by preparing a residue plot of the results in contrast to the linear curve as shown in Figure 54 for the first type of the second order approximation.
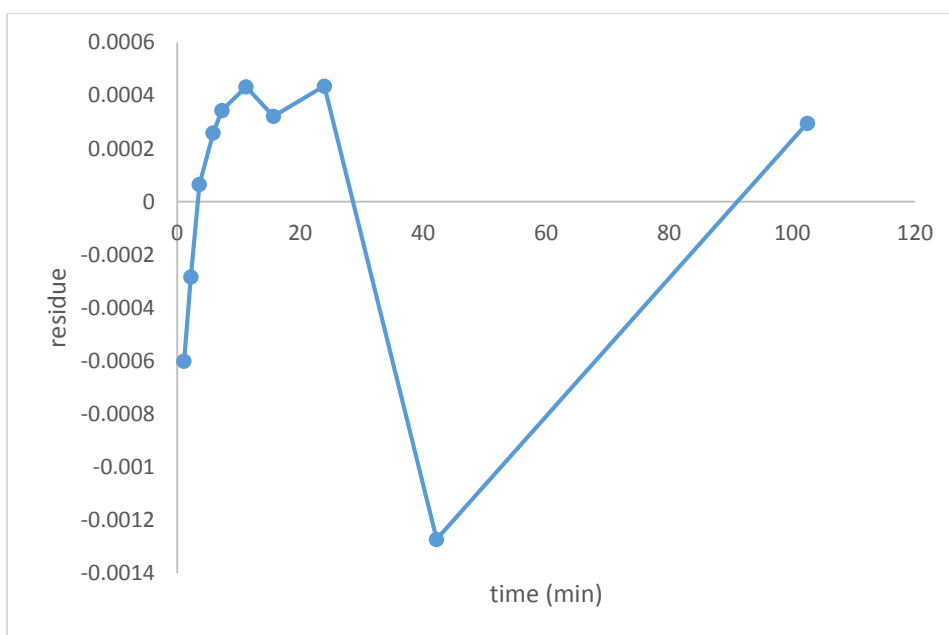
Figure 54: Residue plot of results in contrast to the linear curve when using the first type of second order

The gradient of the results shows that in the beginning of the reaction, the approach deviates from a linear approximation. This can be explained by the fact that the SM-coupling is a catalytic reaction which exists of three different steps. It is possible that the reaction rate goes much faster at higher concentrations of the beginning product iodobenzene, but after a while when the substrate concentration is lowered, the reaction rate goes slower [59]. This phenomenon is studied by Amore et al. [42].

Amatore et al. studied the kinetics of the different steps in the catalytic cycle. In their study, it is concluded that the overall reactivity is controlled by the concentration of the base. Namely, the base has been shown to be crucial in the transmetalation step. However, the base does not only promote the transmetalation, it also has a big influence on the reductive elimination step. The function of the base is already discussed in chapter 2.3.3.2, here it was said that the base has two roles (see Scheme 6).

The first role is the formation of a hydroxo-palladium(II) complex which reacts with phenylboronic acid (see Scheme 6), and the second role is the promotion of the reductive elimination. However, Amore et al. also believe that the transmetalation can proceed via the boronate pathway A (see Scheme 6). In this pathway, the poorly reactive $ArB(OH)_3^-$ is formed, which slows down the reaction drastically. This pathway would be the case at higher concentrations of the base [42]. So in summary, the overall reactivity is controlled by the initial concentration of the base. When the concentration of OH^- is low, it results in a slow reaction because the formed amount of the reactive hydroxo-palladium(II) complex is too little. On the other hand, when the concentration of OH^- is too high, the reaction also goes slow because of the lower concentration of the reactive $ArB(OH)_2$. This lower concentration is due to the transformation of $ArB(OH)_2$ to the less reactive $ArB(OH)_3^-$.

4.1.2 Influence of the temperature on the SM reaction

The temperature usually has a large influence on the reaction rate. This influence is due to the temperature dependence of the rate constant which is well described by the Arrhenius equation shown in Formula 34.

$$k = A \cdot e^{\frac{-E_a}{R.T}}$$

(34)

75

Here, A is the pre-exponential factor and E_a is the activation energy. In addition, the Arrhenius law implies that the reaction rate generally increases exponentially with the temperature. So by increasing the reaction temperature, the reaction will proceed much faster resulting in higher yields of biphenyl in the same reaction time [60]. The biphenyl yields are examined on different reaction times at different temperatures, the results are shown in Figure 55.
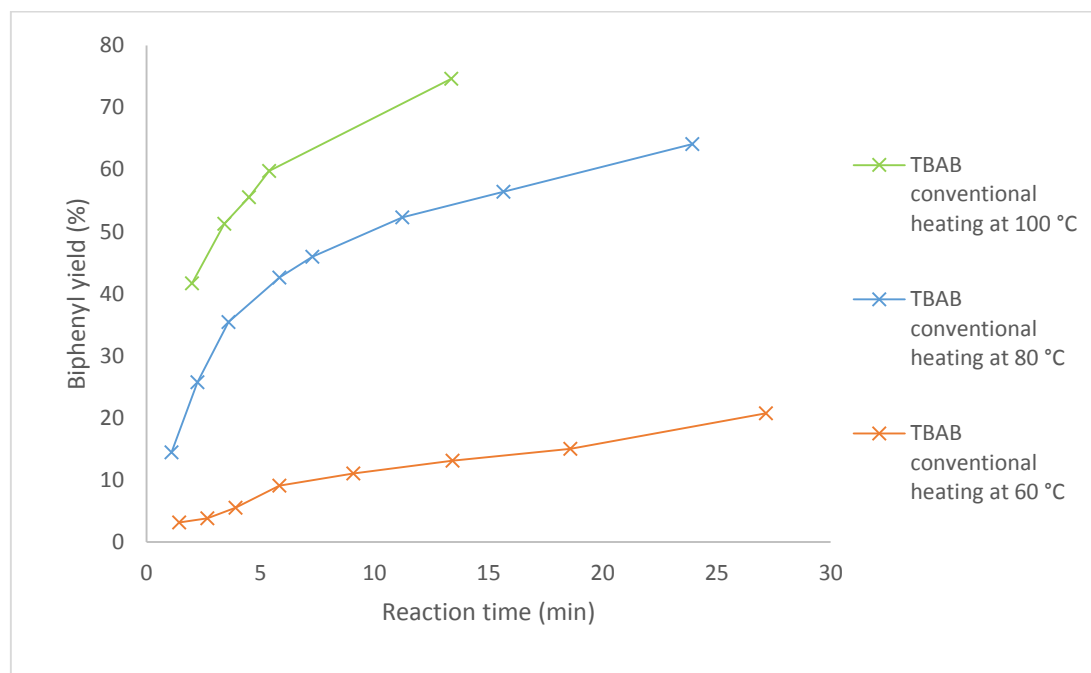
Figure 55: Temperature dependency of the biphenyl yields

Significantly higher yields are obtained when performing the reaction at higher temperatures. For example, after a reaction time of 10 minutes, a product yield of 11.5 % is obtained at 60 °C, a yield of 51.2 % at 80 °C and a yield of 68.4 % at 100 °C. Normally, at 100 °C, water reaches its boiling point but the reactor solution consists of water with a lot of dissolved components which results in a lower vapor pressure relative to the vapor pressure of pure water. This lower vapor pressure ensures that the reactor solution has a boiling point slightly above 100 °C making it possible to work at 100 °C. However, vapor losses must be avoided as these change the concentration in the solution. This is done by placing a vapor reflux on the reactor.

In addition, by observing the trend in Figure 55, it can be expected that even higher yields can be obtained when the reaction is performed at higher temperatures. However, this cannot be investigated as the vapor formation would result in higher pressures against which the reactor is not equipped.

4.1.3 Determination of the rate constant k

First, the reaction rate at a specific temperature is investigated. According to the law of mass action, the rate of a chemical reaction at a constant temperature only depends on the concentrations of the substances that influence the rate [61].

To determine the rate constant, the Suzuki-Miyaura reaction in this study is approached by the first type of the second order equation. This equation is once more below (formula 35) to explain the determination of the rate constant k.

$$\frac{1}{c_{IB}} = k.t + \frac{1}{c_{IB,0}} \tag{35}$$

As explained earlier in chapter 4.1.1, a linear relationship is obtained by plotting the inverse of the concentration of iodobezene as a function of the reaction time. This linear relation is represented by the equation above (formula 35), where the slope corresponds to the rate constant k and the intercept corresponds to the inverse of the initial concentration of iodobenzene. So by plotting the relation between the inverse concentration of iodobenzene and the reaction time, the rate constant k can be extracted from the slope of the equation.

This is done for the SM-coupling at 80 °C in the conventional reactor with the TBAB-water system. Here, the inverse concentration of iodobenzene is plotted against the corresponding reaction time, resulting in Figure 56.
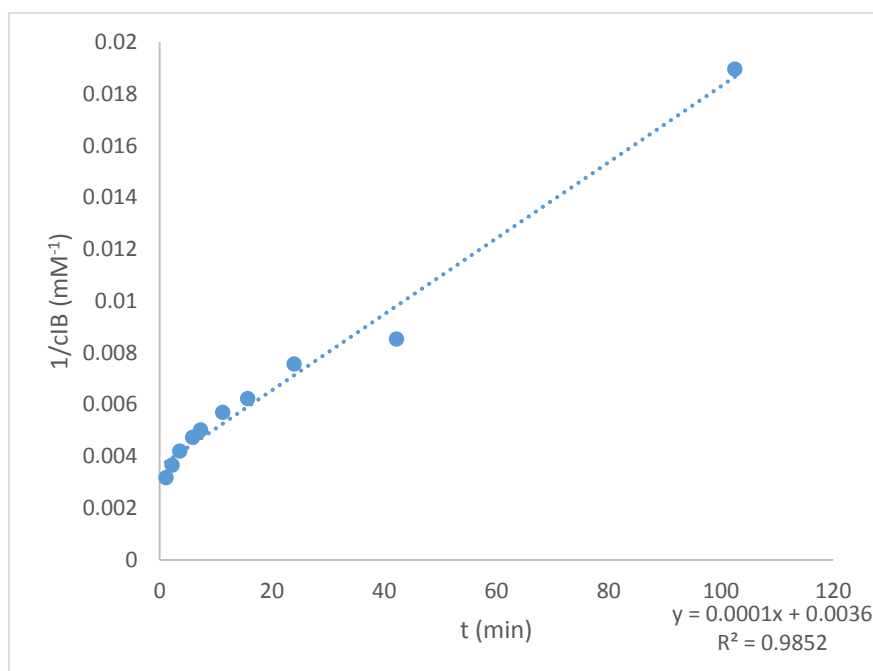
Figure 56: Determination of the rate constant k by the first type of the second order approximation

By performing a regression analysis, a rate constant of 0.000147 $mM^{-1}min^{-1}$ and an inverse initial iodobenzene concentration of 0.00361 mM^{-1} are obtained. This last value corresponds to an initial iodobenzene concentration of 277 mM, while the exact initial concentration of iodobenzene is 369 mM. So the initial concentration obtained via the second order equation deviates 24.8 % of the applied concentration. This deviation is quite large and can be explained by the deviation of the second order approach at the beginning of the reaction. Besides that, the obtained intercept is higher than the actual value of the initial inverse concentration. So this corresponds to a lower initial concentration of iodobenzene obtained by the second order equation. This also can be seen visually in Figure 56 in which the gradient of the curve at the beginning slightly deviates from the linear approximation.

4.1.4 Temperature dependency of the rate constant k

As earlier discussed and shown in chapter 4.1.2, the temperature has a significant influence on the SM-reaction. In order to look at the reaction kinetics at different temperatures, the temperature dependency of the rate constant is therefore investigated by performing the SM-reaction at different temperature e.g., 60 °C, 80°C and 100 °C. After plotting the inverse concentration of iodobenzene as a function of the reaction times, following rate constants are obtained from the slope of the equations (see Table 22).

Table 22: Rate constants at different temperatures performed in the EasyMax® 102

T(°C)	T (K)	k (l/mmole.min)	k (l/mole.s)
60	333	0.0000186	0.000309
80	353	0.0001468	0.002447
100	373	0.0006548	0.010914

The results are obtained by performing the SM-reaction with the TBAB-H_2O system in the conventional batch reactor. As shown in Table 22, the rate constants increase significantly with temperature. Based on the Arrhenius equation, a relation between the rate constant and temperature is obtained. This relation is represented in formula 36, which is received by transforming the Arrhenius equation.

$$\ln(k) = -\frac{E_a}{R} \cdot \frac{1}{T} + \ln(k_0) \tag{36}$$

So by plotting ln(k) as a function of the inverse temperature (in K^{-1}), the pre-exponential factor and the activation energy are determined. With the knowledge of these two values, the reaction rate can be calculated at any temperature. The relation is also shown in Figure 57.
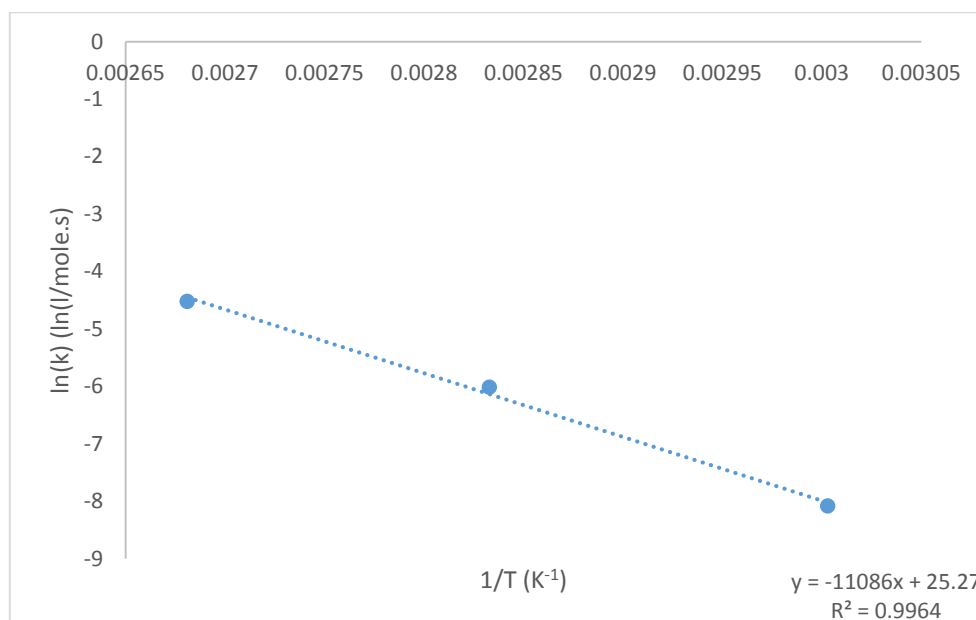
Figure 57: Influence of temperature on the rate constant

Figure 57 shows a linear relation between the inverse temperature and the natural logarithm of the rate constant. This linear relationship can be used to predict the reaction rate at higher temperatures and to determine the activation energy of the reaction. Later in this study, the reaction kinetics will also be used to compare different reaction methods such as the influence of microwave irradiation on the SM-reaction.

4.1.5 Comparison of the TBAB- with the PEG 2000 method

As discussed in the chapters 3.1.1 and 3.1.2, the SM-coupling in this study is investigated by the use of two different mediums. The first medium is TBAB-H_2O and the second medium is PEG 2000-H_2O, where TBAB and PEG 2000 function as the phase transfer catalyst. The reactions are performed in batch as described in 3.1.1 and 3.1.2 at different temperatures and different reaction times. In this way, both reaction mediums

are compared based on their product yields as a function of the reaction time. This comparison is done at different reaction temperatures as shown in Figure 58.
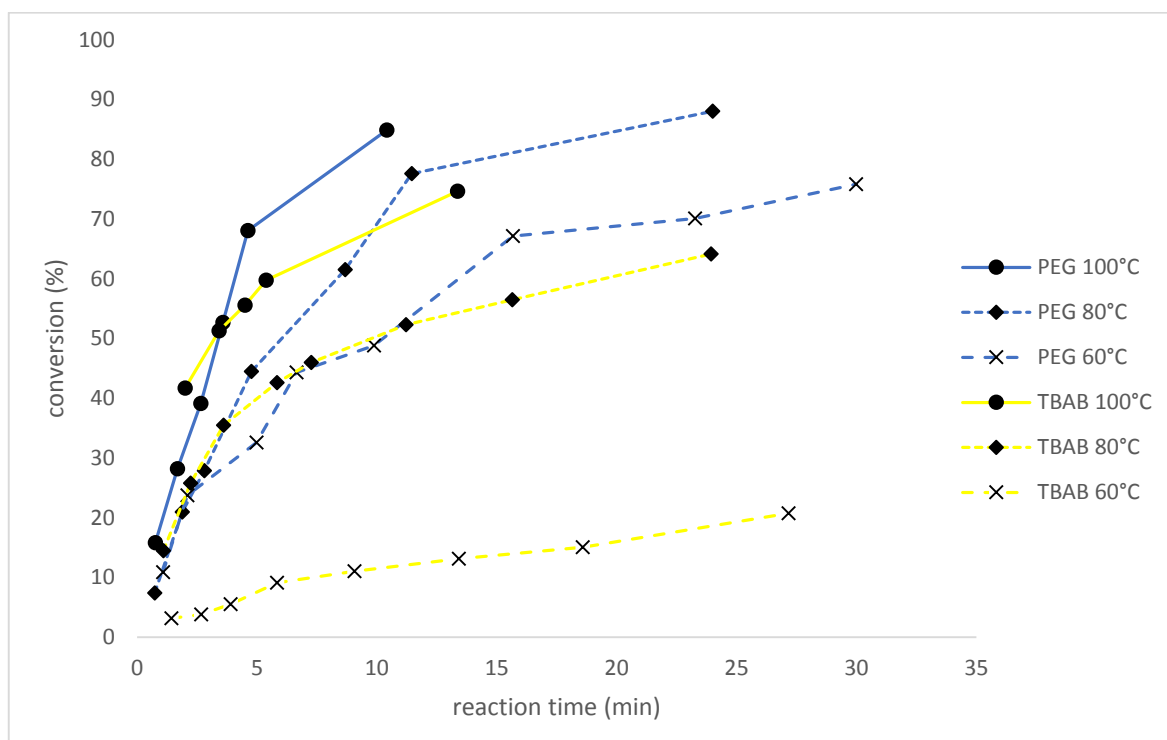
Figure 58: Comparison of the PTC at various temperatures

Based on the biphenyl yields as a function of the reaction time, it can be concluded that the PEG 2000-water medium shows significantly better yields than the TBAB-water medium. This is probably due to the solubility properties of PEG 2000. Namely, PEG 2000 does not only functions as phase transfer agent, it also functions as a co-solvent next to water. And as earlier discussed, the same molar amount of PTC results in a bigger volume of PEG 2000-water than TBAB-water because of the larger molecular mass of PEG 2000. This bigger volume ensures that all components are better dissolved resulting in a better contact between the reagents. This was also found in the study of Liu et al. [9], where it is reported that the $Pd(OAc)_2$-H_2O-PEG system is more efficient than the $Pd(OAc)_2$-H_2O-TBAB due to the properties of PEG as co-solvent and phase transfer catalyst [9].

Based on the results of the different catalysts systems (see also Figure 58), the rate constants are determined. These rate constants, for both the PEG system and the TBAB system, are plotted in contrast to inverse of the temperature. This is represented in Figure 59.
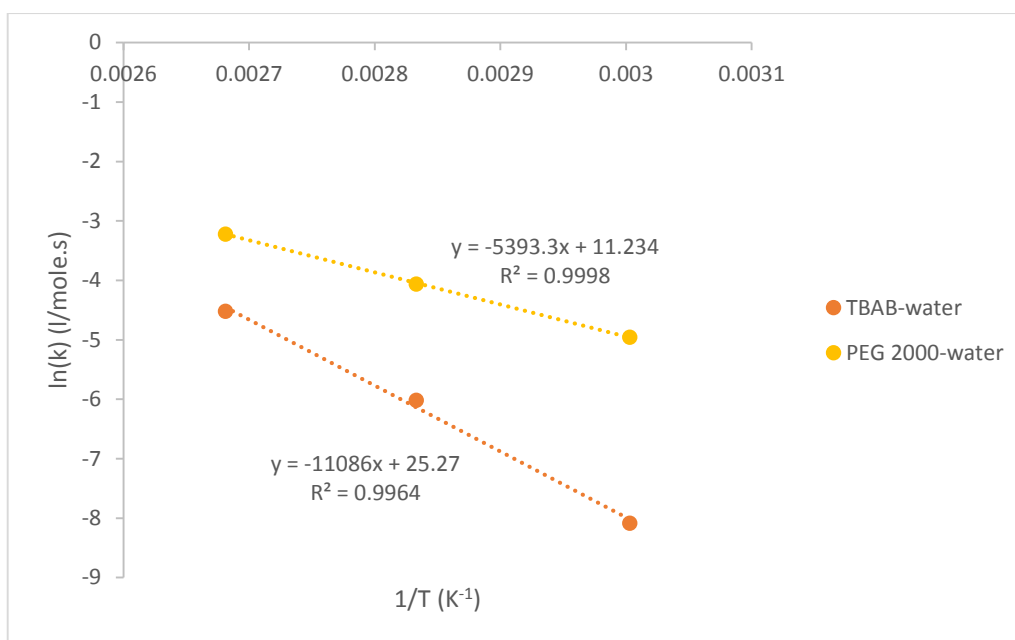
Figure 59: Comparison of the rate constants of the TBAB and PEG system

The activation energy and the pre-exponential factor are determined by the slopes and the intercepts of the equations shown in Figure 59. The pre-exponential factor and the activation energy of the TBAB-water system are $9.4*10^{10}$ l/mole.s and 92178 J/mole. For the PEG-water system, the pre-exponential factor is $7.6*10^4$ l/mole.s and the activation energy is 44842 J/mole. As the activation energy of the PEG-water medium is lower than the TBAB-water medium, the PEG-water medium is energetically favored because less energy is necessary to initiate the reaction. In addition, the pre-exponential factor of the TBAB-water medium is much higher. So at higher temperatures, where the exponential term of the Arrhenius equation can be neglected, the rate constant of the TBAB-water medium will be higher. This temperature is examined by calculating the intercept of both equations. The intercept of both curves lies at an inverse temperature (K^{-1}) of 0.002467, which corresponds to a temperature of 132 °C. So from this temperature and higher, it is possible that the TBAB-water medium is a better system to perform the reaction.

4.1.6 Use of microwaves as energy source for the Suzuki-Miyaura reaction

The main objective of this study is to evaluate the use of microwaves as an energy source for the Suzuki-Miyaura reaction. This is done based on the product yields obtained at different temperatures, similar to the results discussed in chapter 4.1.2. The Miniflow® 200SS batch reactor is used to perform the reactions. The results at temperatures of 60 °C, 80 °C and 100 °C are shown in Figure 60. Here, the results are obtained using the TBAB-water medium.
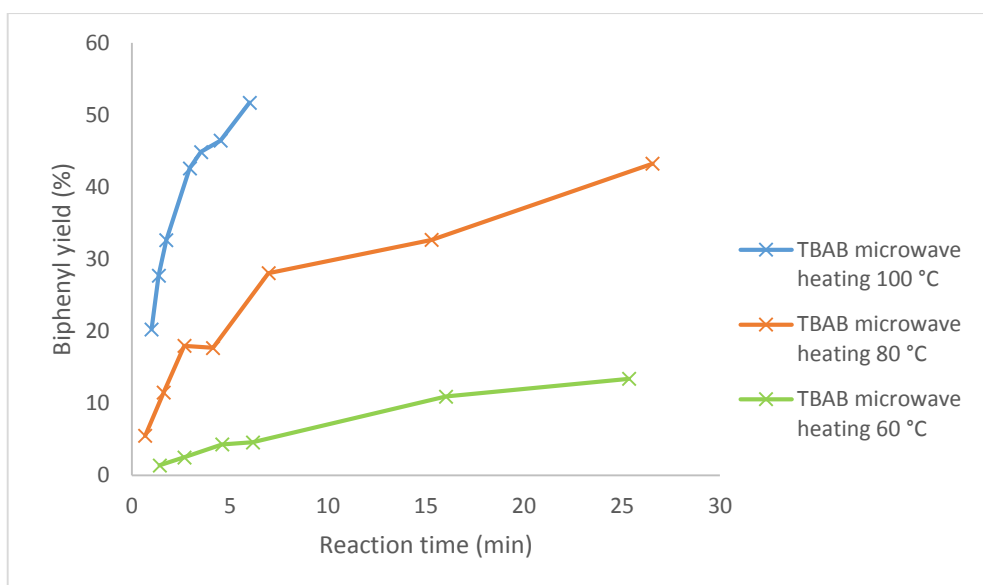
Figure 60: Biphenyl yields in the microwave reactor

The results obtained with the Miniflow® show a greater spread than the results in the conventional reactor. This is also the reason why more outliers were detected, which are not included in the curve. The greater spread is due to the spread of the reaction temperature and other reaction conditions as the temperature in the Miniflow® cannot be controlled as precisely as the EasyMax®. Also stirring and vapor losses are less controllable in the Miniflow® despite using the same refluxing method. Namely, the microwave batch reactor is not completely closed off at the top so more vapor losses are possible in comparison with the conventional batch reactor. These vapor losses result in a bigger spread of the product yields as they influence the concentration. To minimize this influence, the reaction is performed rapidly and samples are taken in less than 10 minutes at 100°C.

Nevertheless, the temperature dependency of the reaction looks good in Figure 60. This shows that the product yields presumably are obtained due to the temperature of the reactor solution and not any side effect of microwaves. The temperature dependency is also examined by plotting the rate constants as a function of the inverse temperature (see Figure 61).
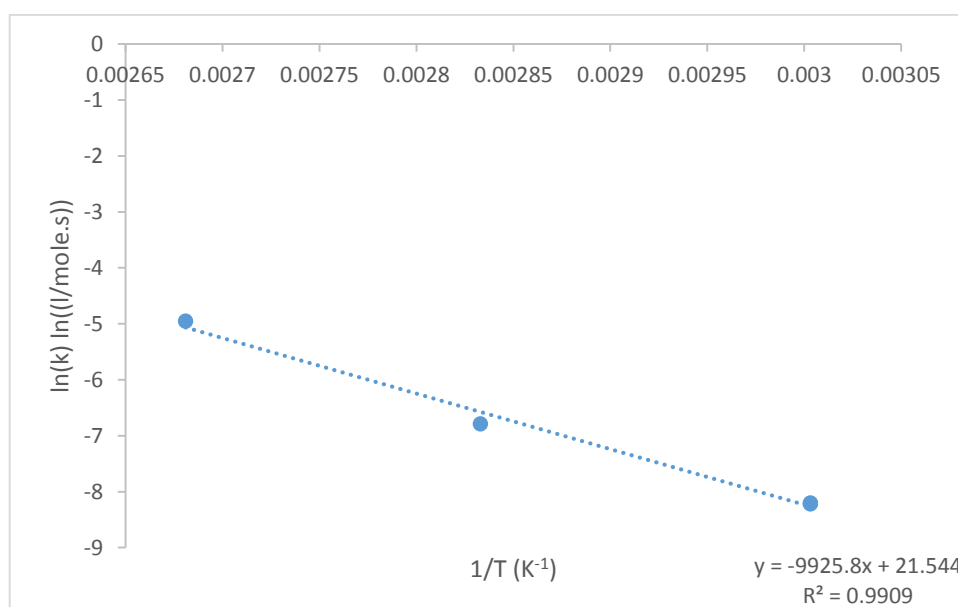
Figure 61: Temperature dependency of the rate constant in the microwave reactor

The relation between the rate constant and the inverse temperature is linear. So it can be concluded that the values shown in Figure 60 are a correct representation of the yields obtained in the microwave reactor. The activation energy and pre-exponential factor when using microwaves are 84915 J/mole and $4.5*10^9$ l/mole.s which is comparable with the activation energy and pre-exponential factor of the TBAB-water system in the conventional reactor. So it can be concluded that the activation energy and pre-exponential factor mainly depend on the catalyst system.

Next to the TBAB-water system, the PEG 2000-water system is also carried out in the presence of microwave radiation. This system is also investigated in order to see if the choice of the phase-transfer catalyst has an influence on the use of microwaves. The results of the experiments in the microwave batch reactor are obtained similar to the results obtained in the conventional reactor (see 4.1.5) and these are shown in Figure 62.
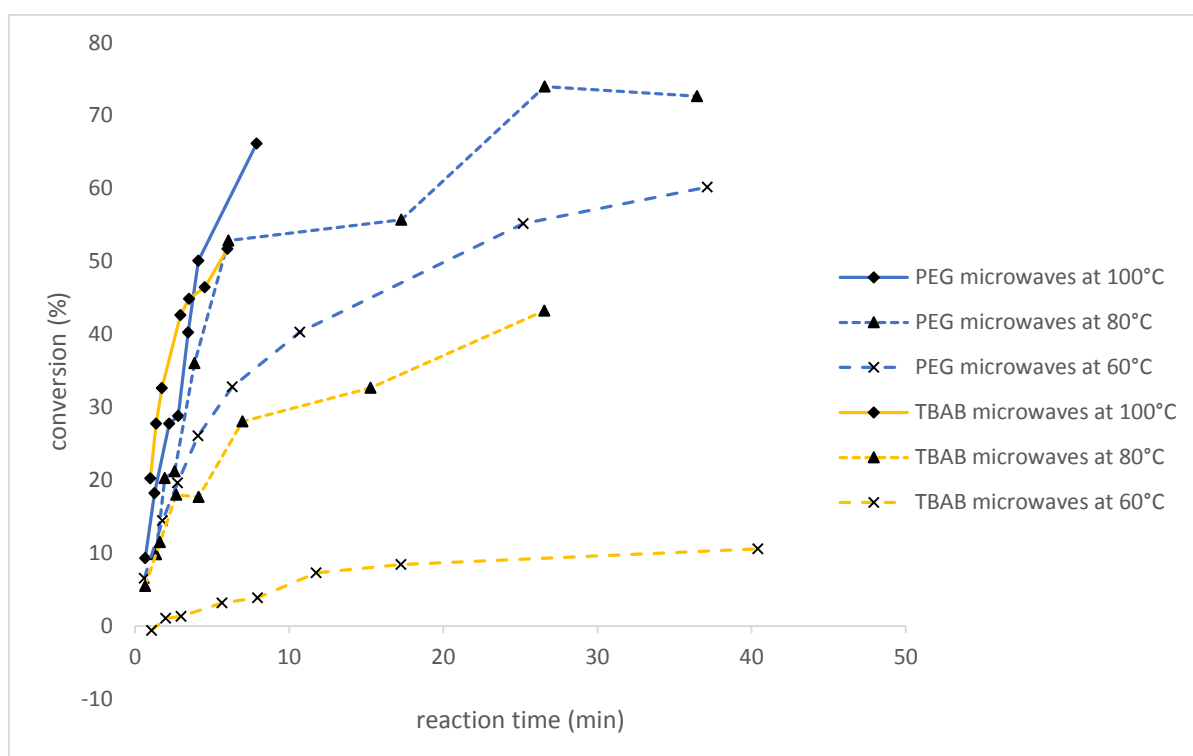
Figure 62: Comparison of TBAB and PEG at different temperatures in the microwave reactor

Especially at the lowest temperature of 60 °C, a great difference exists between the biphenyl yields with PEG and those with TBAB. As the reaction temperature increases, this difference is reduced ending in comparable yields for both phase transfer catalysts at 100 °C. This indicate that it might be possible that the TBAB system will react faster than the PEG system at higher temperatures. To see if this trend is correct, the rate constants are plotted as a function of the temperature (see Figure 63). Therefore, it should be looked at the slopes of the equations to verify whether the predicted trend is correct.
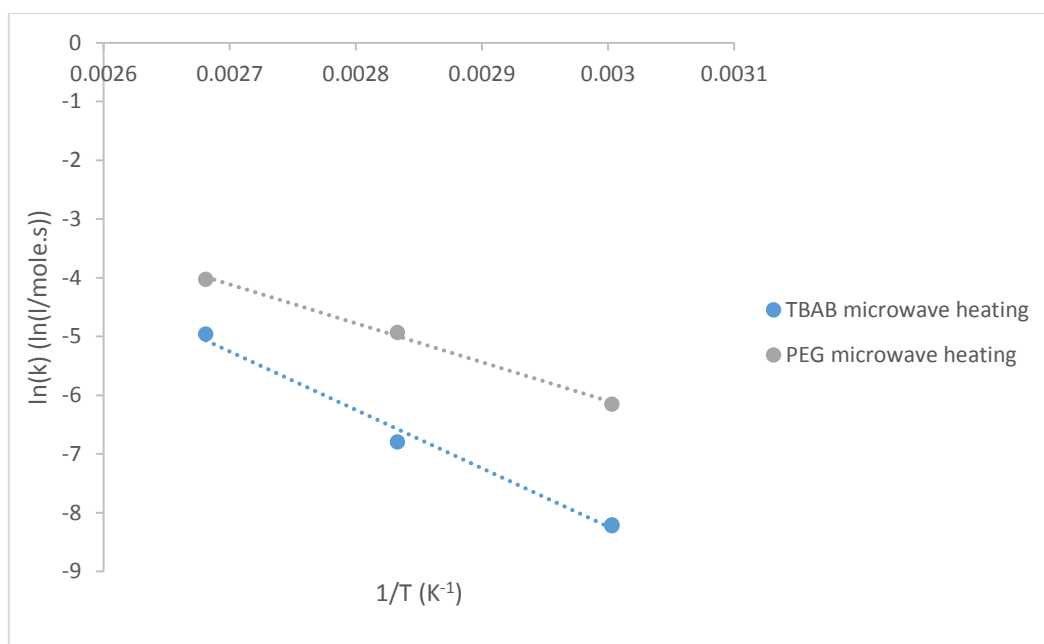
Figure 63: Comparison of the rate constants of the TBAB and PEG system in the microwave reactor

Just as predicted, the slope of the equation obtained with the TBAB system is steeper than the equation obtained with the PEG system. This verifies the previous conclusion. Based on the equation (see also Figure 63), the rate constants are extrapolated to the intersection point of both PTC-systems. The equations intersect at 0.002395, which corresponds to a temperature of 145 °C. This means that both systems probably react similarly fast at a temperature of 145 °C. This temperature also corresponds well to the results obtained in the conventional reactor where equally fast reactions are obtained at 134 °C.

However, just as with the results in the conventional reactor, it is not possible to achieve these temperatures since the batch reactor cannot withstand the elevated pressures. Therefore, the PEG-water system is more interesting in order to achieve good product yields.

4.1.7 Comparison of microwave energy with conventional energy

The comparison of microwaves and conventional heating as energy source is based on the reaction kinetics as a function of the temperature. Therefore, the rate constants are investigated at different temperatures, in both the microwave reactor and the conventional reactor. These rate constants are also investigated for both catalyst systems used in this study. The results obtained with the TBAB-H_2O medium and PEG-H_2O medium are shown in Figure 64.
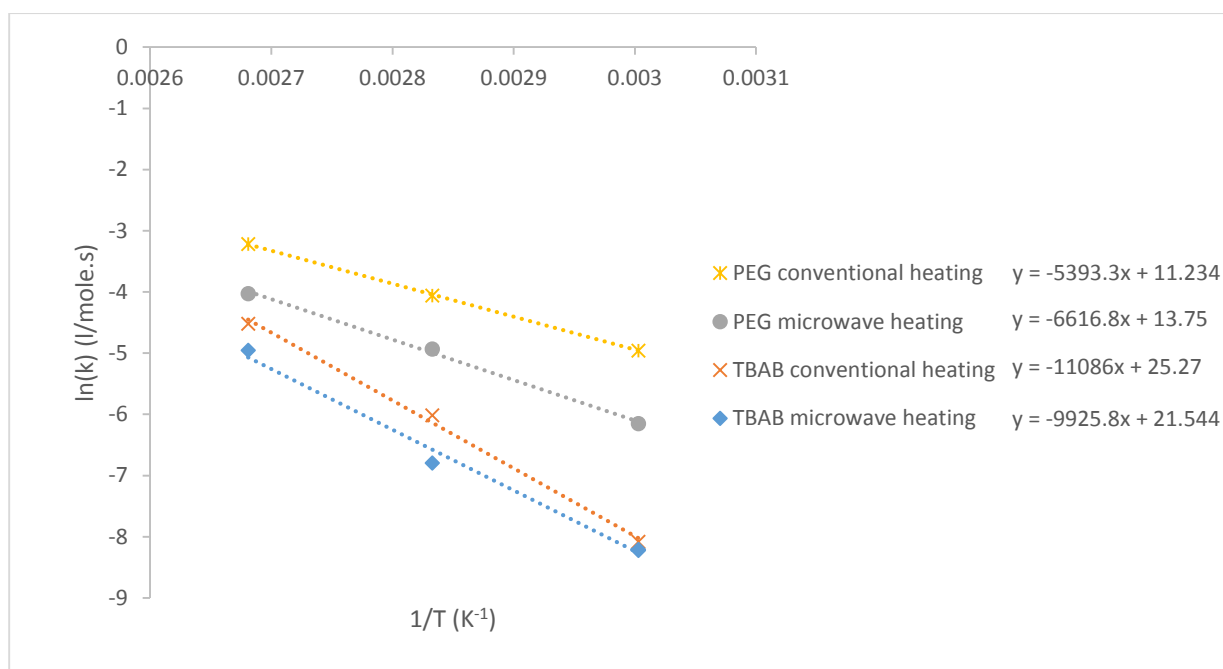
Figure 64: Comparison of microwave- and conventional heating for both PTC-mediums

In both cases, the rate constant obtained with microwaves are significantly lower than the rate constants obtained with conventional heating. So based on these observations, microwaves are not as good as conventional heating for the Suzuki-Miyaura coupling performed in this study. The pre-exponential factor and the activation energy are determined based on the equation of the rate constants as a function of the temperature, which is also shown again in formula 37. The results for the pre-exponential factor and the activation energy are shown in Table 23.

$$\ln(k) = -\frac{E_a}{R} \cdot \frac{1}{T} + \ln(k_0) \qquad (37)$$

Table 23: Comparison of the activation energy and pre-exponential factor for the heating method

catalyst system	heating source	Correlation R^2	k_0 (l/mole.s)	E_a (J/mole)
PEG	Conventional	0.99979	7.57E+04	44843
PEG	Microwaves	0.99719	9.37E+05	55016
TBAB	Conventional	0.99642	9.43E+10	92178
TBAB	Microwaves	0.99091	2.27E+09	82528

The pre-exponential factor and the activation energy depend mainly on the type of phase-transfer agent used for the reaction. The values calculated for the TBAB-H_2O medium are way higher than the PEG 2000-H_2O medium. However, this is mainly due to the steeper slope observed by the TBAB-water medium. The pre-exponential factor or frequency factor includes the total number of collisions between molecules, so collision which may or may not lead to a reaction. Since this is a high value, the possible collisions of the reaction increase which is beneficial for the reaction. The activation energy is the minimum energy that molecules must possess in order to form the biphenyl product. So in this case, it is favourable that the activation energy is low because less energy must be added for initiating the reaction [59],[62]. So on perspective of the activation energy, the PEG-H_2O medium is better.

The comparison of the energy source is more difficult when it is based on the activation energy and the pre-exponential factor. This is more difficult because in the PEG 2000-water medium, k_0 and E_a are both higher by the use of microwaves, while in the TBAB-

water medium, k_0 and E_a are both lower by the use of microwaves. So a specific trend is not observed. However, with the knowledge of the activation energy and the pre-exponential factor, the relation of the rate constant as a function of the temperature can be plotted graphically as shown in Figure 65.
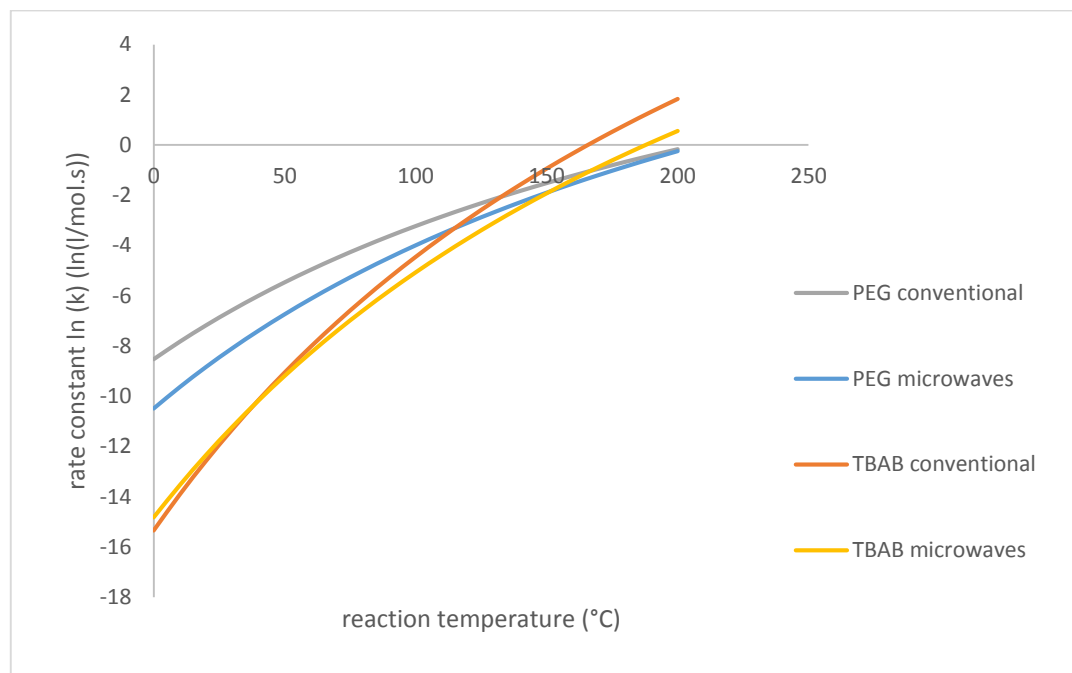
Figure 65: Comparison of the reaction rates at different temperatures

This plot shows visually the variation of the rate constant as a function of the temperature. Since the reaction rate is directly dependent on the rate constant, this also corresponds to the rate of reaction. Within the represented temperature range of 0 °C to 200 °C, it can be concluded that conventional heating provides the highest reaction rates for each specific catalyst system as the reaction rates are higher at each temperature. As all the experiments in the conventional reactor and microwave reactor are performed at the same temperatures, the difference in rate constants is due to another effect but the temperature. This means that the microwaves have another effect beside heating that ensures a lower reaction rate. As the rate determining step consists of different steps as shown in Scheme 12, it could be possible that in the presence of microwave irradiation, one part of the rate determining step proceeds slower as microwaves can cause a different reaction selectivity. This could then result in lower reaction rates and lower product yields within the same reaction times.

Another explanation for the lower reaction rates could be that the transmetalation step proceeds via a different pathway when the reaction is performed in the presence of microwave irradiation. As earlier discussed, pathway A proceeds much slower than pathway B because the formation of the poorly reactive $ArB(OH)^-$. It could be possible that in the presence of microwaves, the share of pathway A increases due to microwave effects. This has as consequence that the overall reaction slows down resulting in the lower rate constants that are observed in the microwave experiments [42].

Finally, it was also found in the study of Liu et al. [9] that the $Pd(OAc)_2$-H_2O-PEG system is less efficient under microwave conditions. Normally, the polyethylene oxide chains in PEG form complexes with the metal ions. These PEG-metal cation complexes bring the activated $ArB(OH)_3$ to the other phase where it reacts with the palladium intermediates. But it could be possible that these large PEG-metal cation complexes are instable in the presence of microwave radiation, so the efficiency decreases [9]. This last explanation could also have an impact on the reaction rate of the Suzuki-Miyaura reaction in the presence of microwaves.

4.2 Suzuki-Miyaura reaction in continuous flow

The Suzuki-Miyaura reaction is also performed in a continuous manner using two different flow set-ups. The first flow system uses microwave irradiation of 200 W as heating source, while the second flow system uses conventional heating delivered by a hot water bath at 90 °C. These two types of flow systems are compared in order to investigate the use of microwave irradiation as energy source for a continuous flow system. The comparison is based on the product yields obtained at different residence times, as well for the microwave-assisted flow as the conventional flow system. Afterwards, continuous flow processing is compared with the batch process in order to investigate the influence of continuous flow processing on the Suzuki-Miyaura reaction.

4.2.1 Comparison of microwave-assisted flow with conventional flow

The results for the comparison of microwave-assisted flow processing to conventional flow processing are obtained by performing the SM-coupling with the PEG-water medium by maintaining the same reaction conditions. These reaction conditions include similar flows, inlet temperature, residence times and molar ratio's, so the only variable is the energy source.

The comparison is based on the product yields as a function of the residence times. Residence times are varied based on the flowrate which at their turn, are set based on the calibration of the reactor solution flow as a function of the pump rate (see also 3.3.1.2). As described before, the flow rate of iodobenzene is adjusted to the flow rate of the reactor solution to obtain a molar ratio of 1.3.

The samples are collected and measured with UV-vis spectrophotometry and the results are shown in Table 24 and Table 25 and visualized in Figure 66 (for calculations, it is referred to appendix 6.3). Beside the product yields, the inlet temperature and outlet temperature of the reactor are also given. These were calculated based on the heat characterisation with the Wilson Plot (see Figure 39). A detail of these calculations can be found in Appendix 6.2.1 and 6.2.2.

Table 24: Product yields as a function of the residence time in the microwave-assisted flow

flow reactor solution (ml/min)	flow iodobenzene (ml/min)	moleratio	residence time (min)	T inlet reactor (°C)	T outlet reactor (°C)	conversion (%)	average
1.91	0.062	1.16	2.84	53.6	103.41	52.14	72.60
1.91	0.062	1.16	2.84	53.6	106.19	72.60	
2.53	0.075	1.26	2.15	58.6	102.50	79.58	77.63
2.53	0.075	1.26	2.15	58.6	104.88	75.69	
3.15	0.089	1.33	1.73	62.0	93.82	76.12	71.69
3.15	0.089	1.33	1.73	62.0	105.02	67.26	
3.77	0.109	1.29	1.44	64.5	102.27	66.75	68.16
3.77	0.109	1.29	1.44	64.5	103.12	69.56	
7.18	0.198	1.36	0.76	71.2	86.74	33.01	27.94
7.18	0.198	1.36	0.76	71.2	81.59	22.86	
10.59	0.293	1.35	0.51	73.9	60.69	0.09	23.79
10.59	0.293	1.35	0.51	73.9	62.73	23.79	

flow reactor solution (ml/min)	flow iodobenzene (ml/min)	moleratio	residence time (min)	T inlet reactor (°C)	T outlet reactor (°C)	conversion (%)	average
3.77	0.109	1.29	1.44	64.5	85.71	2.33	15.04
3.77	0.109	1.29	1.44	64.5	85.07	15.04	
3.15	0.089	1.32	1.73	62.0	84.23	28.17	28.78
3.15	0.089	1.32	1.73	62.0	84.76	29.40	
2.53	0.075	1.26	2.15	58.6	85.71	24.52	24.56
2.53	0.075	1.26	2.15	58.6	84.84	24.60	
1.91	0.055	1.30	2.85	53.6	84.87	27.19	30.14
1.91	0.055	1.30	2.85	53.6	83.99	33.09	
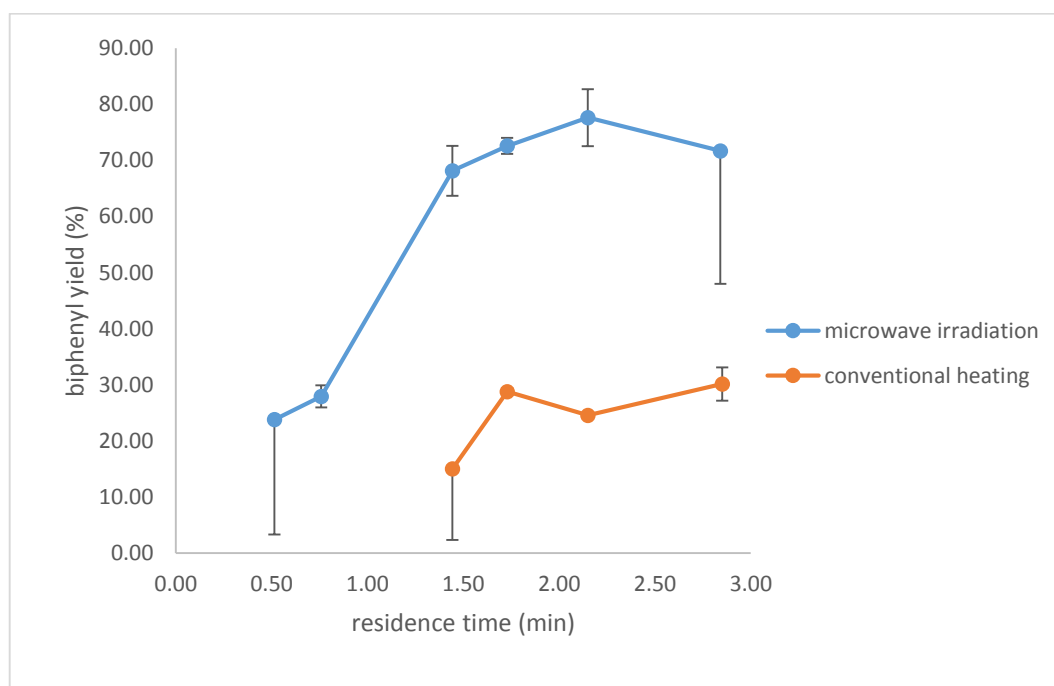
Figure 66: Product yields as a function of the residence time in the different flow systems

An increasing trend of the product yields as a function of the residence time is observed. As the residence time increases, higher conversions are obtained. This is a logical trend, because the reagents have more time to react and to reach a higher temperature which is beneficial for the reaction rate. Table 24 and Table 25 show that with flowrates of 7.18 and 10.59 ml/min, a temperature of 86.7 °C and 62.7 °C is reached, while the flowrates of 3.77 ml/min and lower reach temperatures around 103 °C.

In addition, it is also concluded that the flow system reaches a maximum temperature of about 106 °C, which means that this is about the boiling point of the reactor solution. This is why the flowrate of 3.77 ml/min is the most interesting because at this flowrate, the boiling point is achieved the fastest. When higher flowrates are set, the boiling point is not reached so the flow system is not working at maximum temperature. This is also observed by the flow rate of 3.77 ml/min, where high product yields are obtained, while at higher flowrates these product yields are no longer achieved.

The comparison of the microwave-assisted flow with the conventional flow clearly shows that product yields obtained with the microwave-assisted flow are significantly higher than those in the conventional heated flow. These higher product yields can be directly linked to the higher temperature increase induced by the microwaves. As earlier

indicated in Figure 40, the microwave reactor transmits microwaves with a power of 200 W, thereof is 87 W reflected and 113 W absorbed by the flow set-up. This absorbed power ensures a rapid warming of the reactor solution so that outlet temperatures around 103 °C are observed. This outlet temperature is not achieved in the conventional flow since the hot water bath has a maximum temperature of 90 °C resulting in outlet temperatures around 85 °C.

However, as the product yields mainly depends on the increased temperature, it is difficult to say that microwave-assisted flow is better than the conventional flow. This is because the hot water bath cannot reach similar temperatures as the microwave reactor. In order to make a correct comparison, a hot oil bath at higher temperatures should be used.

4.2.2 Comparison of continuous processing with batch

The fact that continuous flow processing allows higher temperatures than the boiling point of water could be interesting for obtaining good product yields in low residence times. That is why the continuous flow system is compared with the batch process, both in the presence of microwave irradiation as energy source. The comparison is based on the product yields obtained within similar reaction times. These product yields are obtained by keeping most reaction conditions in the flow system similar to the batch reaction conditions. These reaction conditions include molar ratio's, reaction times and concentrations. So, the main difference between the two methods is the reaction temperature. In batch, the temperature has been reached to 100 °C since this is the maximum attainable temperature, while in flow the temperature before reaction depends on the set flowrate and thus on the residence time or reaction time. Figure 67 shows some of the initial temperatures at the entrance of the reactor and temperatures at the end of the reactor as a function of the flow rate. The calculations of the inlet temperatures are based on the Wilson plot in chapter 3.3.1.3.
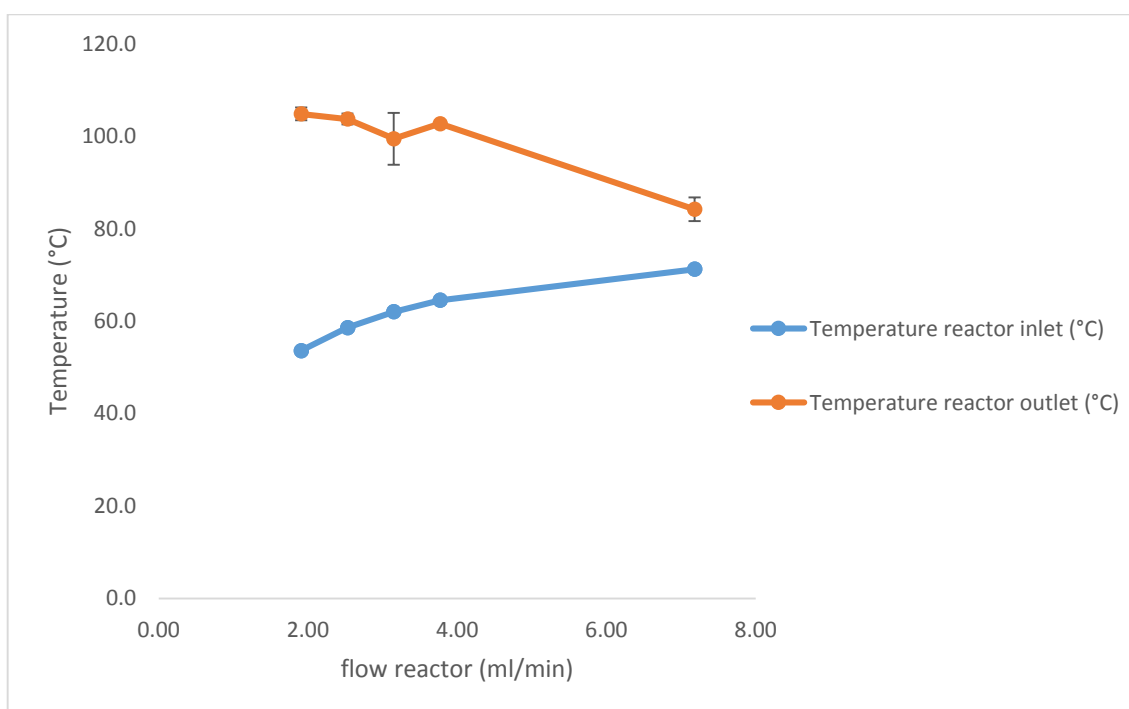

Figure 67: Temperature rise at different flow rates

Figure 67 shows the flow dependency of the temperature over the reactor. Here, it is clear that the temperature increases the most at lower flowrates. This is logical, as the residence time increases with lower flow rates so that there is more time to warm up. So

a difference between the flow reactor and the batch reactor is the initial temperature, as the initial temperature of the flow reactor is lower than the initial temperature of 100 °C achieved in the batch reactor. This lower temperature is not beneficial for the reaction kinetics, although on the other hand, the temperature at the end of the reactor is higher than 100 °C which is favorable for the reaction kinetics.

In Figure 68, the product yields are plotted as a function of the reaction time, as well for the microwave-assisted continuous flow as for the microwave-assisted batch system.
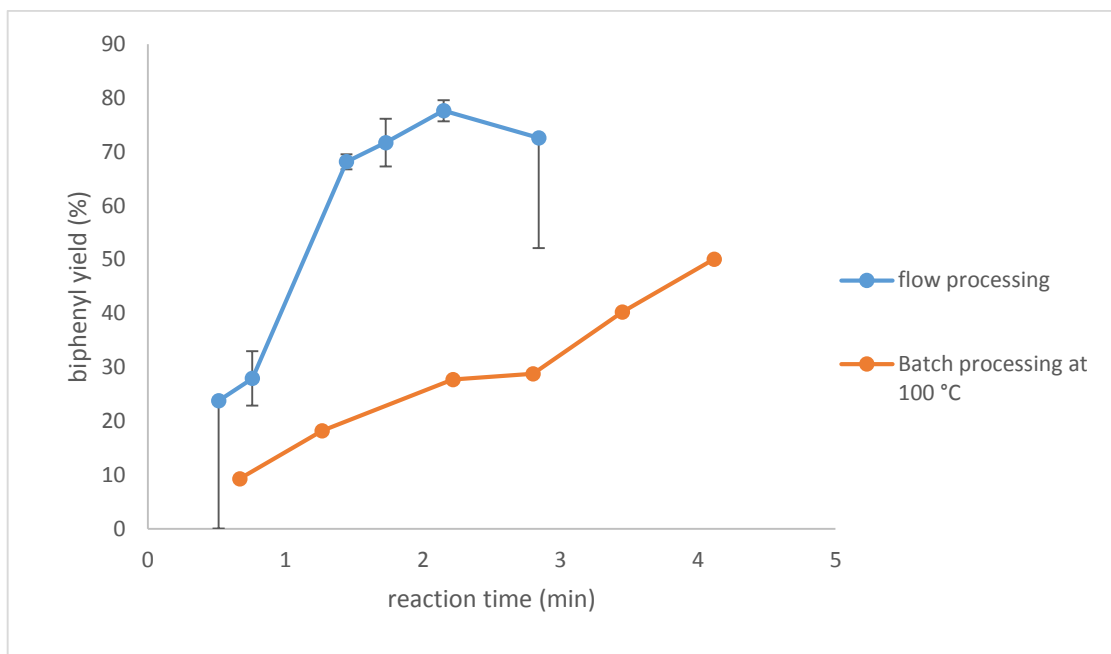
Figure 68: Comparison of flow processing and batch processing on the SM-coupling

The trend of flow processing shows significantly higher yields as batch processing. At first impression, this is against expectations because the initial temperature of approximately 60 °C in the flow system is much lower than the initial temperature of 100 °C in batch. It was expected that the reaction kinetics at the beginning are lower due to the temperature dependence of the rate constants. However, the trend clearly shows that this expectation is incorrect. Here, multiple explanations are possible for the higher yields obtained in the flow system.

First, it could be due to the rapid heating of the microwaves. In this way, the temperature increases quickly to the temperatures above 100 °C which affords higher reaction rates. Therefore, the temperature profile over the continuous reactor should be measured which, unfortunately, was not possible to measure within the reactor vessel. So it is not known how quick a temperature of 100 °C is achieved.

Second, beside the first effect, it is possible that the actual temperature inside the reactor even reached higher temperatures than 105 °C. This can be explained by, for example a piece of tubing at the end of the reactor where no microwaves arrive. As no microwaves arrive in this piece of tubing, the reactor solution already cools down rather than to heat up. As a consequence, the temperature in the reactor was even higher than the temperature which is indirectly measured.

Third, the large pressure drop over the reactor and the fact that the reactor solution with the PEG-water medium is viscous, ensure that a lot of fluctuations in the flowrate are observed. These fluctuations result in variations of the flowrate and thus in the residence time. As a result, the actual residence time could be longer than the residence time based on the calibration curve. This longer residence time, then, results in higher product yields which could explain the observed product yields in the continuous reactor. In

addition, due to the fluctuations, local hotspots could be created because at some points in the flow, the reactor solution will stand still and absorb more of the microwave power. These hotspots result in an increased reaction rate as the temperature increases locally. However, to verify this, the temperature profile over the reactor should also be observed.

Last, another difference between batch processing and continuous processing is the mixing behaviour. As a result, the reactants move towards each other on a different manner. This difference in mixing behaviour could have an influence on the contact of the reactants, and thus, on the reaction kinetics. However, to verify a possible difference in mixing behaviour, the mixing model should be investigated, both for batch processing and continuous processing. However, this seems a little bit farfetched since this has less to do with the effect of microwave radiation on continuous processing.

In order to verify these observations, more research should be performed on the comparison of microwave-assisted flow and microwave-assisted batch processing. Here, the temperature profile should correspond better to each other to see if the differences are mainly due to the temperature profile or flow processing.

5 Conclusion

The use of microwaves as an energy source for the Suzuki-Miyaura coupling of phenylboronic acid and iodobenzene is successfully evaluated.

First, based on validation, UV-Vis spectrophotometry proved to be a suitable analysis method to measure the formed biphenyl product. This analysis method is supported by preceding sample preparation to isolate biphenyl from background substances such as phenylboronic acid and the phase transfer catalyst PEG 2000 or TBAB. Only iodobenzene is found to have an interference at 247.5 nm by the used calibration curve method. However, this interference is 28.16 times smaller than the absorption of biphenyl at 247.5 nm. Nevertheless, by preparing a second calibration curve of iodobenzene and adapting the calculations for the biphenyl concentration, this interference is taken into account.

Next, the Suzuki-Miyaura reaction is performed in batch and continuous flow, both by conventional heating as with microwave irradiation. Here, the reaction is approached by the first type of the second order system to determine the rate constants which are essential for the evaluation of the reaction conditions. However, there still exists some uncertainty about this approximation as different studies consider that the reaction rate depends on the different substances. In addition, up to the present day, the exact role of the base in the Suzuki-Miyaura reaction is not known, so different assumptions for the reaction kinetics are possible.

Prior to the evaluation of microwaves on the reaction, two different catalyst systems are investigated, where the first is a $Pd(OAc)_2$-H_2O-TBAB medium and the second is a $Pd(OAc)_2$-H_2O-PEG 2000 medium. Based on the rate constants and the product yields, the $Pd(OAc)_2$-H_2O-PEG 2000 proves to be a more efficient medium for performing the reaction under the investigated temperatures of 60 °C, 80 °C and 100 °C. By extrapolating the results, it is concluded that the $Pd(OAc)_2$-H_2O-PEG 2000 medium stays more efficient at temperature conditions beneath 132 °C. This is due to better properties of PEG 2000 as a phase transfer catalyst and because of the fact that PEG 2000 also functions as a co-solvent. However, at higher temperatures than 132 °C, it could be possible that the $Pd(OAc)_2$-H_2O-TBAB medium is a more efficient catalyst system. This can be concluded from the results of the pre-exponential factor since the pre-exponential factor obtained with $Pd(OAc)_2$-H_2O-TBAB ($9.4*10^{10}$ l/mole.s) is significantly higher than that of the $Pd(OAc)_2$-H_2O-PEG 2000 ($7.6*10^4$ l/mole.s). This could be further investigated by performing the Suzuki-Miyaura reaction in both catalyst systems at higher temperatures such as 130 °C and 150 °C, but therefore, there should be worked at increased pressure due to the boiling point of the solvent.

Subsequently, the main objective of this master's thesis is investigated by examining the influence of microwaves on the Suzuki-Miyaura reaction. In batch, the results at the investigated temperatures show that microwaves lead to lower reaction rates resulting in lower product yields within the same reaction times. This applies especially to the reaction performed at lower temperatures, while at higher temperatures such as 100 °C, less significant differences are observed between conventional heating and microwave irradiation. So within the investigated temperatures of 60 °C, 80 °C and 100 °C it is concluded that microwave irradiation is a worse energy source than conventional heating.

However, microwave irradiation causes higher heating rates than conventional heating so despite the fact that microwave irradiation is considered as a worse energy source for the Suzuki-Miyaura reaction, it does not mean it is less efficient. This is observed in the microwave-asssisted continuous flow reactor where significantly higher product yields are

obtained within the same residence times in comparison with the conventional flow reactor. For example, after a residence time of 1.73 minutes, a product yield of 71.69 % is obtained with the microwave-assisted flow reactor while only 28.78 % conversion is observed in the conventional flow reactor. This difference is clearly a result of the higher heating rate due to microwave irradiation since a temperature increase of 43 °C over the reaction is observed with microwaves as energy source, while only a temperature increase of 23 °C is observed with conventional heating. However, the heating circumstances are difficult to compare because a hot water bath of 90 °C is used as conventional heating while the microwave-assisted flow uses a microwave power of 200 W.

To compare these heating sources, the same amount of power as the absorbed power (113 W) in the microwave-assisted flow should be used to heat the conventional flow reactor. Here, the heat losses of the hot water bath and power efficiency should be taken into account. Then, it can be observed which temperature is achieved in the conventional flow and compare this with the temperature achieved in the microwave-assisted flow.

Another way to evaluate the efficiency of the heating source is to compare the product yields and the required energy (in kWh) as a function of the flowrate for each flow system. In this way, it is possible to determine which flow system is energetically the most efficient. However, since these measurements are not performed in this study, this could still be a point of research in future study.

Bibliography

[1]   "https://iiw.kuleuven.be/onderzoek/lab4U/." [Online]. Available: https://iiw.kuleuven.be/onderzoek/lab4U/. [Accessed: 08-Mar-2016].

[2]   "https://iiw.kuleuven.be/onderzoek/lab4U/dienstverlening." [Online]. Available: https://iiw.kuleuven.be/onderzoek/lab4U/dienstverlening. [Accessed: 08-Mar-2016].

[3]   "http://www.janssen.com/belgium/nl/over-janssen." [Online]. Available: http://www.janssen.com/belgium/nl/over-janssen. [Accessed: 08-Mar-2016].

[4]   A. K. Gupta, G. Tirumaleswara Rao, and K. N. Singh, "NiCl 2·6H 2O as recyclable heterogeneous catalyst for N-arylation of amines and NH-heterocycles under microwave exposure," *Tetrahedron Lett.*, vol. 53, no. 17, pp. 2218–2221, 2012.

[5]   R. B. Bedford, M. E. Blake, C. P. Butts, and D. Holder, "The Suzuki coupling of aryl chlorides in TBAB-water mixtures.," *Chem. Commun. (Camb).*, vol. 2, no. 4, pp. 466–467, 2003.

[6]   E. G. Berthier, M. J. S. Dewar, H. Fischer, K. Fukui, H. Hartmann, H. H. Jaffe, J. Jortner, W. Kutzelnigg, K. Ruedenberg, E. Scrocco, and W. Zeil, *Lecture Notes in Chemistry*, vol. 80. Springer, 1978.

[7]   T. Thomas and A. Thompson, "A reassessment of the transition-metal free Suzuki-type coupling methodology.," *Chemtracts*, vol. 18, no. 4, pp. 246–250, 2005.

[8]   "http://flowlink.nl/proces-technologie/van-batch-naar-continu/." [Online]. Available: http://flowlink.nl/proces-technologie/van-batch-naar-continu/. [Accessed: 10-Mar-2016].

[9]   L. Liu, Y. Zhang, and Y. Wang, "Phosphine-Free Palladium Acetate Catalyzed Suzuki Reaction in Water- reported . 13a Howe," no. 3, pp. 6122–6125, 2005.

[10]   A. Neves, "Lecture 1 - The nature of electromagnetic radiation," *Tissue Eng.*, no. Nt Ii, pp. 1–12, 2009.

[11]   E. Wiers, S. Wouters, and D. C. Giancoli, *Fysica voor industrieel ingenieurs*, 2e editon. Harlow: Pearson 2012, 2012.

[12]   "http://slideplayer.com/slide/4137310/." [Online]. Available: http://slideplayer.com/slide/4137310/. [Accessed: 27-Apr-2016].

[13]   H. D. Young and R. A. Freedman, "Chapter 32 Electromagnetic Waves," *Powerpoint Lect. Univ. Phys.*, vol. twelfth ed, 2008.

[14]   E. Radiation, "Electromagnetic Radiation Principles CHAPTER 2 :," *Image (Rochester, N.Y.)*, pp. 1–23, 2007.

[15]   M. E. Malainey, "A Consumer's Guide to Archaeological Science Analytical Techniques," *Zhurnal Eksp. i Teor. Fiz.*, p. 624, 2011.

[16]   S. Ravichandran and E. Karthikeyan, "Microwave synthesis - A potential tool for green chemistry," *Int. J. ChemTech Res.*, vol. 3, no. 1, pp. 466–470, 2011.

[17]   V. G. Gude, P. Patil, E. Martinez-guerra, and S. Deng, "Microwave energy potential for biodiesel production," *Sustain. Chem. Process.*, no. c, pp. 1–31, 2013.

[18]   D. F. Stein, *Microwave Processing of Materials*. 1994.

[19]   "Microwave road: microwaves and application areas." [Online]. Available: http://www.microwaveroad.se/microwaves-and-application-areas.html. [Accessed: 01-May-2016].

[20]   M. a. Surat, S. Jauhari, and K. R. Desak, "A brief review : Microwave assisted organic reaction," *Appl. Sci. Res.*, vol. 4, no. 1, pp. 645–661, 2012.

[21] "http://chemwiki.ucdavis.edu/Core/Materials_Science/Optics/Dielectric_Polarizatio n." [Online]. Available: http://chemwiki.ucdavis.edu/Core/Materials_Science/Optics/Dielectric_Polarization . [Accessed: 06-May-2016].

[22] E. Gjuraj, R. Kongoli, and G. Shore, "Combination of Flow Reactors with Microwave-Assisted Synthesis: Smart Engineering Concept for Steering Synthetic Chemistry on the 'Fast Lane,'" *Chem. Biochem. Eng. Q.*, vol. 26, no. 3, pp. 285– 307, 2012.

[23] "Chapter one, microwave assisted organic chemistry." [Online]. Available: http://shodhganga.inflibnet.ac.in/bitstream/10603/3197/8/08_chapter 1.pdf. [Accessed: 06-Apr-2016].

[24] CPI, "Magnetron Theory of Operation," p. 10, 2014.

[25] "http://www.britannica.com/technology/electron-tube," *Encyclopaedia Britannica, inc*. [Online]. Available: http://www.britannica.com/technology/electron-tube. [Accessed: 06-Apr-2016].

[26] "http://hyperphysics.phy-astr.gsu.edu/hbase/waves/magnetron.html." [Online]. Available: http://hyperphysics.phy-astr.gsu.edu/hbase/waves/magnetron.html. [Accessed: 06-May-2016].

[27] C. L. Brace, "Microwave Ablation Technology: What Every User Should Know," *Curr. Probl. Diagn. Radiol.*, vol. 38, no. 2, pp. 61–67, 2009.

[28] "http://www.this-is-synthesis.com/mainnav/crash-course/instrument-types/." [Online]. Available: http://www.this-is-synthesis.com/mainnav/crash-course/instrument-types/. [Accessed: 06-May-2016].

[29] A. Suzuki, "Organoborane coupling reactions (Suzuki coupling)," *Proc. Japan Acad. Ser. B*, vol. 80, no. 8, pp. 359–371, 2004.

[30] "http://pubs.acs.org/JACSbeta/jvi/issue15.html." [Online]. Available: http://pubs.acs.org/JACSbeta/jvi/issue15.html. [Accessed: 07-May-2016].

[31] U. Kazmaier, "Cross-Coupling Reactions via," no. 0, pp. 531–583, 2004.

[32] K. N. H. C. A. Hunter, M. J. K. J. Lehn, S. V. L. M. Olivucci, J. T. M. Venturi, and C. W. H. W. H. Yamamoto, *Topics in current chemistry*, 266th ed. Springer, 2001.

[33] H. G. Gudmundsson, "The Suzuki-Miyaura Recation and Boron Reagents - Mechanism, Synthesis and Application," 2014.

[34] "http://www.name-reaction.com/suzuki-cross-coupling." [Online]. Available: http://www.name-reaction.com/suzuki-cross-coupling. [Accessed: 15-May-2016].

[35] D. Kovala-Demertzi, "Palladium homogeneous catalysis: Suzuki-Miyaura cross-coupling reaction," *NCBI. U.S. Natl. Libr. Med.*, no. 0, pp. 1–23, 2013.

[36] A. Haidle, C. Coletta, and E. Hansen, "Analysis of Elementary Steps in the Reaction Mechanism," *J. Org. Chem. J. Am. Chem. Soc. Acc. Chem. Res. Transmetallation Can. J. Chem. J. Angew. Chem., Int. Ed. Engl. J. Chem. Rev*, vol. 576, no. 95, pp. 147–168, 1999.

[37] "http://everything.explained.today/Suzuki_reaction/#Ref-14." [Online]. Available: http://everything.explained.today/Suzuki_reaction/#Ref-14. [Accessed: 15-May-2016].

[38] "https://organometallicchem.wordpress.com/2012/10/14/oxidative-addition-of-polar-reagents/." [Online]. Available: https://organometallicchem.wordpress.com/2012/10/14/oxidative-addition-of-polar-reagents/. [Accessed: 17-May-2016].

[39] B. U. W. Maes, S. Verbeeck, T. Verhelst, A. Ekomi??, N. Von Wolff, G. Lef??vre, E. A. Mitchell, and A. Jutand, "Oxidative addition of haloheteroarenes to palladium(0): Concerted versus S<inf>N</inf>Ar-type mechanism," *Chem. - A Eur. J.*, vol. 21, no. 21, pp. 7858–7865, 2015.

[40] "http://www.ilpi.com/organomet/oxidative.html." [Online]. Available: http://www.ilpi.com/organomet/oxidative.html. [Accessed: 17-May-2016].

[41] E. Van Hoof, *Organische chemie 2A*. Universiteit Hasselt, 2014.

[42] C. Amatore, A. Jutand, and G. Le Duc, "Kinetic data for the transmetalation/reductive elimination in palladium-catalyzed Suzuki-Miyaura reactions: Unexpected triple role of hydroxide ions Used as Base," *Chem. - A Eur. J.*, vol. 17, no. 8, pp. 2492–2503, 2011.

[43] A. J. J. Lennox and G. C. Lloyd-Jones, "Selection of boron reagents for Suzuki-Miyaura coupling.," *Chem. Soc. Rev.*, vol. 43, no. 1, pp. 412–43, 2014.

[44] M. D. Angelica and Y. Fong, "NIH Public Access," *October*, vol. 141, no. 4, pp. 520–529, 2008.

[45] "http://everything.explained.today/Transmetalation/." [Online]. Available: http://everything.explained.today/Transmetalation/. [Accessed: 17-May-2016].

[46] "https://organometallicchem.wordpress.com/2012/10/19/reductive-elimination/." [Online]. Available: https://organometallicchem.wordpress.com/2012/10/19/reductive-elimination/. [Accessed: 17-May-2016].

[47] A. Mastracchio, "Phase-Transfer Catalysis," 2008.

[48] I. Maluenda and O. Navarro, "Recent developments in the Suzuki-Miyaura reaction: 2010-2014," *Molecules*, vol. 20, no. 5, pp. 7528–7557, 2015.

[49] P. C. Chemistry, "Palladium-Catalysed Coupling Chemistry," *Acros Org.*

[50] R. Jana, T. P. Pathak, and M. S. Sigman, "Advances in Transition Metal (Pd, Ni, Fe)-catalyzed Cross-Coupling Reactions Using Alkyl-Organometallics as Reaction Partners," *October*, vol. 111, no. 3, p. 295, 2011.

[51] "Bedienungsanleitung: EasyMax 102," pp. 1 –52, 2008.

[52] "http://us.mt.com/us/en/home/products/L1_AutochemProducts/Chemical-Synthesis-and-Process-Development-Lab-Reactors/Synthesis-Reactor-Systems/EasyMax-Synthesis-Reactor.html." [Online]. Available: http://us.mt.com/us/en/home/products/L1_AutochemProducts/Chemical-Synthesis-and-Process-Development-Lab-Reactors/Synthesis-Reactor-Systems/EasyMax-Synthesis-Reactor.html. [Accessed: 23-May-2016].

[53] R. Miniflow, "MINIFLOW 200SS, 200W, 2450 MHz Ref. MiniFlow 200SS," pp. 1–5.

[54] "http://gestis-en.itrust.de/nxt/gateway.dll/gestis_en/013450.xml?f=templates$fn=default.htm$3.0." [Online]. Available: http://gestis-en.itrust.de/nxt/gateway.dll/gestis_en/013450.xml?f=templates$fn=default.htm$3.0. [Accessed: 26-May-2016].

[55] C. H. Bartholomew, "Mechanisms of catalyst deactivation," *Appl. Catal. A Gen.*, vol. 212, no. 1–2, pp. 17–60, 2001.

[56] W. Manuals, "Watson-Marlow 120 cased pumps 120U / DV Contents."

[57] "http://omlc.org/spectra/PhotochemCAD/html/043.html." [Online]. Available: http://omlc.org/spectra/PhotochemCAD/html/043.html. [Accessed: 31-Mar-2016].

[58] "H5: kinetiek," pp. 1–36.

[59]   L. Thomassen and M. Lynen, "Industriële ingenieurswetenschappen Reactorkunde."

[60]   V. Aquilanti, K. C. Mundim, M. Elango, S. Kleijn, and T. Kasai, "Temperature dependence of chemical and biophysical rate processes: Phenomenological approach to deviations from Arrhenius law," *Chem. Phys. Lett.*, vol. 498, no. 1–3, pp. 209–213, 2010.

[61]
        "http://chemwiki.ucdavis.edu/Core/Physical_Chemistry/Kinetics/Rate_Laws/The_R ate_Law." [Online]. Available: http://chemwiki.ucdavis.edu/Core/Physical_Chemistry/Kinetics/Rate_Laws/The_Ra te_Law. [Accessed: 02-Jun-2016].

[62]
        "http://chemwiki.ucdavis.edu/Core/Physical_Chemistry/Kinetics/Modeling_Reactio n_Kinetics/Temperature_Dependence_of_Reaction_Rates/The_Arrhenius_Law/The _Arrhenius_Law%3A_Arrhenius_Plots." [Online]. Available: http://chemwiki.ucdavis.edu/Core/Physical_Chemistry/Kinetics/Modeling_Reaction _Kinetics/Temperature_Dependence_of_Reaction_Rates/The_Arrhenius_Law/The_ Arrhenius_Law%3A_Arrhenius_Plots. [Accessed: 03-Jun-2016].

6 Appendix

6.1 Calculations of the equations for the order approximations

6.1.1 Pseudo first order approach

In the pseudo first order approach it may be assumed that the concentration of phenylboronic acid stays the same as this reagent is in excess. So the concentration of phenylboronic acid during the reaction is equal to the initial concentration and can be considered as a constant value.

$$[PBA] = cst$$

Here, the reaction rate mainly depends on the concentration gradient of iodobenzene.

$$-r_{IB} = k\,[PBA_0][IB] = \frac{dC_{IB}}{dt}$$

This differential equation is solved by integrating over the concentration of iodobenzene and the time.

$$\int_{C_{IB,0}}^{C_{IB}} \frac{dC_{IB}}{C_{IB}} = k\,C_{PBA,0} \int_0^t dt$$

This is further elaborated and transformed to the equation of the concentration of iodobenzene as a function of the reaction time.

$$\ln|C_{IB}| - \ln|C_{IB,0}| = k\,C_{PBA,0}\,t$$

$$\ln|c_{IB}| = C_{PBA,0}.k.t + \ln|c_{IB,0}|$$

6.1.2 First type of the second order approach

In the first type of the second order approach, the reaction rate is proportional to the product of the concentrations of two reactants.

$$-r_{IB} = \frac{dC_{IB}}{dt} = k\,[IB][PBA]$$

Here, an assumption is made that the concentration of phenylboronic acid is equal to the iodobenzene concentration during the reaction. The consequence of this assumption is that the concentration of iodobenzene is squared so this can be further elaborated.

$$-r_{IB} = \frac{dC_{IB}}{dt} = k\,C_{IB}^2$$

This differential equation is solved by integrating over the concentration of iodobenzene and the time. Subsequently, the equation is further transformed to the concentration of iodobenzene as a function of the reaction time.

$$k \int_0^t dt = \int_{C_{IB,0}}^{C_{IB}} \frac{dC_{IB}}{C_{IB}^2}$$

$$k\,t = \frac{1}{C_{IB}} - \frac{1}{C_{IB,0}}$$

$$\frac{1}{c_{IB}} = k.t + \frac{1}{c_{IB,0}}$$

6.1.3 Second type of the second order approach

In the second type of the second order approach, the reaction rate is proportional to the product of the concentrations of two reactants. In this approach, it is not assumed that the concentration of phenylboronic acid is equal to the concentration of iodobenzene during the reaction. However, an expression of the phenylboronic acid concentration as a function of the iodobenzene concentration during the reaction is made. This expression makes it possible to solve the equation to the concentration of iodobenzene.

$$C_{PBA} = C_{IB} + (C_{PBA,0} - C_{IB,0})$$

The expression of the phenylboronic acid concentration is filled in the second order rate equation and further elaborated.

$$-r_{IB} = \frac{dC_{IB}}{dt} = k\, C_{IB}\, (C_{IB} + (C_{PBA,0} - C_{IB,0}))$$

$$-r_{IB} = \frac{dC_{IB}}{dt} = k\, (C_{IB}^2 + C_{IB}(C_{PBA,0} - C_{IB,0}))$$

This differential equation is solved by integrating over the concentration of iodobenzene and the time. Then it is further elaborated and transformed to the concentration of iodobenzene as a function of the reaction time.

$$\int_0^t k\, dt \int_{C_{IB,0}}^{C_{IB}} \frac{dC_{IB}}{C_{IB}^2 + C_{IB}(C_{PBA,0} - C_{IB,0})}$$

$$k\, t\, (C_{PBA,0} - C_{IB,0}) = (\ln|C_{IB}| - \ln|C_{IB} + C_{PBA,0} - C_{IB,0}|) - (\ln|C_{IB,0}| - \ln|C_{PBA,0}|)$$

$$\ln|c_{IB}| - \ln|c_{IB} + c_{PBA,0} - c_{IB,0}| = (c_{PBA,0} - c_{IB,0}).k.t + \ln|c_{IB,0}| - \ln|c_{PBA,0}|$$

6.2 Temperature calculation in flow based on the Wilson plot

Based on the Wilson plot, following equation has been prepared.

$$\frac{1}{U} = 0.0002 * \frac{1}{q_v} + 0.028$$

Based on this equation, it is possible to calculate the overall heat-transfer coefficient which is necessary for the temperature calculation.

The relation between the overall heat-transfer coefficient and the temperature is given in following equation.

$$U = \frac{\dot{Q}}{A\,.\,\Delta T_{lm}}$$

Here, $\dot{Q}$ is the exchanged heat represented by $\dot{m}\,c_p\,\Delta T$, A is the surface of the tubing where heat exchange is possible so this is represented by d ⊓ l, and ΔT_m is the logarithmic temperature difference, which is calculated with following formula.

$$\Delta T_{lm} = \frac{[(T_{hi} - T_{co}) - (T_{ho} - T_{ci})]}{ln\left[\frac{T_{hi} - T_{co}}{T_{ho} - T_{ci}}\right]}$$

Here, the cold heat flow is represented by the environment, so T_{co} and T_{ci} can be considered equal to the room temperature so also equal to each other.

Subsequently, all the parameters are filled in the equation of the overall heat-transfer coefficient as a function of the temperature. This gives following formula.

$$U = \frac{\dot{m}\, c_p (T_{ho} - T_{hi})}{\dfrac{T_{ho} - T_{hi}}{\ln(\dfrac{T_{hi} - T_r}{T_{ho} - T_r})} \pi\, d\, l}$$

This equation is further elaborated, which gives following formula.

$$U = \frac{\dot{m}\, c_p \ln(\dfrac{T_{hi} - T_r}{T_{ho} - T_r})}{\pi\, d\, l}$$

Based on the equation shown above, the temperature of the reactor inlet and the temperature outlet are calculated.

6.2.1 Temperature of the reactor inlet

By transforming the equation to the temperature of the reactor inlet, T_{ho} can be calculated when the temperature at the beginning of the flow system is measured. In this case, T_{ho} represents the temperature at the inlet of the reactor.

$$T_{ho} = \frac{T_{hi} - T_r}{e^{(\frac{U \pi d l}{\dot{m}\, c_p})}} + T_r$$

6.2.2 Temperature of the reactor outlet

By transforming the equation to the temperature of the reactor outlet, T_{hi} can be calculated when the temperature at the end of the flow system is measured. In this case, T_{hi} represents the temperature at the outlet of the reactor.

$$T_{hi} = (T_{ho} - T_r)\, e^{(\frac{U \pi d l}{\dot{m}\, c_p})} + T_r$$

6.3 Calculation method of the product yields in flow system

The flows of the reactor solution and the iodobenzene flow are calculated based on the calibration curves of the pumps. The residence time is determined by the volume of the reactor divided by the total flow, which is the sum of the two flowrates.

In order to calculate the product yields of the sample, the initial concentration of iodobenzene at the beginning of the reactor needs to be determined. This concentration is determined by calculating the initial mass of iodobenzene in the sample. As the sample is weighed, it is possible to determine the initial mass of iodobenzene by means of the mass percentage of pure iodobenzene. This mass percentage of iodobenzene in the reactor solution is based on the molar ratios in contrast to the amount of moles of phenylboronic acid. The amount of mole of phenylboronic acid is known since this is exactly weighed by the preparation of the reactor solution. Following formula shows the calculation of the initial mass of iodobenzene.

$$m_{IB,0} = m_{sample} \cdot m\%_{IB}$$

Here, following formula is used to calculate the mass percentage of iodobenzene.

$$m\%_{IB} = \frac{m_{IB}}{m_{IB} + m_{reactorsolution}} \cdot 100\% = \frac{\frac{n_{PBA,0}}{n_{PBA/IB}} MM_{IB}}{(\frac{n_{PBA,0}}{n_{PBA/IB}} MM_{IB}) + m_{reactorsolution}} \cdot 100\%$$

Then, the initial concentration of iodobenzene is calculated by the amount of mole iodobenzene in the volume of hexane extract. Note that a volume correction factor of the volume of iodobenzene has been taken into account for this volume of hexane.

$$C_{IB,0 \ in \ extract} = \frac{\frac{m_{IB,0}}{MM_{IB}}}{V_{hexane} + \frac{m_{IB,0}}{\rho_{IB}}}$$

Finally, the conversion is calculated similar to the calculation in the batch experiments, therefore is referred to 3.4.8.

Auteursrechtelijke overeenkomst

Ik/wij verlenen het wereldwijde auteursrecht voor de ingediende eindverhandeling:
Optimisation of the Suzuki-Miyaura-coupling and conversion from batch to continuous flow with microwaves as energy source

Richting: **master in de industriële wetenschappen: chemie**
Jaar: **2016**

in alle mogelijke mediaformaten, - bestaande en in de toekomst te ontwikkelen - , aan de Universiteit Hasselt.

Niet tegenstaand deze toekenning van het auteursrecht aan de Universiteit Hasselt
behoud ik als auteur het recht om de eindverhandeling, - in zijn geheel of gedeeltelijk -,
vrij te reproduceren, (her)publiceren of distribueren zonder de toelating te moeten
verkrijgen van de Universiteit Hasselt.

Ik bevestig dat de eindverhandeling mijn origineel werk is, en dat ik het recht heb om de rechten te verlenen die in deze overeenkomst worden beschreven. Ik verklaar tevens dat de eindverhandeling, naar mijn weten, het auteursrecht van anderen niet overtreedt.

Ik verklaar tevens dat ik voor het materiaal in de eindverhandeling dat beschermd wordt door het auteursrecht, de nodige toelatingen heb verkregen zodat ik deze ook aan de Universiteit Hasselt kan overdragen en dat dit duidelijk in de tekst en inhoud van de eindverhandeling werd genotificeerd.

Universiteit Hasselt zal mij als auteur(s) van de eindverhandeling identificeren en zal geen wijzigingen aanbrengen aan de eindverhandeling, uitgezonderd deze toegelaten door deze overeenkomst.

Voor akkoord,

Verhoeven, Douwe

Datum: **13/06/2016**